# Structural insights into ligand-receptor interaction of Equine herpesvirus type 1 and 4

Inaugural-Dissertation
to obtain the academic degree
Doctor rerum naturalium (Dr. rer. nat.)

submitted to the Department of Biology, Chemistry, Pharmacy
of Freie Universität Berlin

by

VIVIANE KREMLING

2020

Angefertigt im Zeitraum März 2017 bis Juni 2020 am Institut für Virologie und am Institut für Chemie und Biochemie der Freien Universität Berlin unter der Leitung von Walid Azab, Nikolaus Osterrieder und Markus Wahl.

1. Gutachter: Univ.-Prof. Dr. Nikolaus Osterrieder

2. Gutachter: Prof. Dr. Markus C. Wahl

Disputation am 4 November 2020

"I have never tried that before,
so I think I should definitely be able to do that."
– Astrid Lindgren, Pippi Longstocking

## Zusammenfassung

Die zwei nahverwandten Alphaherpesviren Equines Herpesvirus Typ 1 (EHV-1) und Equines Herpesvirus Tpy 4 (EHV-4) binden mit Hilfe des Oberflächenproteins Glykoprotein D (gD) den Haupthistokompatibilitätskomplex (MHC-I) um in Zellen einzudringen. In dieser Studie wurde die gD-MHC-I Interaktion charakterisiert. Die Proteine (gD1, gD4, MHC-I) wurden mit dem Baculovirus/Insektenzellsystem hergestellt und anschließend kristallisiert. Die Strukturen von gD1 und gD4 wurden mit einer Auflösung von 2,45 und 1,9 Å gelöst und zeigen eine V-Set Immunglobulin (IgV-like) Faltung vergleichbar mit dem von HSV-1 gD. Die Helices und Loop-Regionen unterscheiden sich aber zwischen EHV-1 und 4 gD Strukturen und denen verwandter Alphaherpesviren. Außerdem wurde die Bindeaffinität von recombinanten gDs zu equinem MHC-I mittels Oberflächenplasmonresonanz (SPR) bestimmt und gezeigt, dass lösliches gD Plaqueanzahl und EHV-1 und EHV-4 Infektionsraten in equinen Zellen reduzieren kann. Mit Hilfe von molekularer Modellierung konnten plausible Bindehypothesen und Schlüsselaminosäuren für die Ligand-Rezeptor-Interaktion identifiziert und durch Molekulardynamiksimulationen und EHV-1 und EHV-4 Viren mit mutiertem gD evaluiert werden. Die Punktmutationen führten zu einem reduziertem Viruswachstum und es konnte bestätigt werden, dass die Aminosäuren F213 und D261 eine Rolle im Viruseintritt in die Zelle spielen. Zusammgefasst tragen unsere Ergebnisse dazu bei, die Interkation zwischen Herpesviren und Zellen besser zu verstehen und sie können dazu genutzt werden, um gezielt antivirale Wirkstoffe und Impfstoffe zu entwickeln.

## Summary

The two closely related alphaherpesviruses equine herpesvirus 1 (EHV-1) and EHV-4 bind to the equine major histocompatibility complex I (MHC-I) through their surface glycoprotein D (gD) to enter host cells. In this study, we characterized the gD-MHC-I interaction. Proteins (gD1, gD4, MHC-I) were produced using the baculovirus/insect cell system and crystallized. The structures of recombinant gD1 and gD4 were solved at resolutions of 2,45 and 1,9 Å, respectively, and revealed a V-set immunoglobulin-like (IgV-like) core comparable to that of HSV-1 gD. However, the alpha helices and loop regions differ from resolved gD structures of related alphaherpesviruses. Moreover, binding of the recombinant gDs to equine MHC-I was determined using surface plasmon resonance, and soluble gDs reduced plaque numbers and infection rates of EHV-1 and EHV-4 in equine cells. Molecular modeling yielded plausible binding hypotheses and key residues for the receptor-ligand interaction that were evaluated with molecular dynamics simulations and by using EHV-1 and EHV-4 viruses with mutated gDs. The point mutations in the gDs impaired the growth of the viruses and it can be concluded that the residues F213 and D261 play a role in virus entry into the host cell. Taken together, our results contribute to a better understanding of herpesvirus-cell interactions and could be used for the targeted design of antiviral drugs and vaccine development.

# Contents

**AcNPV** Autographa californica nuclear polyhedrosis virus
**BAC** bacterial artificial chromosome
**BEVS** baculovirus expression vector system
**$\beta$2m** $\beta$2-microglobulin
**CNS** central nervous system
**CPE** cytopathic effect
**cryo-EM** cryogenic electron microscopy
**DHB** 2,5-dihydroxybenzoic acid
**DMEM** Dulbecco's Modified Eagle's Medium
**DNA** deoxyribonucleic acid
**dssp** hydrogen bond estimation algorithm
**DTT** dithiothreitol
**CSPG** chandrotin sulfate proteoglycans
***E. coli*** *Escherichia coli*
**EBV** Epstein-Barr Virus
**ED** equine dermal
**EDTA** ethylendiamine tetraacetic acid
**EHM** Equine herpesvirus myeloencephalopathy
**EHV-1** Equine herpes virus type 1
**EHV-4** EHV-4
**ELA** Equine Leucocyte Antigen
**ELISA** enzyme-linked immunosorbent assay
**EC** endothelial cell
**ER** endoplasmic reticulum
**E** early
**FAK** focal adhesion molecule
**FBS** fetal bovine serum
**FHK** fetal horse kidney
**FR** functional region
**GAG** glycosaminoglycan
**gD** glycoprotein D
**gD1** EHV-1 gD
**gD4** EHV-4 gD
**GFP** green fluorescent protein
**gp64** major envelope glycoprotein
**GlcNAc** *N*-acetyl-D-glucosamine
**HEPES** 4-(2-hydroxyethyl)-1-piperazineethanesulfonic acid
**HLA** human leukocyte antigen
**HPLC** high-performance liquid chromatography
**HSPG** surface heparan sulfate proteoglycans
**HSV-1** Herpes Simplex Virus 1
**HSV-2** HSV-2
**HSV** Herpes Simplex Virus
**HVEM** herpesvirus entry mediator
**ICTV** International Committee on Taxonomy of Viruses
**IE** immediate-early
**Ig** immuneglobulin
**IMAC** immobilized metal ion affinity chromatography
**IMDM** Iscove's Modified Dulbecco's Medium

**$IP_3$** inositol 1,4,5-triphosphate
**IPTG** isopropyl-$\beta$-D-thiogalactopyranosid
**IR** inverted repeat
**KyA** Kentucky A
**L** late
**MALDI-TOF-MS** matrix-assisted laser desorption ionization-time of flight mass spectrometry
**MALS** multi-angle static light scattering
**MD** molecular dynamics
**MDV** Marek's disease Virus
**MEM** Minimal Essential Medium Eagle
**MES** 2-(N-morpholino)ethanesulfonic acid
**MHC-I** major histocompatibility complex class I
**mRNA** messenger RNA
**MOI** multiplicity of infection
**MS** mass spectrometry
**NEAA** non-essential amino acids
**Ni-NTA** nickel-NTA
**NTA** nitrilotriacetic acid
**ORF** open reading frame
**P/S** penicillin/streptomycin
**PBMC** Peripheral blood mononuclear cell
**PBS** phosphate buffered saline
**PCR** polymerase chain reaction
**PDB** protein data base
**PEI** polyethylenimine
**PEG** polyethylene glycol
**PFU** plaque forming units
**PISA** Proteins, Interfaces, Structures and Assemblies
**PLC** phospholipase C
**PPI** protein-protein interaction
**PrV** Pseudorabies Virus
**PS** phosphatidylserine
**PTM** post translational modification
**q-PCR** quantitative PCR
**RFLP** Restriction fragment length polymorphism
**rmsd** root-mean-square deviation
**ROCK1** serine/threonine Rho kinase
**RPMI** Roswell Park Memorial Institute Medium
**SA** sinapinic acid
**SD** standard deviation
**SDS** sodium dodecyl sulfate
**SDS-PAGE** sodium dodecyl sulfate-polyacrylamide gel electrophoresis
**SEC** size exclusion chromatography
**SSM** Secondary Structure Matching
**SPR** surface plasmon resonance
**TAE** tris-acetate-EDTA buffer
**TCR** T-cell receptor
**TEV** Tobacco Etch Virus

| | |
|---|---|
| **TM** | transmembrane region |
| **TR** | terminal repeat |
| **Tris** | tris(hydroxymethyl)aminomethan |
| **$U_L$** | unique long |
| **$U_S$** | unique short |
| **URT** | upper respiratory tract |
| **VZV** | Varicella Zoster Virus |
| **XDS** | X-ray detector software |
| **YFP** | yellow fluorescence protein |

# List of Figures



# List of Tables

# 1. Introduction

Herpesviruses are a diverse group of large deoxyribonucleic acid (DNA) viruses which comprise more than 200 species. They have been assigned to the order *Herpesvirales* on the basis of their genome sequences, similarity of encoded proteins, site of latency, and other biological properties by the International Committee on Taxonomy of Viruses (ICTV) (Davison et al., 2009). The order accommodates three families: The family *Herpesviridae* infecting mammals, birds and reptiles, the family *Alloherpesviridae* incorporating viruses infecting amphibians and fish and the family *Malacoherpesviridae* containing two gastropod viruses (Domingo et al., 2008). The family *Herpesviridae* has been classified into three subfamilies *Alphaherpesvirinae* , *Betaherpesvirinae*, *Gammaherpesvirinae*, and contains nine human herpesviruses (Arvin et al., 2007). Equine herpes virus type 1 (EHV-1) and EHV-4 (EHV-4) are members of the subfamily *Alphaherpesvirinae* and the genus *Varicellovirus* which they share with eighteen other species and are in line with four other viruses infecting equids: EHV-3 (Coital exanthema virus), EHV-6 (Asinine herpesvirus 1), EHV-8 (Asinine herpesvirus 3) and EHV-9 (Gazelle herpesvirus 1). The other three equine viruses are members of the *Gammaherpesvirinae*: EHV-2, EHV-5 and EHV-7 (Asinine herpesvirus 2) (Davison et al., 2009). EHV-1 and 4 are the most important equine pathogens that cause great suffering in horses and economic losses to the equine industry worldwide (Patel and Heldens, 2005).

## 1.1. Epidemiology and diagnostic tests for EHV-1 and EHV-4

EHV-1 and 4 are endemic in horse populations (Lunn et al., 2009) with periodic outbreaks around the world (Ferrera et al., 1950; Donald, 1998; Gilkerson et al., 1999; Van Maanen et al., 2000; Foote et al., 2003; Kydd et al., 2012; Aharonson-Raz et al., 2014; Azab et al., 2019). They can be detected throughout the year, however, the occurrence seams to peak during late winter, spring and early summer (Gilkerson et al., 1994; Wilson, 1997). The distinction between the two viruses was problematic for a long time due to the strong antigenic cross-reactivity (Patel and Heldens, 2005; Ma et al., 2013). In the 1990s a type-specific enzyme-linked immunosorbent assay (ELISA) was developed when variability in the extracellular C-terminal region of gG was found (Crabb et al., 1992; Crabb and Studdert, 1993). Today, standard diagnostic methods include virus isolation, alternatively quantitative PCR (q-PCR) (Pusterla et al., 2005), virus neutralization test and type specific ELISA (Lang et al., 2013).

## 1.2. Tropism

Most herpesviruses are specialized for one host, intriguingly some alphaherpesviruses display a broader host cell tropism (Spear, 1993). Interestingly, although EHV-1 and 4 are genetically very close related, EHV-1 can infect many mammalian species *in vivo*, whereas EHV-4 seems to be restricted only to equines and *in vitro* to equine epithelial cell lines (Osterrieder and Van de Walle, 2010). Experimentally rabbits, hamster and mice (Stokes et al., 1989; Baxi et al., 1996; Mori et al., 2012; Kanitz et al., 2015) have been infected with EHV-1 and natural infections have been documented in black bear, Thomson's gazelles, guinea pigs (Wohlsein et al., 2011), blackbuck, cattle (Chowdhury et al., 1988), alpacas, lamas, polar bears (Greenwood et al., 2012) and rhinoceros (Greenwood et al., 2012; Abdelgawad et al., 2014, 2015). *In vitro* EHV-1 enters and replicates in cell lines derived from equine, bovine, rabbit, hamster, mouse, monkey, pig, cat, and human (Studdert and Blackney, 1979; Ahn et al., 2010). Interestingly, it has been shown that an envelope protein needed for host cell receptor binding named glycoprotein D (gD) determines the host cell tropism. Exchanging the gDs between EHV-1 and 4 leads to an inversion of the

tropism (Whalley et al., 2007; Azab and Osterrieder, 2012). The exact regions and residues of gD responsible for the tropism have not been determined yet.

## 1.3. Clinical symptoms

EHV-1 and 4 are important pathogens that cause great suffering in *Equidae* and other mammals as well as big economic losses to the equine industry (Patel and Heldens, 2005). Both viruses cause respiratory disease often associated with secondary bacterial infections (Thomson et al., 1979). Clinical symptoms are more severe in EHV-1 infections including neurological signs termed Equine herpesvirus myeloencephalopathy (EHM), abortion often late in gestation, early neonatal death in foals and in some cases death of the infected horse. EHV-4 is mainly restricted to the upper respiratory tract (URT) and induces only occasionally abortions and EHM (Burrows and Goodridge, 1974; Edington et al., 1986; Ostlund, 1993; Tewari et al., 1994; Patel and Heldens, 2005). For EHV-1, neurotrophic isolates are known that cause vasculitis, thrombosis, and necrosis (Edington et al., 1986; Slater et al., 1994; Wilson, 1997). In these viruses a mutation in the DNA polymerase gene in the open reading frame (ORF) 30 is prevalent which seems to lead to a more efficient infection of the endometrium causing abortions and the central nervous system (CNS) leading to EHM (Nugent et al., 2006; Patel et al., 1982; Whitwell and Blunden, 1992). This variable region in ORF 30 can be exploited to differentiate between neuropathogenic (Ab4) and non-neuropathogenic (V592) EHV-1 isolates using polymerase chain reaction (PCR) (Allen, 2007; Leutenegger et al., 2008) although not all strains causing EHM harbor this mutation (Nugent et al., 2006; Perkins et al., 2008).
Clinical symptoms in non-definite hosts are more stroke-like and deviate with that from infections in horses (Ma et al., 2013). In theses cases the infection may progress into fatal encephalitis and present a problem especially in zoos where many species live together in a confined area. This is even more important if endangered and irreplaceable species are involved (Greenwood et al., 2012; Azab et al., 2018).

## 1.4. Virus particle morphology

Morphologically, herpesviruses share a common architecture which is distinct from all other viruses. The herpes virion has four characteristics. (1) The densely packed double-stranded, linear DNA genome with a size ranging from 125 to 290 kbp is contained within (2) an icosahedral capsid (diameter of 90 to 110 nm), which is embedded in (3) the tegument, an amorphous proteinaceous layer. (4) This complex is enveloped by a protein-lipid membrane termed envelope (Figure 1). Mature virions are approximately 200 nm in diameter (Domingo et al., 2008).

### 1.4.1. Genome architecture

EHV-1 and 4 are genetically very close with a homology of individual proteins ranging from 55 to 84% on the DNA level and 55 to 96% in the amino acid sequence. The linear double stranded DNA genome has a size of approximately 150 kbp. It is categorized as a type D genome and comprised of a unique long ($U_L$) and unique short ($U_S$) region. The $U_S$ segment is bracketed by the inverted repeat (IR) and terminal repeat (TR) sequence. Both viruses share their 76 genes, which can encode 77 proteins due to splicing. EHV-1 has four duplicated genes (64, 65, 66, 67), EHV-4 three (64-66) which results in 80 and 79 ORFs, respectively (Telford et al., 1992, 1998). Recently, it has been shown that the EHV-1 strains RacL11 and Kentucky A (KyA) are missing ORF 1 and ORF 2 (Shakya et al., 2017).

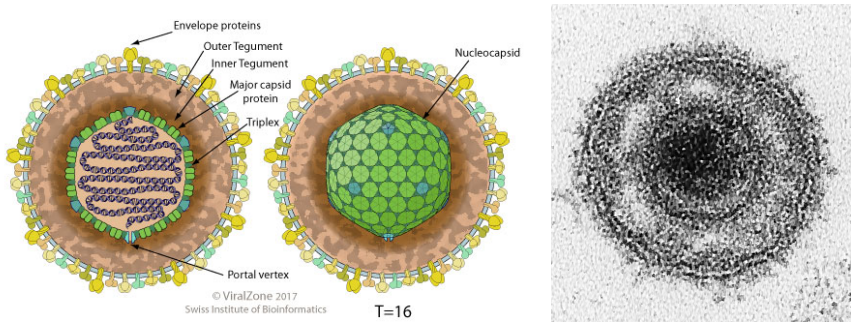


(a) (b)

Figure 1: (a) Schematic morphology of herpesvirus virion. The icosahedral capsid, containing the linear DNA genome, is surround by the tegument and enveloped with embedded glycoproteins (`viralzone.expasy.org`). (b) Electron microscopic picture of extracellular Virion of EHV-1 with a diameter of approximately 150 nm (Granzow et al., 2001).

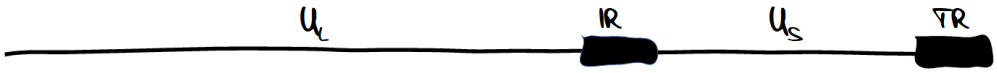


Figure 2: Schematic genome organization of EHV-1 and 4. $U_L$ = unique long, IR = inverted repeat, $U_S$ = unique short, TR = terminal repeat.

## 1.5. Transmission

Primary infection of the URT with EHV-1 and EHV-4 occurs when horses inhale virus-loaded aerosol droplets or have direct contact with infected horses, nasal discharge, fetal or placental tissue from abortions (Patel et al., 1982; Kydd et al., 1994). Fomites like contaminated food and equipment are also a source for transmission (Reed and Toribio, 2004; Harless and Pusterla, 2006). Recently it has been shown that EHV-1 can stay infectious in water bodies for up to three weeks under experimental conditions (Dayaram et al., 2017) although overall stability of virus particles is low in the environment (Reed and Toribio, 2004; Harless and Pusterla, 2006).

## 1.6. Primary infection

Once the virus particles have been inhaled or otherwise taken up, they come in contact with mucus and epithelium lining the nasal septum, the nasopharynx, the soft palate, and the trachea where EHV-1 and 4 primarily replicate. After an incubation time of 2 to 10 days (Allen, 1986) the destruction of infected cells leads to plaque formation in the tissue and causes clinical symptoms like fever, anorexia, depression, nasal discharge, swelling of the submandibular and retropharyngeal lymph nodes and sometimes conjunctivitis with ocular discharge (Patel et al., 1982; Allen, 1986).
Peripheral blood mononuclear cells (PBMCs), namely mononuclear cells ($CD172^+$) and T- and B-lymphocytes that patrol the respiratory epithelium and ganglia can be infected as well through either cell-to-cell spread or by newly synthesized virus particles budding from infected respiratory tissue. By hijacking leukocytes the virus can cross the otherwise confining basement membrane and reach the lymphatic system and blood vessels (Vandekerckhove et al., 2010; Gryspeerdt et al., 2010). This enables EHV-1 to spread to the secondary site of infection in endothelial

cells (ECs) of the endometrium in the pregnant uterus leading to abortion or arrive at the CNS causing EHM (Edington et al., 1991; Smith et al., 1992, 1993).
This is only rarely seen in EHV-4 (Burrows and Goodridge, 1974; Edington et al., 1986; Ostlund, 1993; Tewari et al., 1994; Patel and Heldens, 2005), potentially because EHV-4 infects PBMCs only inefficiently in contrast to EHV-1 (Van de Walle et al., 2008; Osterrieder and Van de Walle, 2010). Moreover, EHV-1 might have a better immune evasion strategy by interrupting chemokine signaling using gG (Van de Walle et al., 2009; Osterrieder and Van de Walle, 2010). However, Azab and Osterrieder (2012) showed that EHV-4 can infect PBMCs independent of integrins and as efficient as EHV-1. Further research will be needed to elucidate why EHV-1 frequently but EHV-4 only rarely lead to systemic infections.
EHV-1 might also disseminate cell free to the secondary site of replication through damaged respiratory tissue by entering the bloodstream (Bryans and Prickett, 1970). The virus transfer has also been observed by exploiting trans- and paracellular migrations of PBMCs through ECs (unpublished data). The exact mechanisms for viral spread between the different cells and tissues are still under investigation (Kamel et al., 2020).

## 1.7. Latency and secondary infection

As all herpesviruses, EHV-1 and 4 establish a lifelong latency from where they can reactivate. This is important for the survival and spread of the virus and it is a way to circumvent neutralizing antibodies and cytotoxic T lymphocytes (Slater et al., 1994). The site of latency is subject to discussion, however, both viruses are known to establish latency in trigeminal ganglia (Slater et al., 1994) and PBMCs (Welch et al., 1992; Pusterla et al., 2005), where the viruses lie dormant until reactivation.
The exact factors for reactivation remain elusive, however, stressful situations like weaning, castration, relocation and terminal illness were shown to induce spontaneous viral shedding (Burrows and Goodridge, 1974; Van Maanen et al., 2000). The reactivation can also proceed asymptomatic leading to so called "silent shedders" (Reed and Toribio, 2004).

## 1.8. Replication cycle

Although EHV-1 and 4 have a high genetic and antigenic similarity their pathogenesis differs greatly, apart from central steps, which are common among all alphaherpesviruses (Spear and Longnecker, 2003). EHV-1 has been studied to a greater extent than EHV-4, nevertheless, the mechanisms in many steps during the replication cycle of both viruses remain elusive (Azab and Osterrieder, 2017).

### 1.8.1. Entry into the host cell

One of the most essential steps for virus replication is the entry into a host cell. For EHV-1 and EHV-4, as for other herpesviruses, this is a complex multistep process involving five (gB, gC, gD, heterodimer gH/L) of twelve glycoproteins (gB, gC, gD, gE, gG, gH, gI, gK, gL, gM, gN, and gp2 (Osterrieder and Van de Walle, 2010).
The first attachment is generally a charged-based contact and relatively non–specific to concentrate virus particles at the cell surface (Spear and Longnecker, 2003). In alphaherpesviruses this is facilitated via a reversible interaction of gB and/or gC (Neubauer et al., 1997; Osterrieder, 1999; Azab et al., 2010) with surface heparan sulfate proteoglycans (HSPG) and chandrotin sulfate proteoglycans (CSPG) (Banfield et al., 1995; Spear and Longnecker, 2003; Neubauer et al., 1997). HSPGs are the most negatively charged biopolymers in nature and present on essentially

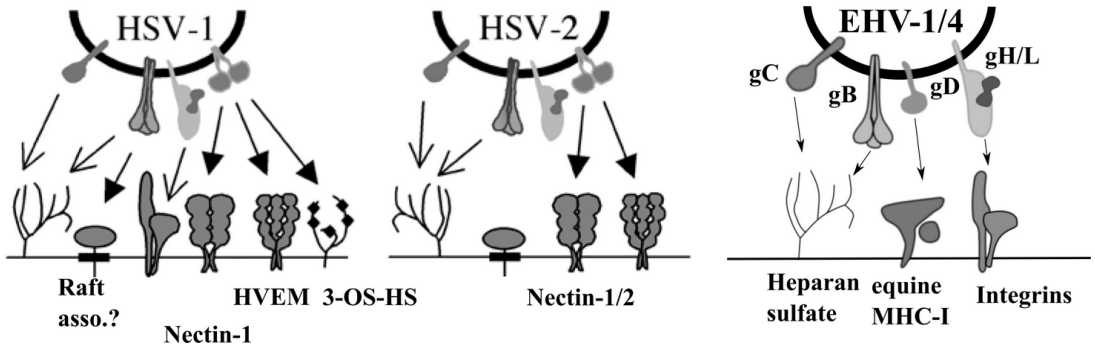


Figure 3: Receptor usage of HSV-1/2 (Krummenacher et al., 2013) and EHV-1/4.

all cell types (Sarrazin et al., 2011). To stabilize the binding (Csellner et al., 2000), gD interacts with its putative receptor which is, to date, equine major histocompatibility complex class I (MHC-I) for EHV-1 and EHV-4 (Kurtz et al., 2010; Sasaki et al., 2011a; Azab et al., 2014) (Figure 3). EHV-1 must be employing so far unknown receptors besides equine MHC-I, since it can enter and replicate in a wide range of cells that do not harbor this receptor (see section 1.2). Equine herpesvirus entry mediator (HVEM) has been shown to not allow entry of EHV-1 (Azab and Osterrieder, unpublished data).

**Glycoprotein D** The main receptor-binding protein is gD (Cole and Grose, 2003) and conserved among alphaherpesviruses (Campadelli-Fiume et al., 2007; Heldwein and Krummenacher, 2008; Krummenacher et al., 2013; Spear, 1993). Exceptions are Varicella Zoster Virus (VZV) which has no homolog (Davison and Scott, 1986), Marek's disease Virus (MDV) which does not express gD in cell culture (Tan et al., 2001) and Herpes B virus with gD-dependent and -independent entry pathways (Perelygina et al., 2015).
The first DNA sequence of EHV-1 gD was determined for the KyA strain (Flowers et al., 1991). Full length DNA sequences of EHV-1 and 4 were available from 1992 and 1998, respectively (Telford et al., 1992, 1998). The gD sequences are 76% homolog on the amino acid level. The gene is encoded within the $U_S$ region (Henry et al., 1981) in ORF 72 and is 1209 nucleotides long which translates into 402 amino acids from which 367 constitute an approximately 58-60 kDa native protein including N-linked oligosaccharides (Flowers and O'Callaghan, 1992; Love et al., 1993; Whittaker et al., 1992). The protein is comprised of a signal peptide (aa 1-35) for correct displacement in the host cell which is cleaved between aa 35 and 36 from the mature protein, a large N-terminal region where the suspected entry receptor binding site is located, a C-terminus, predicted to be mainly unstructured, followed by a transmembrane region (aa 349-370) composed of $\alpha$-helices and a cytoplasmic tail (aa 371-402), which is thought to trigger fusion during the entry process (Azab and Osterrieder, 2017).
The structure of gD is predicted to contain a V-like immuneglobulin (Ig) domain as the homologs in Herpes Simplex Virus (HSV) and Pseudorabies Virus (PrV) with three disulfide bonds and four predicted sites, where N-linked glycans are added to amide nitrogen.

In Herpes Simplex Virus 1 (HSV-1) and HSV-2 (HSV-2) gD can bind four receptors (Figure 3). The main receptor seems to be HVEM from the tumor necrosis factor receptor family (Montgomery et al., 1996; Warner et al., 1998). The interaction is exclusively N-terminal on the

side of gD. The residues 7-15, 24-32, and 35-37 are binding the HVEM residues 17-26, 30-39, and 74-76 and the key residue Y23 (Carfi et al., 2001; Connolly et al., 2002, 2003; Krummenacher et al., 2005; Lazear et al., 2008). The second and third receptor used by HSV to enter cells are nectin-1 and nectin-2, both from the poliovirus receptor family and structurally from the Ig-superfamily (Geraghty et al., 1998). Nectin-2 is only used by HSV-2 wild type virus (Lopez et al., 2000). The region facilitating binding overlap in some residues with HVEM binding ones. The gD residues 35-38, 199-201, 214-217, 219-221, and 223 interact with the nectin-1 residues Y38 and F129 (Di Giovine et al., 2011). In the unbound form of HSV gD, the N-terminal binding sites are covered by the flexible C-terminus which is displaced upon receptor binding. For binding of HVEM, this C-terminal movement allows the formation of an N-terminal hairpin loop that binds the receptor (Carfi et al., 2001; Connolly et al., 2002). The fourth receptor exploited for HSV-1 entry is a modified form of heparan sulfate, 3-O-sulfated heparan sulfate (Shukla et al., 1999).
PrV, Bovine herpesvirus type 1 and 5 and Herpes B virus are known to use nectin-1 as entry receptor as well. Additionally, PrV enters through nectin-2 and poliovirus receptor CD155 (Geraghty et al., 1998; Connolly et al., 2001; Gabev et al., 2010; Dummer et al., 2014).

**Equine major histocompatibility complex class I** MHC-I plays a crucial role in the adaptive immunity by presenting proteolytically processed intracellular proteins on the cell surface to T-cells and natural killer cells (Bjorkman and Parham, 1990). In case of an infected cell, virus derived peptides are presented and the recognition by T-cell receptor (TCR) initiates an immune response (Germain and Margulies, 1993). The structure of MHC-I molecules is composed of a heavy chain ($\alpha$-chain) with three helices ($\alpha$1-3), a transmembrane domain, and a cytoplasmic tail. The helices $\alpha$1 and $\alpha$2 form the peptide binding groove for T-cell presentation (Bjorkman and Parham, 1990). The heavy chain is stabilized by a protein termed $\beta$2-microglobulin ($\beta$2m) in the presence of a peptide in the binding groove (Yewdell and Bennink, 1992). The equine MHC-I has been designated Equine Leucocyte Antigen (ELA).
In comparison to humans, horses express a restricted set of MHC-I genes, however, with so far 30 classical and non-classical MHC-I loci and pseudogenes identified (Vaiman et al., 1986; Carpenter et al., 2001) (Figure 4). The ELA is located on chromosome 20 (Ansari et al., 1988; Makinen et al., 1989) and up to seven expressed loci have been detected in an MHC-I homozygous horse (Tallmadge et al., 2005).
MHC-I seems to be an unlikely receptor for viral entry since it is present on all somatic cells (David-Watine et al., 1990) and therefore restricts tissue specificity. Additionally, it is one of the most polymorphic proteins among mammalian proteins with 10 to 25% difference (Tallmadge et al., 2010; Gilcrease, 2007). Few other viruses are known to utilize MHC molecules. Coxsackievirus A9 co-receptor GRP78 has been shown to interact with MHC-I (Triantafilou et al., 2002), Simian virus 40 bind to but do not enter by using MHC-I (Atwood and Norkin, 1989; Norkin, 1999), the fiber knob of Adenovirus type 5 binds to the $\alpha$2 region of human leukocyte antigen (HLA) (Hong et al., 1997), and the functional gD homolog gp42 in Epstein-Barr Virus (EBV) binds to MHC-II to activate the membrane fusion (Mullen et al., 2002).
Not all MHC-I genes allow entry of EHV-1 and 4 (Kurtz et al., 2010; Sasaki et al., 2011b; Azab et al., 2014). Interestingly, the residue A173 in the $\alpha$2 region of MHC-I seems to be necessary but not sufficient for virus entry (Ellis et al., 1995; Sasaki et al., 2011b; Azab et al., 2014).

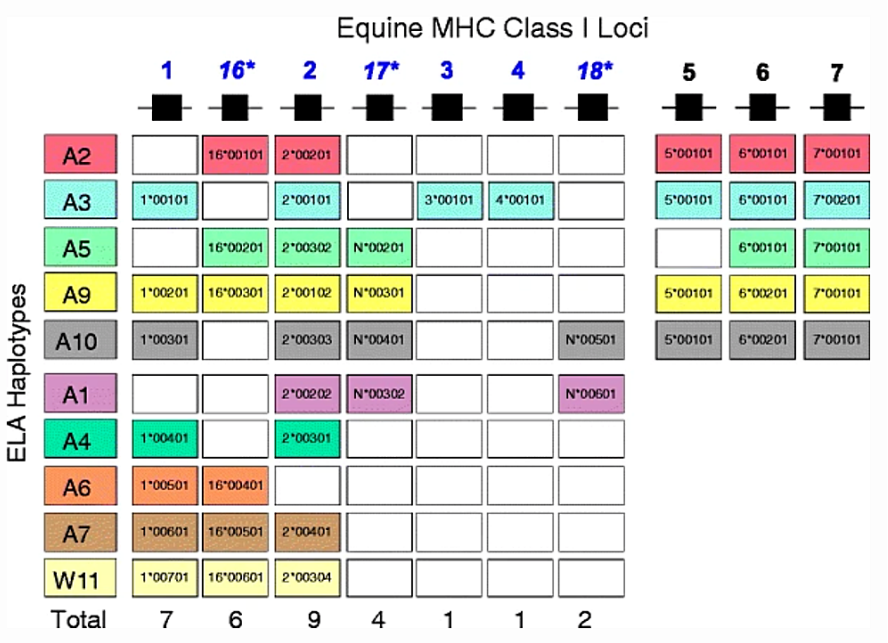


Figure 4: ELA haplotypes with genomic structure model of classical (blue numbering) and non-classical (black numbering) MHC-I loci. The upper half reperesents horeses homozygous for MHC-I and the lower half heterozygous horses (Tallmadge et al., 2010).

### 1.8.2. Signaling

After gD has bound the entry receptor, it triggers the entry process by activating the gH/gL complex. Glycoprotein H interacts with $\alpha_4\beta_1$- integrins via a serine-aspartate-isoleucine (SDI) motif which is not present in EHV-4 gH which has instead an alanine-aspartate-isoleucine (ADI) motif (Azab et al., 2012). The signal from gD and the integrin receptor leads to disintegration of the gH/gL heterodimer and gH is now in its activated form. The co-receptor binding of gH to integrins initiates a cellular signaling cascade resulting in $Ca^{2+}$ release from the endoplasmic reticulum (ER) based on phospholipase C (PLC)-inositol 1,4,5-triphosphate ($IP_3$) receptor and focal adhesion molecule (FAK) activation. This in term flips phosphatidylserine (PS) to the outside of the plasma membrane of the host cell (Azab et al., 2012). The role of PS in the entry process is not yet clear, however, the virus particles were found to co-localize with exposed PS (Heldwein et al., 2006; DuBois et al., 2013).

### 1.8.3. Fusion

The fusion process of the viral envelope with the plasma membrane is mainly facilitated by gB after activation by gH (Azab et al., 2015; Azab and Osterrieder, 2017). EHV-1 can enter cells by direct fusion with the plasma membrane induced by conformational changes of gB that forms a complex with the heterodimer gH/gL after binding of gD to MHC-I (Frampton et al., 2007; Van de Walle et al., 2008). For EHV-1, the non-classical caveolin-dependent endocytic pathway was observed in PBMCs in case the calcium release during EHV-1 infection is disrupted (Azab et al., 2015). This process can be pH-dependent or -independent (Frampton et al., 2007; Van de Walle et al., 2008; Hasebe et al., 2009; Azab et al., 2013). The endocytic pathway involves the

interaction of the gD arginine-serine-aspartatic acid (RSD) motif which is conserved between EHV-1 and 4 with $\alpha$ V integrins (Van de Walle et al., 2008) activating serine/threonine Rho kinase (ROCK1) and leads to productive infection of EHV-1 (Frampton et al., 2007; Frampton Jr et al., 2010). The route of entry for EHV-1 also differs between cell lines (Frampton et al., 2007; Van de Walle et al., 2008; Hasebe et al., 2009; Frampton Jr et al., 2010). No increase in $Ca^{2+}$ can be observed after EHV-4 gD (gD4) binds to the entry receptor and the virus is known to enter through caveolin/raft-dependent endocytosis (Azab et al., 2012).

### 1.8.4. Transport of nucleocapsid

Following fusion and the removal of the envelope, naked nucleocapsids and tegument proteins are released into the cytoplasm (Frampton Jr et al., 2010). The capsids travel along microtubules to the nucleus where viral DNA is injected through nuclear pores (Frampton Jr et al., 2010; Lyman and Enquist, 2009).

### 1.8.5. Replication

Transcription of viral DNA is a highly controlled process with three phases: immediate-early (IE), early (E), and late (L) gene expression (Caughman et al., 1985; Albrecht et al., 2005). First, the tegument proteins initiate the transcription of IE proteins and the degradation of cellular messenger RNA (mRNA) which is a preparation for the virus to take over the cell metabolism for replication (Taddeo and Roizman, 2006). Immediate early proteins regulate the translation of E proteins which are mostly required for DNA replication, coding among others for the DNA polymerase and thymidine kinase (Boehmer and Lehman, 1997). Late genes translate into structural proteins like capsid, tegument and glycoproteins (Boehmer and Nimonkar, 2003).

### 1.8.6. Budding

The capsids assemble in the nucleus around the newly synthesized viral DNA together with tegument proteins and bud from the inner leaflet of the nuclear membrane (Nii, 1992; Roizman, 1996). This primary envelope is lost when the particles leave the perinuclear space by fusion (Granzow et al., 1997). The secondary and final envelope is acquired from the *trans*-Golgi complex and the mature virus particles are budding from the cell by exocytosis (Granzow et al., 2001) (see Fig 1b).

## 1.9. Vaccines

For about 60 years, efforts have been made to find efficient vaccines against EHV-1 (Kydd et al., 2006). However, the protection is usually limited in time and efficacy and with that does not prevent infection, resulting in frequent outbreaks (Allen, 1986; Burrows and Goodridge, 1974; Goehring et al., 2010; Goodman et al., 2012). Different types of vaccines have been studied with good potential for protection. Modified live or inactivated whole virus (Mayr et al., 1968; Hübert et al., 1996; Gilkerson et al., 1997; Schnabel et al., 2019), recombinant glycoproteins (Awan et al., 1990; Tewari et al., 1994; Osterrieder et al., 1995; Stokes et al., 1997; Packiarajah et al., 1998; Zhang et al., 1998) and injected DNA of gD (Ruitenberg et al., 1999a,b) were partially protective in mouse models and in the horse. The vaccines Rhinomune® (Boehinger Ingelheim) and Prevaccinol® (MSD Tiergesunheit) are currently in use in the United States and in Europe, respectively, containing the EHV-1 vaccine strain RacH. This altered attenuated strain is lacking several genes, including ORF1, 2, and 67 (Hübert et al., 1996).

The humoral immune response, especially the mucosal, has been thought to play a main role in infection control by preventing the entrance of the virus into the respiratory epithelium (Wilkie, 1982; Israel et al., 1992; Brandtzaeg et al., 1997). Nevertheless, the main aim is to activate cell-mediated immune resoponses which last longer and should prevent systemic distribution of the virus thus prohibiting viremia, EHM and abortion (Allen et al., 1995; Schnabel et al., 2019). In alphaherpesviruses, gD often induces proliferation of virus-specific T-cells (Krishna et al., 1989; Blacklaws et al., 1990), however, T-cell responses against EHV-1 are short lived probably due to immune evasion strategies.

### 1.10. Project introduction

The entry of viruses into the host cell is a crucial step during virus replication. Recently the entry receptor equine MHC-I has been identified for the clinically and economically important alphaherpesviruses EHV-1 and 4. However, it is not known how the viral envelope protein gD interacts with this receptor. The knowledge of the residues facilitating binding would allow to manipulate and even inhibit entry of the viruses into host cells, possibly leading to an efficient vaccine. The aim of this work is to elucidate the interaction of EHV-1 and 4 gD with equine MHC-I by using recombinant, soluble proteins for crystallography, biochemical characterization and cell culture based assays.

The aims of this study are:

1. Production of soluble gD1, gD4, and MHC-I in insect cells and *Escherichia coli*
2. Structure solving of soluble, recombinant proteins
3. Testing the gD-MHC-I interaction with soluble, recombinant proteins
4. Determination of interacting residues of the receptor-ligand complex
5. Testing the proposed interacting residues with virus mutants

## 2. Materials and Methods

### 2.1. Materials

#### 2.1.1. Chemicals

| **Name** | **Feature/Cat.No.** | **Company** |
|---|---|---|
| Acrylamid | 3029-1 | Carl-Roth, Karlsruhe |
| Acetic acid (CH3COOH) | A3686, 2500 | Applichem, Darmstadt |
| Acetone ((CH3)2CO) | A160, 2500 | Applichem, Darmstadt |
| Agar (agar bacteriological) | 2266.2 | Applichem, Darmstadt |
| Arabinose L (+) | A11921 | Carl-Roth, Karlsruhe |
| $\beta$-mercaptoethanol | 28625 | Serva, Heidelberg |
| Bluo-Gal | | Invitrogen, Germany |
| Calcium chloride (CaCl2) | T885,2 | Carl-Roth, Karlsruhe |
| Casyton (buffer for Casy TT counter) | | Roche, Germany |

| **Name** | **Feature/Cat.No.** | **Company** |
|---|---|---|
| Coomassie brilliant blue G-250 | | Serva, Germany |
| Dimethyl sulfoxide (DMSO) | A3672,0250 | Applichem, Darmstadt |
| dNTP Mix (10mM total) | BIO-39053 | Bioline, Luckenwalde |
| 0.1 % Diethylpyrocarbonat (DEPC) water | 750023 | Thermo Fisher Scientific Inc |
| 1,4-Dithiothreitol (DTT) | | Roth, Germany |
| Ethidium bromide 1% | 2218.2 | Carl-Roth, Karlsruhe |
| Ethanol den. absolute | A1613 | Applichem, Darmstadt |
| Ethylene glycol | | Serva, Germany |
| Ethylendiaminetetraacetic acid (EDTA) | A2937,1000 | Applichem, Darmstadt |
| FACS rinse | 340346 | BD, San Jose |
| FACS clean | 340345 | BD, San Jose |
| FACS sheath fluid | B51503 | Beckman Coulter, Krefeld |
| FACS FlowClean | A64669 | Beckman Coulter, Krefeld |
| G-10 beads | GE 17-0010-01 | GE Healthcare, Piscataway, NJ |
| FBS (fetal bovine serum) | P30-1506 | PAN-Biotech GmbH |
| Formamide | A2156,1000 | Applichem, Darmstadt |
| Gentamycin Sulfate | 17-518Z | Biowitthaker, France |
| Gibco® trypsin | 27250-018 | Thermo Fisher Scientific Inc |
| Glycerol | A2926,2500 | Applichem, Darmstadt |
| 37% hydrochloric acid (HCl) | 4625.2 | Carl-Roth, Karlsruhe |
| 4-(2-hydroxyethyl)-1-piperazineethanesulfonic acid (HEPES) | | Roth, Germany |
| Hygromycin B | 380-306-G001 | Enzo Life Sciences |
| Isopropyl alcohol (2-propanol) | 20842.330 | VWR International, West Chester |
| IgepalR CA-630 (NP-40) | | Sigma-Aldrich, Germany |
| Imidazole | | Merck, Germany |
| Isopropyl-$\beta$-D-1-thiogalactopyranoside (IPTG) | | Roth, Germany |
| Magnesium chloride hexahydrate ($MgCl_2$) | 5833.025 | Merck, Darmstadt |
| 2-(N-morpholino)ethanesulfonic acid (MES) | | |
| Methanol | 20847.422 | VWR International, West Chester |
| Methyl cellulose | M0262 | Sigma-Aldrich, St. Louis |
| Non-fat milk powder | 68514-61-4 | Carl-Roth, Karlsruhe |
| sodium chloride (NaCl) | A3597,5000 | Applichem, Darmstadt |
| sodium hydroxide (NaOH) | 1.06462 | Merck, Darmstadt |
| Optimem | 31985062 | Life Tech., Carlsbad |
| Phenol/Chloroform | A0889,0500 | Applichem, Darmstadt |
| Phytohemagluttinin-L | 11249738001 | Roche, Mannheim |
| Polyethyleneimine (PEI) | P3143 | Sigma-Aldrich, St Louis |

| Name | Feature/Cat.No. | Company |
|---|---|---|
| Polyethylene glycol 200-8000 | | Sigma-Aldrich, Germany |
| sodium dodecyl sulfate (SDS) | A7249.,000 | Applichem, Darmstadt |
| SYPRO Orange Protein Stain | | Invitrogen, USA |
| Sodium acetate (NaAc) | A4279,0100 | Applichem, Darmstadt |
| Sodium azide (NaAz) | UN1687 | Applichem, Darmstadt |
| tetramethylethylendiamin (Temed) | 2367.3 | Roth, Karlsruhe |
| Tris(hydroxymethyl) aminomethane (Tris) | 443864E | VWR International, West Chester |
| Triton X-100 detergent | 8603 | Merck, Darmstadt |
| Tween-20 | 0777-1L | VWR International, West Chester |
| Universal-Agarose, peqGOLD | 35-1020 | VWR International, West Chester |
| Urea | | Merck, Germany |
| X-tremeGene 9 Transfection Reagent | | Roche, Germany |

### 2.1.2. Consumables

| Name | Feature/Cat.No. | Company |
|---|---|---|
| Acupuncture needle | | Moxom Medical, Germany |
| Concentrators (Amicon Ultra) | | Millipore, USA |
| Cover slides | glass, 22 mm | Hampton Research, USA |
| Crystallization plates MRC | 96 well, sitting drop | Molecular Dimensions, UK |
| Dialysis membranes | | Spectra/Por, USA |
| Electroporation cuvettes | | Bio-Rad, Germany |
| Cell culture dishes | 6-well, 96-well | Sartsedt, Nümbrecht |
| Parafilm®M | | Bemis, Neenah |
| Whatmann blotting paper | 0,35 mm | Carl-Roth, Karlsruhe |
| ECOJECT®Syringes | 10 ml | Dispomed, Germany |
| Kimtech Science, Precision Wipes | 05511 | Kimberly-Clark, Roswell |
| Roti®-NC Transfermembrane 0,2 µm | 9302.1 | Roth, Karlsruhe |
| PCR tubes | 0.2 ml | Applied biosystems, Berlin |
| PVDF 0.45 | T830.1 | Roth, Karlsruhe |
| Pipettes | 5, 10, 25 ml | Sarstedt, Nümbrecht |
| Petri dishes for cell culture | 100 mm | Sarstedt, Nümbrecht |
| Petri dishes for bacteria | | Sarstedt, Nümbrecht |
| Cell culture flasks | 25 and 75 ml | Sartsedt, Nümbrecht |
| Conical test tubes 17x120 | 15 ml | Sartsedt, Nümbrecht |
| Conical test tubes 30x115 | 50 ml | Sartsedt, Nümbrecht |
| Cryotubes | 1,8 ml | Sartsedt, Nümbrecht |
| Eppendorf tubes | 1.5 and 2 ml | Sartsedt, Nümbrecht |
| Greiner 96-Well U-shape | 650201 | Greiner Bio-One |

| Name | Feature/Cat.No. | Company |
|---|---|---|
| Nitrile gloves | | Hansa-Medical 24, Hamburg |
| Microscope cover glasses | ECN631-1569 | VWR International, West Chester |
| Sterile syringe filters PVDF | 0,2 and 0,45 µm | VWR International, West Chester |
| Pipettes | 5, 10, 25 ml | Sarstedt, Nümbrecht |
| Pipettes tips for Pipetman | P1000, 200, 100 and 10 | VWR International, West Chester |
| SPR sensor chip | HC 200M | XanTec Bioanalytics GmbH |
| U-bottom 96-well plates | 92697 | TPP, Trasadingen |

### 2.1.3. Equipment

| Name | Feature/Cat.No. | Company |
|---|---|---|
| Äkta Explorer, Purifier, Prime, Micro | | GE Healthcare, Little Chalfont Germany |
| Allegra X-15R | | Beckman Coulter, Germany |
| Bacterial incubator | 07-26860 | Binder, Turtlingen |
| Bacterial incubator | shaker Innova 44 | New Brunswick Scientific, New Jersey |
| Beamline 14.3 | | HZB, Berlin, Germany |
| Beamline P14, Petra III | | DESY, Hamburg, Germany |
| Bunsen burner | Type 1020 | Usbeck, Radevormwald |
| CASY TT Counter | | Innovatis, Germany |
| Cartesian crystallization robot | 8 channels | Digilab, USA |
| Cell incubators | Excella ECO-1 | New Brunswick Scientific |
| Cell incubators | Excella ECO-1 | New Brunswick Scientific, New Jersey |
| Centrifuge 5424 | Rotor FA-45-24-11 | Eppendorf, Hamburg |
| Centrifuge 5804R | Rotors A-4-44 and F45-30-11 | Eppendorf, Hamburg |
| Centrifuge Function Line400R | | Heareus, Hanau |
| Chemismart imaging system | 5100 | Peqlab, Erlangen |
| Electrophoresis power supply Power Source 250 V | | VWR International, West Chester |
| FACSCalibur | flow cytometer | BD, San Jose |
| Freezer -20 °C | | Liebherr, Bulle |
| Freezer -80 °C | | GFL, Burgwedel |
| Galaxy mini centrifuge | | VWR International, West Chester |
| Gel electrophoresis chamber | SUB-Cell GT | Bio-Rad, München |
| Gel electrophoresis chamber Mini Electrophorese System | | VWR International, West Chester |
| Ice machine | AF100 | Scotsman, Vernon Hills |
| INTEGRA Pipetboy | | IBS Integrated Biosciences, Fernwald |
| Magnetic stirrer RH basic KT/C | | IKA, Staufen |
| Mosquito® Crystallization robot | | ttlabtech |
| Mounted CryoLoop | | Hampton Research, USA |
| Newbauer counting chamber | | Assistant, Sondheim/Rhön |
| Nitrogen tank | ARPEGE70 | Air liquide, Düsseldorf |
| Orbital shaker | 0S-10 | PeqLab, Erlangen |
| pH-meter | RHBKT/C WTW pH level 1 | Inolab, Weilheim |
| Photospectrometer | Nanodrop 1000 | Peqlab, Erlangen |

| Name | Feature/Cat.No. | Company |
|---|---|---|
| Pipetman | P1000, P100, P10 | VWR International, West Chester |
| SPR GE Biacore J Biomolecular Interaction Analyser instrument | | Uppsala, Sweden |
| Sterile laminar flow chambers | | Bleymehl, Inden |
| Thermocycler | Professional Trio | Analytik Jena, Jena |
| Thermocycler | T-Gradient | Biometra, Göttingen |
| Thermocycler Flexcycler | ThermoFlex | Analytik Jena, Jena |
| Thermomixer | comfort | Eppendorf, Hamburg |
| Ultracentrifuge | L7-65 | Beckman, Krefeld |
| Ultraflex-II TOF/TOF instrument | 200 Hz solid-state Smart beam™ laser | Bruker Daltonics, Bremen, Germany |
| UV Transiluminator | Bio-Vision-3026 | PeqLab, Erlangen |
| Vortex | Genie 2™ | Bender&Hobein AG, Zurich |
| Water bath shaker | C76 | New Brunswick Scientific, New Jersey |
| Water baths | TW2 and TW12 | Julabo, Seelbach |

## Microscopes

| Type | Name | Company |
|---|---|---|
| Fluorescence microscope | AxioVert S 100 | Carl Zeiss MicroImaging GmbH, Jena |
| Fluorescence microscope | AxioVert.A1 | Carl Zeiss MicroImaging GmbH, Jena |
| Microscope AE20 | AE20 | Motic, Wetzlar |
| Microscope AE31 | AE31 | Motic, Wetzlar |

## Software

| | | |
|---|---|---|
| Chemi-Capt | | Vilber-Lourmat, Eberhardzell |
| Collaborative Computational Project Number 4 (CCP4i) program suite | | Potterton et al. (2002) |
| Coot | | Emsley et al. (2010) |
| Corel Draw | | Corel Corporation, USA |
| CytoFLEX CytExpert Software | 1.2.11.0 | Beckman Coulter Life Sciences, Krefeld |
| Fiji-Image J | 1.41 | NIH, Bethesda |
| Graphpad Prism 5 | 5 | Graphpad Software inc, La Jolla |
| iMosflm | 1.0.7. | Battye et al. (2011) |
| Inkscape | 0.92.4 | Software Freedom Conservancy, Brooklyn |
| ND-1000 | 3.0.7 | PeqLab, Erlangen |
| software for Zeiss microscopes | Axiovision 4.8 | Carl Zeiss MicroImaging GmbH, Jena |
| SnapGene® Viewer | 4.3.11 | GSL Biotech LLC |
| FlexAnalysis | 2.4. | Bruker Daltonics, Bremen, Germany |
| Phaser | | McCoy et al. (2007) |
| Phenix suite | | Adams et al. (2010) |
| Pymol Schrödinger | | LLC, USA |
| Vector NTI | 9 | Invitrogen Life Technologies, Grand Island |
| Vision-Capt | | Vilber-Lourmat, Eberhardzel |
| XDS | | Kabsch (2010) |

### 2.1.4. Enzymes and markers

| Name | Cat.No. | Company |
|---|---|---|
| BamHI | R0136 | New England Biolabs, Ipswich |
| DpnI | ER1701 | New England Biolabs, Ipswich |
| RNase A | 7528.2 | Carl-Roth, Karlsruhe |
| Phusion Hot Start High-Fidelity DNA Polymerase | M0530S | Finnzymes, Thermo Scientific, Rochester |
| Proteinase K | 7528.2 | Finnzymes, Thermo Scientific, Rochester |
| PstI | R0140S | New England Biolabs, Ipswich |
| EcoRI | R0101 | New England Biolabs, Ipswich |
| EcoRI HF | R3101 | New England Biolabs, Ipswich |
| EcoRV | R0195 | New England Biolabs, Ipswich |
| HindIII | R0104 | New England Biolabs, Ipswich |
| NheI | R0131M | New England Biolabs, Ipswich |
| NotI-HF | R3189M | New England Biolabs, Ipswich |
| TEV Protease | | Home-made, recombinant |
| XbaI | R0145S | New England Biolabs, Ipswich |
| XmaI | R0180S | New England Biolabs, Ipswich |
| Quick ligase | M2200S | New England Biolabs, Ipswich |
| T4 ligase | M02025 | New England Biolabs, Ipswich |
| Taq DNA-Polymerase | 01-1020 | PeqLab, Erlangen |
| PageRuler TM Prestained Protein Ladder | 26616 | Thermo Scientific, Darmstadt |
| Precision Plus Protein All Blue Prestained Protein Standards | 1610373 | BioRad |
| GeneRuler 1 kb Plus DNA Ladder | SM1331 | Thermo Scientific, Darmstadt |

### 2.1.5. Oligonucleotides

| Name | Sequence |
|---|---|
| VK1 pACEBac1 fwd P1 | acggtcctaaggtagcgagt |
| VK2 pACEBac1 rev P2 | gatggtgggacggtatgaat |
| VK3 pACEBac1 rev P3 | cgttctgcccaagtttgagc |
| VK4 pACEBac1 rev P4 | ggaagagcgacccaagtcaa |
| VK5 pACEBac1 rev P5 | acgctcagtggaacgaaaac |
| VK6 Ph+gp64SP fwd | attataatcgattcgcgacctactcc |
| VK7 Ph+gp64SP rev | tatatagaattccgcaaaggcagaat |
| VK8 gD1 NcoI bacteria fwd | atattaccatggagaaagccaagcgtgcg |
| VK9 gD1/4 XhoI bacteria rev | tatatactcgaggccctggaagtacaggttc |
| VK10 gD4 NcoI bacteria fwd | atatatccatggaaaattacaggcgtgtggttcg |
| VK11 alpha1-3 insect fwd | atatatgaattcggctcccactccat |
| VK12 alpha1-3 stop ScaI insect rev | tatataagtactttagtggtggtggtggtggt |
| VK13 b2m main EcoRI insect fwd | tatatagaattcgtcccgcgtgttccgaa |
| VK14 b2m main His stop ScaI insect rev | tatataagtactttagtggtggtggtggtggaggtctcgatcccact |
| VK15 alpha1-3 NcoI bacteria fwd | tatataccatgggctcccactccatgagatat |
| VK16 b2m main NcoI bacteria fwd | tatataccatggtcccgcgtgttccgaa |

| | |
|---|---|
| VK17 b2m main TEV XhoI bacteria rev | atatatctcgaggccctggaagtacaggttctcttagaggtctcgatcccact |
| VK20 pETM13 fwd P1 | ttccacagcaatggcatcct |
| VK21 pETM13 fwd P2 | ggggaaaaatgcggttccac |
| VK22 pETM13 fwd P3 | ttcccttcctttctcgccac |
| VK23 pETM13 fwd P4 | taatcgcggcctagagcaag |
| VK24 pETM13 fwd P5 | taccgcctttgagtgagctg |
| VK25 pETM13 fwd P6 | tcatttgatgctcgatgagtttt |
| VK26 pETM13 fwd P7 | tcggtgattcattctgctaacca |
| VK27 gD1 NcoI bac fwd | atattaccatggaaaaggctaagcgtgct |
| VK28 gD1 XhoI bac rev | tatatactcgaggccttggaagtacaggt |
| VK29 gD4 NcoI bac fwd | atatatccatggaaaactaccgtcgtgttgtt |
| VK30 gD4 XhoI bac rev | tatatactcgagtccctggaagtacaggtt |
| VK31 alpha1-3 NcoI bac fwd | tatataccatgggtagccactcaatgaggtac |
| VK32 alpha1-3 XhoI bac rev | tatatactcgagtccttggaagtacaagttttcc |
| VK33 b2m NcoI bac fwd | tatataccatgggttcctagagttcctaaggttca |
| VK34 b2m TEV XhoI bac rev | atatatctcgaggccctggaagtacaggttctccaggtcacggtcccacttaa |
| VK35 alpha1-3 insect fwd | atatatgaattcggtagccactcaatg |
| VK36 alpha1-3 stop ScaI insect rev | tatataagtactttagtggtggtggtgatggtg |
| VK37 b2m EcoRI insect fwd | tatatagaattcgttcctagagttcctaaggttcag |
| VK38 b2m His stop ScaI insect rev | tatataagtactttagtggtggtggtggtggtgcaggtcacggtcccactta |
| VK42 SV40 rev | aagatacattgatgagtttggacaaacc |
| VK43 T7terminator rev | tcaagacccgtttagaggc |
| VK44 T7promotor fwd | taatacgactcactataggggaat |
| VK46 EcoRI gD1 aa 36 fwd | tatatatgaattcgctgtgcgtggtcgtca |
| VK47 gD1 aa 280 rev | tatatattctagattagtggtggtggtgatggtggccttggaagtacaggttttc tgggactggtctagcgaaagc |
| VK48 EcoRI gD1 aa 45 fwd | tatatatgaattcaaggagttccctcctccacg |
| VK49 gD1 aa 276 rev | tatatattctagattagtggtggtggtgatggtggccttggaagtacaggttttc agcgaaagcttgagcttcgtag |
| VK50 EcoRI gD4 aa 36 fwd | tatatatgaattcgttgttcgtggtaaccagaaccag |
| VK51 gD4 aa 280 rev | tatatattctagattagtggtggtggtgatggtggccttggaagtacaggttttc aggaacaggacgagcgaag |
| VK52 EcoRI gD4 aa 45 fwd | tatatatgaattccctgagttcccaccacctagat |
| VK53 gD4 aa 276 rev | tatatattctagattagtggtggtggtgatggtggccttggaagtacaggttttc agcgaaggcctgggc |
| VK54 gD1 aa 280 rev ScaI | tatatatagtactttagtggtggtggtgatggtggccttggaagtacaggttttc tgggactggtctagcgaaagc |
| VK55 gD1 aa 276 rev ScaI | tatatatagtactttagtggtggtggtgatggtggccttggaagtacaggttttc agcgaaagcttgagcttcgtag |
| VK56 gD4 aa 280 rev ScaI | tatatatagtactttagtggtggtggtgatggtggccttggaagtacaggttttc aggaacaggacgagcgaag |
| VK57 gD4 aa 276 rev ScaI | tatatatagtactttagtggtggtggtgatggtggccttggaagtacaggttttc agcgaaggcctgggc |
| VK58 b2m mutagenesis fwd | ttaagaaggagatataccatggttcctagagttcc |
| VK59 b2m mutagenesis rev | tattaggaactctaggaaccatggtatatctccttct |
| VK60 b2m VK33 G deletion fwd | tatataccatggttcctagagttcctaaggt |
| VK61 gD1 D261N fwd | aggagagcatatgacatggttgaagttctggttcgtctacaatggtggaaaccta ccagtgcaaggatgacgacgataagtag |

| | |
|---|---|
| VK62 gD1 D261N rev | atgcctgggcttcataaaactgcactggtaggtttccaccattgtagacgaacca gaacttcacaaccaattaaccaattctg |
| VK63 gD1 F213A fwd | cttttctgtaactattcccagtgaacggtgtccgattgccgctgagcaaaacttt ggcaatccaggatgacgacgataagtag |
| VK64 gD1 F213A rev | ctggagttttacaccgatccggattgccaaagttttgctcagcggcaatcggaca ccgttcaccaaccaattaaccaattctg |
| VK65 gD4 D261N fwd | aggtgtacatttagcatgggtaaaacactggtttgtgcaaaatggtggaaaccttt ccagtacaaggatgacgacgataagtag |
| VK66 gD4 D261N rev | acgcctgggcttcgtaaaactgtactggaaggtttccaccattttgcacaaacca gtgttttacaaccaattaaccaattctg |
| VK67 gD4 F213A fwd | cttttccgtaacaattccgagcagccattgtccgctttctgctgagcagaacttt ggtaatccaggatgacgacgataagtag |
| VK68 gD4 F213A rev | caggagttttacagcgatcaggattaccaaagttctgctcagcagaaagcggaca atggctgccaaccaattaaccaattctg |
| VK69 gD1 rever261 fwd | aggagagcatatgacatggttgaagttctggttcgtctacgatggtggaaaccta ccagtgcaaggatgacgacgataagtag |
| VK70 gD1 rever261 rev | atgcctgggcttcataaaactgcactggtaggtttccaccatcgtagacgaacca gaacttcacaaccaattaaccaattctg |
| VK71 gD1 rever213 fwd | cttttctgtaactattcccagtgaacggtgtccgattgcctttgagcaaaacttt ggcaatccaggatgacgacgataagtag |
| VK72 gD1 revr213 rev | ctggagttttacaccgatccggattgccaaagttttgctcaaaggcaatcggaca ccgttcaccaaccaattaaccaattctg |
| VK73 gD4 revert261 fwd | aggtgtacatttagcatgggtaaaacactggtttgtgcaagatggtggaaaccttt ccagtacaaggatgacgacgataagtag |
| VK74 gD4 revert261 rev | acgcctgggcttcgtaaaactgtactggaaggtttccaccatcttgcacaaacca gtgttttacaaccaattaaccaattctg |
| VK75 gD4 revert213 fwd | cttttccgtaacaattccgagcagccattgtccgctttcttttgagcagaacttt ggtaatccaggatgacgacgataagtag |
| VK76 gD4 revert213 rev | caggagttttacagcgatcaggattaccaaagttctgctcaaaagaaagcggaca atggctgccaaccaattaaccaattctg |
| WA1 gD fwd | gctgcttgtactgtatgtta |
| WA2 gD rev | acatgctcatatgttctccg |

### 2.1.6. Antibodies

| **Name** | **Dilution** | **Company** |
|---|---|---|
| polyclonal anti-gD1 19-mer | 1:200 | Dennis O'Callaghan, Louisiana State University Health Sciences Center, Shreveport, LA |
| polyclonal anti-gD4 antibodies | 1:200 | Ken Maeda, Yamaguchi University, Japan |
| Goat anti-mouse HRP | 1:10.000 | Sigma-Aldrich, St Louis |
| Goat anti-rabbit HRP | 1:10.000 | Cell Signaling, Boston |
| monoclonal anti-equine MHC-I CZ3 | 1:100 | Donaldson et al. (1988) |
| Rabbit anti-6×His | 1:1.000 | Sigma-Aldrich, St Louis |

### 2.1.7. Cells

| **Name** | **Feature** | **Reference** | **Culture media** | **Supplements** | °C |
|---|---|---|---|---|---|
| 293T | Human epithelial kidney cell line, SV-40 T-antigen | ATCC CRL-11268 | DMEM | 10% FBS, 1% P/S | 37 |
| HeLa | Human epithelial cervix cell line, adenocarcinoma | ACTT CCL-2 | DMEM | 10% FBS, 1% P/S | 37 |
| B78H1 | murine melanoma cell line | | DMEM | 10% FBS, 1% P/S | 37 |
| B9C8 | murine melanoma cell line, stable transfection with MHC-I gene | | DMEM | 10% FBS, 1% P/S | 37 |
| P815 | murine mastocytoma cell line | | DMEM | 10% FBS, 1% P/S | 37 |
| P815 3.1 | murine mastocytoma cell line DBA/2 strain, stable transfection with MHC-I gene 3.1 | ATCC TIB-64 | DMEM | 10% FBS, 1% P/S | 37 |
| ED cells | equine dermal cell line | CCLV-RIE 1222, Federal Research Institute for animal health, Greifswald | IMDM | 20% FBS, 1% P/S, 1% NEA, 1% sodium pyruvate | 37 |
| Vero | African green monkey kidney | ATCC CCL-81 | DMEM | 10% FBS, 1% P/S | 37 |
| MDCK II | ATCC CCL-34 | Madin-Darby canine kidney | DMEM | 10% FBS, 1% P/S | 37 |
| RK13 | rabbit kidney cell line | ATCC CCL-37 | DMEM | 10% FBS, 1% P/S | |
| Sf9 cells | clonal isolate derived from parental *Spodoptera frugiperda* (Fall Armyworm) cell line IPLB-Sf21-AE. Originated at the USDA insect Pathology Laboratory (Vaughn et al., 1977) | Invitrogen, Germany | Gibco® Sf-900 III SFM | | 27 |
| High Five ™ cells | BTI-TN-5B1-4, developed by Boyce Thompson Institute for Plant Research, Ithaca, NY and originated from a clonal isolate derived from the ovarian cells of the cappage looper, *Trichopulsia ni* (Wickham et al., 1992) | Invitrogen, Germany | Express Five Medium SFM | | 27 |

### 2.1.8. Viruses

| | | |
|---|---|---|
| EHV-1 strain RacL11 | BAC derived with GFP in Mini-F, $\delta$ORF1/2, $\delta$gp2, $\delta$IR6, GFP+ | (Rudolph et al., 2002) |
| EHV-1 strain RacL11 $gD_{D261N}$ | BAC derived with GFP in Mini-F | |
| EHV-1 strain RacL11 $gD_{F213A}$ | BAC derived with GFP in Mini-F | |
| EHV-4 | BAC derived with GFP in Mini-F | |
| EHV-4 $gD_{D261N}$ | BAC derived with GFP in Mini-F | |
| EHV-4 $gD_{F213A}$ | BAC derived with GFP in Mini-F | |

### 2.1.9. Bacteria

| | | |
|---|---|---|
| TOP10 | F - mcrA $\Delta$(mrr-hsdRMS-mcrBC) $\phi$80lacZ$\Delta$M15 $\Delta$lacX74 nupG recA1 araD139 $\Delta$(ara-leu)7697 galE15 galK16 rpsL(StrR ) endA1 | Invitrogen, Carlsbad |
| DH10BAC | F- endA1 recA1 galE15 galK16 nupG rpsL $\Delta$lacX74 $\phi$80lacZ$\Delta$M15 araD139 $\Delta$(ara,leu)7697 mcrA $\Delta$(mrr-hsdRMS-mcrBC) $\lambda$ | Invitrogen, Carlsbad |
| GS1783 | DH10B $\lambda$cI857 $\Delta$(cro-bioA)<>araC-PBAD, I-SceI | Greg Smith, Northwestern University, Chicaco |
| BL21 (DE3) Rosetta2 | - opmpT hsdScB(rB- mB-) gal dcmpRARE2 (CamR) | Novagen, USA |
| DH10MultiBacY | | Dr. I. Berger, EMBL, Grenoble |

### 2.1.10. Plasmids

| **Name** | **Feature** | **Reference/supplier** |
|---|---|---|
| pACEBac1 | insect cell expression vector | Nie et al. (2016) |
| pEPkan-S | pEP vector containing kanamycin resistance | Tischer et al. (2006) |
| pETM13 | bacterial expression vector | a kind gift from EMBL, Heidelberg |
| pUC-SP | | Bio Basic Inc. (New York) |

### 2.1.11. Cell culture supplements

| **Name** | **Cat.No.** | **Company** |
|---|---|---|
| Fetal calf serum (FCS) | P30-3306 | PAN, Aidenbach |
| L-alanyl-L-glutamine | K 0302 | Biochrom AG, Berlin |
| Non-essential amino acids (NEAA) | K 0293 | Biochrom AG, Berlin |
| Sodium pyruvate | L 0473 | Biochrom AG, Berlin |

### 2.1.12. Kits for molecular biology

| Name | Cat.No. | Company |
|---|---|---|
| GF-1 AmbiClean PCR/Gel Purification Kit | GF-GC-050 | Vivantis, USA |
| Hi Yield Plasmid Mini Kit | 30 HYDF100 | SLG, Gauting |
| PeqGold Plasmid Miniprep Kit I | 12-6942-02 | Peqlab, Erlangen |
| MiniElute Gel Extraction Kit | 28604 | Qiagen, Hilden |
| Monarch DNA Gel extraction kit | | New England biolabs, Ipswich |
| RNeasy Mini Kit (250) | 74106 | Qiagen, Hilden |
| RTP DNA-RNA virus mini kit | | Stratec Molecular, Berlin |
| Qiagen Plasmid mini kit | | Qiagen, Hilden |

### 2.1.13. Buffers

| Buffer | Composition |
|---|---|
| 1x phosphate buffered saline (PBS) | 2 mM $KH_2PO_4$, 10 mM $Na_2HPO_4$, 137 mM NaCl, 2,7 mM KCl, pH 7.3 |
| 1x tris-acetate-EDTA buffer (TAE) | 40 mM Tris, 1 mM $Na_2EDTAx$ 2 $H_2O$, 20 mM HCl 99%, pH 8.0 |
| LB medium (1 L) | 10 g Bacto™Tryptone, 5 g Bacto™Yeast Extract, 10 g NaCl, 15 g Bacto™Agar |
| Buffer (P1) | 50 mM Tris HCL, pH 8.0, 10 mM EDTA, 100 µg/ml RNAse , |
| Lysis Buffer (P2) | 200 mM NaOH, 1% sodium dodecyl sulfate (SDS) |
| Neutralization Buffer (P3) | 3 M K-Acetate, pH 5.5 |
| Buffer TE | 10 mM Tris HCl, pH 7.4, 1 mM $Na_2EDTA$ |
| Trypsin | 1,5 M NaCl, 0,054 M KCl, 0,055 M $C_6H_{12}O_6$, 0,042 M $NaHCO_3$, 106 U Penicillin (P), 1457.4 U Streptomycin (S), 0,0084 M Versene (EDTA), Trypsin 1:250 |
| 5×SDS loading buffer | 250 mM Tris pH 6.8, 8% (w/v) SDS, 10% (v/v) $\beta$-ME, 30% (v/v) Glycerol, 0.02% (w/v), Bromophenol blue |
| 10×SDS running buffer | 250 mM Tris pH 6.8, 2 mM Glycine, 1% (w/v) SDS |
| Binding buffer for $His_6$-tagged MHC-I | 20 mM tris(hydroxymethyl)aminomethan (Tris)-HCl at pH 7,5, 200 mM NaCl, 5% glycerol |
| Binding buffer for $His_6$-tagged gDs | 20 mM 2-(N-morpholino)ethanesulfonic acid (MES) at pH 6, 200 mM NaCl, 5% glycerol |
| Elution buffer for $His_6$-tagged MHC-I | 20 mM Tris-HCl at pH 7,5, 200 mM NaCl, 5% glycerol, 200 mM imidazole |
| Elution buffer for $His_6$-tagged gDs | 20 mM MES at pH 6, 200 mM NaCl, 5% glycerol, 200 mM imidazole |
| Coomassie staining solution | 0.025% (w/v) Coomassie (R250), 0.025% (w/v) Coomassie(G250), 30% (v/v) isopropanol, 7.5% (v/v) acetic acid |
| Destaining solution | 10% (v/v) acetic acid |
| SEC buffer for $His_6$-tagged gDs | 20 mM MES at pH 6, 50 mM NaCl, 5% glycerol |
| SEC buffer for $His_6$-tagged MHC-I | 20 mM Tris-HCl at pH 7,5, 50 mM NaCl, 5% glycerol |
| Citrate buffer | 40 mM citric acid, 10 mM potassium chloride, 135 mM sodium chloride, to pH 3 |

### 2.1.14. Media

| Name | Cat.No. | Company |
|---|---|---|
| Dulbecco's Modified Eagle's Medium (DMEM) | PO4-04500 | PAN-Biotech GmbH |
| Roswell Park Memorial Institute Medium (RPMI) | PO4-18500 | PAN-Biotech GmbH |
| Minimal Essential Medium Eagle (MEM) | PO4-09500 | PAN-Biotech GmbH |
| Iscove's Modified Dulbecco's Medium (IMDM) | P04-20256 | PAN-Biotech GmbH |
| Sf-900 III SFM | 12659017 | Thermo Scientific, Darmstadt |
| Express Five Medium | B85502 | Thermo Scientific, Darmstadt |

### 2.1.15. Antibiotics

| Name | Cat. No | Working concentration | Company |
|---|---|---|---|
| Ampicillin (Amp) | K0292 | 100 µg/ml in ddH2O | Roth, Karlsruhe |
| Chloramphenicol | 3886.3 | 30 µg/ml diluted in 96% ethanol | Roth, Karlsruhe |
| Kanamycin sulphate (Kana) | T832.3 | 50 µg/ml in ddH2O | Roth, Karlsruhe |
| Penicillin (P) | A1837 | 100 U/ml in MEM | Applichem, Darmstadt |
| Streptomycin (S) | A1852 | 100 U/ml in MEM | Applichem, Darmstadt |
| Hygromycin B-solution (Hygro) | 10687010 | 400 µg/ml in ddH2O | Thermo Scientific, Darmstadt |
| G418 (Geniticinsulfat) | 10131027 | 800 µg/ml in ddH2O | Thermo Scientific, Darmstadt |
| Gentamicin (Gent) | 15710072 | 10 µg/ml in ddH2O | Thermo Scientific, Darmstadt |

## 2.2. Methods

### 2.2.1. Virus propagation

The EHV-1, strain RacL11, and EHV-4, strain TH20p, are bacterial artificial chromosome (BAC) derived with green fluorescent protein (GFP) inserted into the Mini-F (Rudolph et al., 2002; Azab et al., 2009, 2011). In EHV-1, the gene 71 has been exchanged for the BAC vector sequence (Rudolph et al., 2002). For EHV-4 the BAC DNA was inserted between the non essential genes 58 and 59 (Azab et al., 2011). Viruses were reconstituted by transfection of 293T cells using polyethylenimine (PEI), harvested by freeze-thawing and further propagated in equine dermal (ED) cells using IMDM supplemented with 20% fetal bovine serum (FBS), 1% penicillin/streptomycin (P/S), 1% non-essential amino acids (NEAA) and 1% sodium pyruvate at 37 °C under a 5% $CO_2$ atmosphere. After complete infection of the cells, the viruses were harvested, freeze-thawed and titrated using ED cells and 7-fold serial dilutions and overlaid with semi-fluid methyl cellulose. Plaque numbers were counted for titer calculations.

### 2.2.2. Construct design for protein production

To identify an efficient system for high yield protein production for crystallography, the bacterial and the baculovirus expression vector system were tested.
Synthetic genes were constructed for EHV-1 gD (gD1) (GenBank M59773.1), gD4 (GenBank S65633.1), and the MHC-I complex Eqca-1*00101 (GenBank ID DQ083407.1). All synthetic genes contain a Tobacco Etch Virus (TEV) cleavage site (ENLYFQG), a C-terminal $His_6$-tag,

and are flanked by EcoRI and ScaI restriction sites (Figure 6). N-terminal tagging of proteins is more common, however, the interacting region of gD with MHC-I is suspected to be rather at the N-terminus (Azab and Osterrieder, 2017). To not disrupt complex formation, the C-terminus was chosen for the tag. For cloning into the bacterial vector pETM-13, NcoI and XhoI restriction sites were added using PCR and primer pairs displayed in Figure 5.
The MHC-I construct includes the $\alpha$-chain, separated from $\beta$2m (GenBank ID AY124653.1) with a linker sequence (GGGGSGGGSGGGS) (White et al., 1999) and a peptide by the ribosomal scipping site P2A. A high affinity peptide (SDYVKVSNI, IC50 0,66 nM) for the equine MHC-I Eqca-1*00101 binding groove was chosen (Bergmann et al., 2015) to secure stable MHC-I complex formation. The native signal peptide was substituted with major envelope glycoprotein (gp64) signal peptide (synonym: gp67) from Autographa californica nuclear polyhedrosis virus (AcNPV) to direct the secretion of recombinant proteins into the cell culture media (Whitford et al., 1989; Stewart et al., 1991). For that gp64 of the AcNPV baculovirus was added to the vector plasmid pACEBac1 (Geneva Biotech) already containing a polyhedrin promotor.

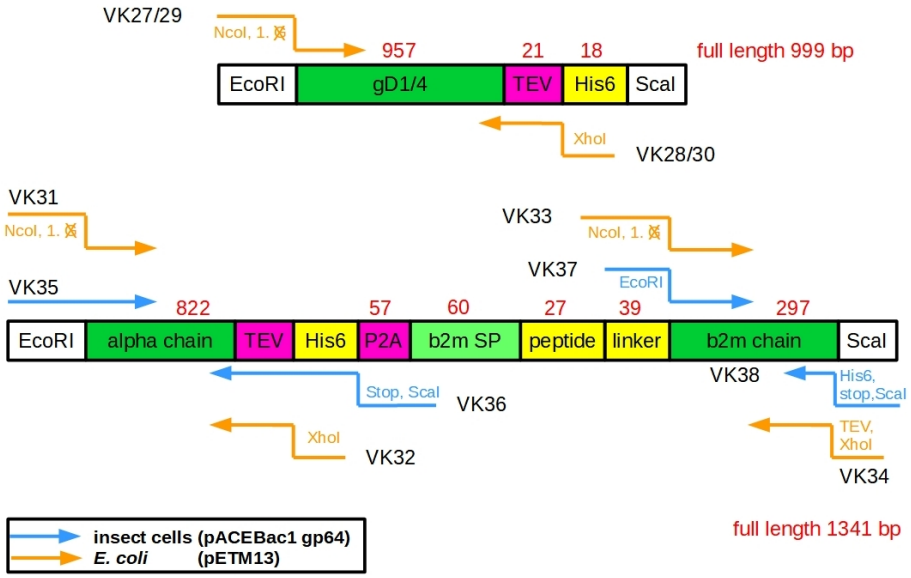


Figure 5: Cloning strategy from synthetic genes. Shown are the synthetic genes together with the primers (Table 2.1.5) used to amplify constructs for cloning into pACEBac1 and pETM-13 plasmids. Red numbers are lenght of construct fragments.

### 2.2.3. Molecular cloning of constructs for protein production in *E. coli* and insect cells

Five constructs were amplified using PCR with in Figure 5 indicated primer pairs (sequences can be found in Table 2.1.5) from synthetic genes for protein production in insect cells and four for the bacterial system. These PCR products were digested with EcoRI and ScaI or NcoI and XhoI restriction enzymes for insertion into pACEBac1 and pETM13, respectively. The transfer vectors were digested with the same restriction enzymes and ligated with the digested PCR products. These plasmids were transformed into DH10MultiBac and Rosetta electrocompetent cells for the production of recombinant bacmids and recombinant bacteria, respectively.

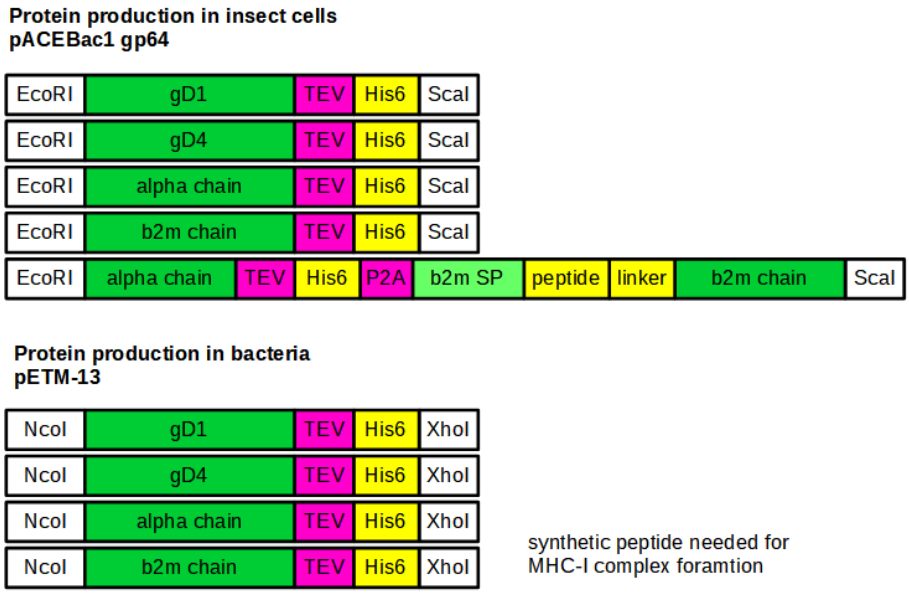


Figure 6: Schematic constructs for protein production in insect cells using pACEBac1 vector plasmid and *E. coli* using pETM-13 vector plasmid after amplification from synthetic genes. For MHC-I complex assembly from separately produced $\alpha$-chain and $\beta$2m, synthetic peptide is needed.

### 2.2.4. Protein production and purification from insect cells

Bacmid DNA was isolated from recombinant DH10MultiBac cells and adherent Sf9 cells in 6-well plates transfected using x-treme Gene9 DNA Transfection Reagent (Roche). The V0 virus was harvested after complete infection by collecting the cell supernatant. For production of a higher titer V1 stock, the V0 supernatant was used to infect 50 ml Sf9 cell culture in a shaker flask. The viruses were harvested as before and used to infect High5 cells in a shaker flask for protein production. Cell supernatant was harvested after 48 to 72 h post infection, the pH adjusted to 7 with 1 M Tris-HCl buffer at pH 9 on ice and incubated for at least 1 h with washed nickel-NTA (Ni-NTA) beads for immobilized metal ion affinity chromatography (IMAC). The beads with the bound recombinant protein were collected with a gravity flow column and protein eluted with a buffer containing 20 mM Tris-HCl at pH 7,5 or MES at pH 6 for gDs and MHC-I, respectively, and 200 mM NaCl, 5% glycerol, and 200 mM imidazole. All buffers were prepared on ice. Concentrated protein was loaded onto a buffer washed 16/600 Superdex 200 gel filtration column (GE Healthcare, Piscataway, NJ) for size exclusion chromatography (SEC). The buffer conditions were the same as in IMAC but with 20 mM NaCl and no imidazole. Protein collected from SEC was concentrated, aliquoted and directly used for crystallization or stored at −80 °C. A more detailed protocol can be found in supplement section A.2.1.

### 2.2.5. Protein production and purification from *E. coli* inclusion bodies

To produce recombinant protein in *Escherichia coli* (*E. coli*), the Rosetta strain was transformed with the vector plasmid pETM13 containing the protein construct. A 1:100 dilution of a starter culture of this transformed bacteria was grown in ZYM-5052 media until $OD_{200}$ 0,6 at 37 °C and

transferred to 15 - 20 °C over night.
For purification of recombinant protein from inclusion bodies produced in *E. coli*, the pellet was harvested by centrifugation, lysed with a buffer containing 20 mM Tris-HCl at pH 8, 200 mM NaCl, and 1 mM dithiothreitol (DTT). After 1 h treatment with DNase on ice and sonication, the pellet was washed three times with lysis buffer containing 1% Triton-X 100 and again with lysis buffer and rotated for 1 h in different solubilization buffers (Table 1). Proteins were analyzed by sodium dodecyl sulfate-polyacrylamide gel electrophoresis (SDS-PAGE). A more detailed protocol can be found in supplement section A.2.2.

Table 1: Non-denaturing solubilization buffer conditions for purification tests of recombinant proteins in *E. coli* inclusion bodies.

| Label | NaCl (mM) | Detergent | Glycerol (%) |
|---|---|---|---|
| N | 200 | - | - |
| MES | 200 | - | 5 |
| 0,5 S | 500 | - | - |
| 1 S | 1000 | - | - |
| Nonident 40 | 200 | 0, 2% NP 40 | - |
| Triton-X 100 | 200 | 0, 2% Triton-X 100 | - |
| Tween-20 | 200 | 0, 2% Tween-20 | - |
| Glycerol | 200 | - | 10 |

### 2.2.6. Thermal shift assay

To test protein stability, a thermal shift assay was performed according to manufacture's instructions. In short, 0,2 mg protein were mixed with SYPRO Orange dye. The dye binds to denatured protein and emits fluorescence. Proteins were subjected to increasing temperatures and denaturing was monitored by detecting fluorescence levels using a real time q-PCR machine. A more detailed protocol can be found in supplement section A.2.3.

### 2.2.7. Crystallography

Crystals of EHV-1 gD were obtained by the sitting-drop vapor-diffusion method at 18 °C with a reservoir solution composed of 0,1 M Tris/HCl buffer at pH 8.5, 0,2 M $MgCl_2$, and 30% (w/v) polyethylene glycol (PEG) 4000. Crystals of EHV-4 gD were obtained in the same way with a reservoir solution containing 200 mM $MgCl_2$, 100 mM MES at pH 6.5 and 30% (w/V) PEG 400. The TEV cleavage site was not cleaved and the $His_6$-tag present. Initial screens were done in 96-well MRC plates dispensed by a Cartesian liquid dispensing robot 200 nl drops. Refinement was done in 24-well plates.

### 2.2.8. Crystal cryo-preservation

Crystals were cryo-protected in 75% mother liquor and 25% (v/v) glycerol and subsequently flash-cooled in liquid nitrogen.

### 2.2.9. Diffraction data collection and structure solving

Synchrotron diffraction data were collected at the beamline P14 at DESY (Hamburg, Germany) and at the beamline 14-2 of the MX beamline of the BESSY II (Berlin, Germany) and processed with X-ray detector software (XDS) (Kabsch, 2010) (Table 3). The structure was solved by molecular replacement with PHASER (Bunkóczi et al., 2013) using the coordinates of PDB ID 2c36 as search model. A unique solution with two molecules in the asymmetric unit was subjected to the program AUTOBUILD in PHENIX (Adams et al., 2010) and manually adjusted in COOT (Emsley et al., 2010). The structure was refined by maximum-likelihood restrained refinement using PHENIX (Adams et al., 2010; Afonine et al., 2012). Model quality was evaluated with MolProbity (Williams et al., 2018) and the JCSG validation server (Yang et al., 2004). Secondary structure elements were assigned with DSSP (Kabsch and Sander, 1983) and for displaying sequence alignments generated by ClustalOmega (Sievers et al., 2011) ALSCRIPT (Barton et al., 1993) was used. Structure figures were prepared using PyMOL (DeLano, 2002).

### 2.2.10. SEC coupled with MALS

SEC-multi-angle static light scattering (MALS) was used to study the molecular mass of recombinant, soluble gD1. The separation was performed at room temperature on a Superdex 75 10/300 GL (GE Healthcare, Piscataway, NJ) column with 2 mg/ml gD1 and a mobile phase composed of Tris-HCl at pH 7.5, 200 mM NaCl, 5% glycerol, and 0,02% sodium azide, attached to a high-performance liquid chromatography (HPLC) system from Agilent Technologies (USA). The MALS detector was a miniDAWN TREOS detector (Wyatt Technology Corp., USA) and data was acquired and analyzed with the ASTRA® for Windows software package (version 6.1.2) provided with the instrument. A more detailed protocol can be found in supplement section A.2.4.

### 2.2.11. Blocking assays

**Flow cytometry** For dose dependent blocking assays, ED cells in 24-well plates were incubated with recombinant gDs (20 - 150 µg/ml) for one hour on ice, infected with either EHV-1-GFP, strain Racl11, or EHV-4-GFP, strain TH20p, at multiplicity of infection (MOI) 0,1 for one hour at 37 °C. After citrate treatment and two washes with PBS, infection was allowed to proceed for 24 (EHV-1) or 48 h (EHV-4). The intensity of fluorescence was measured with a FACSCalibur flow cytometer (BD Biosciences) and analyzed with the software CytExpert (Beckman Coulter, Krefeld). A more detailed protocol can be found in supplement section A.2.5.
In another experiment, recombinant MHC-I (150 µg/ml) was incubated for one hour on ice with viruses, which were then used to infect cells seeded in 24-well plates at MOI 0,1. It was proceeded as in blocking assays with gDs and infection analyzed by flow cytometry.

**Plaque numbers** To block virus entry, cells were incubated with recombinant gDs as for analysis with flow cytometry. After citrate treatment, cells were overlaid with semi-fluid methyl cellulose and plaque numbers inspected with an inverted fluorescence microscope (Zeiss Axiovert 100) after 48 h. A more detailed protocol can be found in supplement section A.2.6.

### 2.2.12. Surface plasmon resonance analysis

Affinities of gD1, gD4, and $gD4_{36\text{-}280}$ to immobilized MHC-I were measured with a SPR GE Biacore J Biomolecular Interaction Analyser instrument (Uppsala, Sweden) using a HC 200M sensor chip (XanTec Bioanalytics GmbH) according to the protocol provided by XanTec. The

flow cell coated with amine-coupled, recombinant MHC-I was considered to be the active surface, while the negative control (reference surface) was a second flow cell, on the same chip, coated with poly-L-lysine and positive nanogels (size 214 nm) (Dey et al., 2018). The reference sensorgrams were subtracted from reaction sensorgrams and normalized and the data fitted with the Hill-Wand binding model (Schasfoort, 2017). All solutions were freshly prepared, degassed, and filtered through 0,22 µm filter. Measurements were performed at 25 °C in PBS at pH 7.4.
The surface of the sensor chip was cleaned prior to use by injection of 20 mmol/dm$^3$ sodium hydroxide and 80 mmol/dm$^3$ hydrochloric acid. A pre-concentration test was performed to determine the adequate pH for the MHC-I immobilization. After regeneration of the sensor surface with buffer containing 2 M NaCl and 10 mM NaOH, the carboxyl groups on the hydrogel were activated with amine coupling reagent ()N-ethyl-N'-(3-dimethylaminopropyl) carbodiimide (EDC) 200 mM and N-hydroxysuccinimide (NHS) 50 mM) freshly prepared in 500 mM MES buffer. Recombinant MHC-I (50 µg/ml) was diluted in 10 mM sodium acetate at pH 5 and injected at low flow for 30 min on the flow-cell (FC1) where the protein was immobilized through covalent binding by a amino-coupling reaction. Remaining activated COOH groups were blocked by injection of 1 M Ethanol amine (pH 9.5) for 10 minn. This reduced the negative charge of the sensing film surface and thus decreased the potential for non-specific binding. Loosely absorbed proteins where removed with regeneration solution.
Proteins were injected at concentrations ranging from 0 to 12 900 nM. The interaction of gDs with MHC-I was monitored for 15 min at medium flow to give sufficient time for the association phase to reach equilibrium levels (Req). The dissociation phase was monitored for 5 min. After every injection, MHC-I ligand regeneration was performed to wash off bound protein by injecting 2xPBS with 10 mM NaOH at pH 10 shortly. Each experiment was repeated at least three times and with different protein batches.

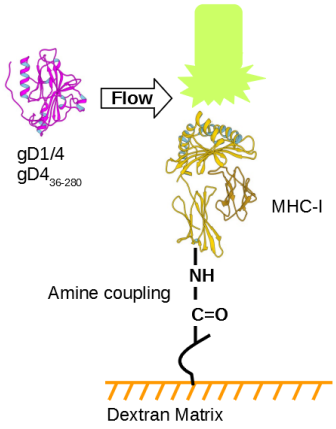


Figure 7: Schematic amine coupling of MHC-I during surface plasmon resonance (SPR) analysis with recombinant gDs as analyte.

### 2.2.13. Mass spectrometry analysis

Intact protein mass of gD1, gD4, and MHC-I was determined by matrix-assisted laser desorption ionization-time of flight mass spectrometry (MALDI-TOF-MS) using an Ultraflex-II TOF/TOF instrument (Bruker Daltonics, Bremen, Germany) equipped with a 200 Hz solid-state Smart beam™ laser by Dr. Christoph Weise (BioSupraMol Core Facility, Bio-Mass Spec-

trometry). Samples were spotted using the dried-droplet technique on sinapinic acid (SA) or 2,5-dihydroxybenzoic acid (DHB) matrix (saturated solution in 33% acetonitrile / 0,1% trifluoroacetic acid). The mass spectrometer was operated in the positive linear mode, and spectra were acquired over an m/z range of 3,000-60,000. Data was analyzed using FlexAnalysis 2.4. software provided with the instrument.
Protein identity was determined by tandem mass spectrometry (MS/MS) of in-gel digested Coomassie stained protein with 12,5 µg/ml Glu-C and trypsin, and 10 µg/ml Asp-N in 25 nM ammonium bicarbonate. A more detailed, general protocol can be found in supplement section A.2.8.
N-terminal c and C-terminal (z+2) sequence ion series were generated by in-source decay (ISD) with 1,5-diaminonaphthalene (1,5-DAN) as matrix (20 mg/ml 1,5-DAN in 50% acetonitrile / 0,1% trifluoroacetic acid). Spectra were recorded in the positive reflector mode (RP PepMix) in the mass range 800–4,000.

### 2.2.14. Generation of gD1/4-MHC-I binding hypothesis

The binding hypothesis of gD1/4-MHC-I were generated by Szymon Pach from the Molecular Design lab at Freie Universität Berlin of Professor Gerhard Wolber by using *in silico* modeling. The available structural data of equine MHC-I Eqca-N*00602 (protein data base (PDB) ID 4ZUU) (Yao et al., 2016) served as a template to generate a model of MHC-I Eqca-1*00101 including the peptide SDYVKVSNI, which was used for the recombinant MHC-I. The peptide was manually fitted into the binding groove based on the peptide CTSEEMNAF in the MHC-I crystal structure 4ZUU and the associated binding-mode analysis by Yao et al. (2016).
The MHC-I alpha chain has 85% sequence identity and 88% similarity with the MHC-I gene Eqca-1*00101. The mouse $\beta$2m has 63% sequence identity and 82% similarity with Eqca-1*00101. Hence, both chains are well suited to create a Eqca-1*00101 model and were assembled and relaxed by molecular dynamics (MD) simulations. The residues of the peptide in 4ZUU were mutated to SDYVKVSNI, sidechain rotamers searched with MOE2019 (Molecular Operating Environment (MOE), Chemical Computing Group ULC: 1010 Sherbrooke St. West, Suite #910, Montreal, QC, Canada, 2019) and finally energy-minimized together with MHC-I sidechains using OPLS-AA force-field (Kaminski et al., 2001).
The MHC-I Eqca-1*00101 structural model together with the structural data from gD1 and gD4 were used to generate binding poses. The search area could be narrowed down since the binding of gD1 and 4 to MHC-I was suspected to be at or close to A173 in the $\alpha$2 chain (Azab et al., 2014). After subsequent selection of statistically most plausible binding poses according to the O-ring theory (Bogan and Thorn, 1998), MD simulations of the obtained gD1-MHC-I complexes were performed.

### 2.2.15. BAC mutagenesis

The protocol for BAC mutagenesis using two-step Red-mediated recombination is adapted from Azab et al. (2011). In short, to insert point mutations into a BAC, first, a transfer construct including the I-SECI-aphAI cassette from the pEPKan-S plasmid was amplified by PCR with primers pairs covering the site of interest containing the mutation (Table 2.1.5). This construct was transformed into electrocompetent *E. coli* GS1783 cells including the BAC. The insertion of the construct was tested by selection for the kanamycin resistance and by Restriction fragment length polymorphism (RFLP) using the restriction enzyme Pst-I-HF. Now the I-SCEI-aphAI cassette is being removed by induction of the Red recombination system. BAC DNA was isolated and purified from correct clones and transfected into 293T cells. The GFP expression should be visible after 16 h. The cells and supernatant were harvested three days post infection and used

to infect ED cells. Viral plaques were visible 1 to 3 days post infection. A more detailed protocol can be found in supplement section A.2.7.

### 2.2.16. Growth kinetics

Multi-step growth kinetics was performed to compare virus growth of wild type and mutant viruses as described previously (Azab et al., 2010). ED cells were grown to confluency in 24-well plates, infected with an MOI of 0,1 and incubated for one hour at 37 °C. All virus particles that did not enter cells after this time were removed by citrate treatment for no longer than 30 s with a sterile filtered buffer with a pH of 3 containing 40 mM citric acid, 10 mM potassium chloride and 135 mM sodium chloride. The buffer was neutralized by adding approximately 500 µl IMDM and the cells were washed twice with PBS and finally overlaid with 500 µl IMDM. At indicated times after the citrate treatment cells and supernatant were collected separately for EHV-1 and together for EHV-4. The samples were frozen at −80 °C until the sample collection was complete. The titers were determined by plating dilution series onto ED cells and counting plaque numbers after one or two days under a methylcellulose overlay. All plates were fixed for 10 min with 4% formaldehyde, washed with PBS and stained for 10 min with crystal violet which was washed away with tab water. Statistical analysis was done using GraphPad Prism 5 software and an unpaired, one-tailed test. P<0,05 was considered significant. A more detailed protocol can be found in supplement section A.2.7.

# 3. Results

## 3.1. Production and purification of recombinant gD1, gD4, $gD4_{36\text{-}280}$ and MHC-I

Previously, recombinant full length and truncated gD1 have been successfully produced several times using the baculovirus expression vector system (BEVS), *E. coli* and yeast (Love et al., 1992; Tewari et al., 1994; Flowers et al., 1995a; Packiarajah et al., 1998; Zhang et al., 1998; Ruitenberg et al., 2001; Fuentealba et al., 2014) but only publications is available for gD of EHV-4 (Azab et al., 2014). Only two structures of equine MHC-I (Eqca-N*00601, Eqca-N*00602) complexed with mouse $\beta$2m are available in the PDB which were produced in *E. coli* and therefore possess no post translational modifications (PTMs). Furthermore, these MHC-I genes have been shown to not support EHV-1 and 4 infection (Azab et al., 2014).
Since the role of gD glycosylations is still unknown, for this study three synthetic genes (for $gD1_{32\text{-}349}$, $gD4_{32\text{-}349}$, MHC-I) were optimized for insect cells (synthesized by Bio Basic Inc. (New York)) and designed in a way that all needed constructs for both expression systems, BEVS and bacterial, could be cloned from these synthetic genes (Figure 5).

### 3.1.1. Protein production in *E. coli* and insect cells

Production in *E. coli* resulted in insoluble proteins in inclusion bodies. Different buffer conditions without denaturing agents were unsuccessful to extract soluble protein from inclusion bodies without unfolding. Further solubility tests showed that 3-4 M urea is sufficient to unfold gD1, gD4, and $\alpha$-chain (example Figure 8). However, since the role of protein glycosylation for the entry process of EHV-1 and 4 remains to be determined (Osterrieder, 1999; Frampton et al., 2005) and bacterial systems do not produce proteins with mammalian-type glycosylations, I focused on the protein production using insect cells. That system is the most widely used expression system for glycoproteins (Jarvis, 2003).

Glycoprotein D1, gD4, $gD4_{36\text{-}280}$, MHC-I and $\beta$2m were successfully produced in High5 and secreted into the media (Figure 10). The heavy chain ($\alpha$-chain) of MHC-I could not be produced in H5 cells. Due to a low protein yield, the Bac-to-Bac system was exchanged for the MultiBac yellow fluorescence protein (YFP) system, which permitted easier monitoring of baculovirus titers due to the expression of YFP in infected cells. Notably, the virus stocks are not as stable as other baculovirus preparations (Jarvis and Garcia, 1994). They can be stored at 4 °C in the dark but loose infectivity over time and cannot be used after approximately six months.

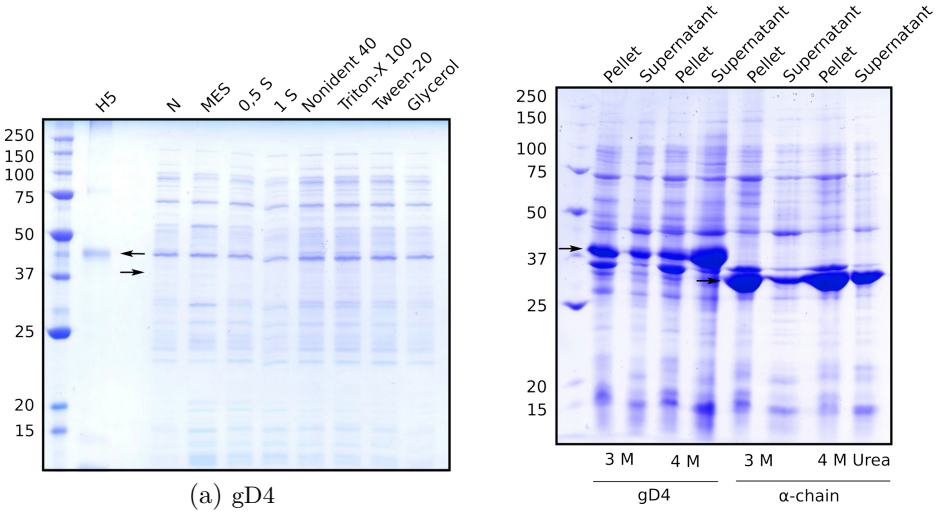


(a) gD4

(b)

Figure 8: Solubility tests with gD4 and $\alpha$-chain from *E. coli* inclusion bodies in (a) different non-denaturing (Table 1) and (b) denaturing buffers. Inclusion bodies were harvested by centrifugation, washed, resuspended in different buffers, supernatant and in (b) supernatant and pellet were run on an SDS-gel, and stained with Coomassie blue. Marker in (a) and (b) lane 1: Bio-Rad Precision Plus Protein™ marker with sizes of reference proteins in kDa, lane 2 in (a) shows gD4 produced in High5 insect cells. Arrows point at expected sizes of glycosylated, non-glycosylated gD4 in (a), and glycosylated gD4 and $\alpha$-chain in (b).

### 3.1.2. Protein purification using a two-step protocol

A two-step protocol proved to be effective to purify proteins to a high degree of purity, however, the procedure had to be optimized due to high losses of protein. In a first step the protein was pulled down from the insect cell media by IMAC with a nickle-charged nitrilotriacetic acid (NTA) agarose affinity resin on a gravity flow column (Figure 9). The affinity of His-tagged proteins to the Ni-NTA beads was very low, since the pH of the insect cell media is approximately 6 and the binding affinity of Ni-NTA decreases dramatically below pH 7 (Crowe et al., 1994). This led to a protocol where media with secreted proteins was cooled to 4 °C and the pH adjusted to 7. A second centrifugation step removed precipitated salts which would have clogged the fritted flow gravity column in the next step. This approach increased the protein yield, however, a substantial

part of the proteins remained in the media. Therefore, the incubation with the Ni-NTA beads at 4 °C was prolonged to one hour and repeated at least two times. During the concentration step, the protein likely interacted with the membrane of the concentrator and the yield could be further increased by using a 15 instead of 50 ml concentrator, as well as a maximum of 10 min centrifugation at a time with subsequent gentle mixing by inversion. Adequate buffer conditions for high protein stability in IMAC and SEC were confirmed by thermal shift assay. With the optimized purification protocol a protein yield of up to 5 mg and approximately 70% purity was obtained from 400 ml insect cell media using IMAC (Figure 10). The protein was further purified using SEC (Figure 11 and 12) and concentrated to a maximum of 25 mg/ml. During SEC the salt concentration in the buffer was lowered from 150 to 50 mM, which proved to be favorable for subsequent crystallization of the proteins.
Taken together, the proteins gD1, gD4, $gD4_{36\text{-}280}$, MHC-I and $\beta$2m were successfully produced using the BEVS and purified to a high degree suitable for crystallization in a two-step purification process.

Figure 9: Harvest of secreted protein from insect cell media using IMAC at 4 °C.

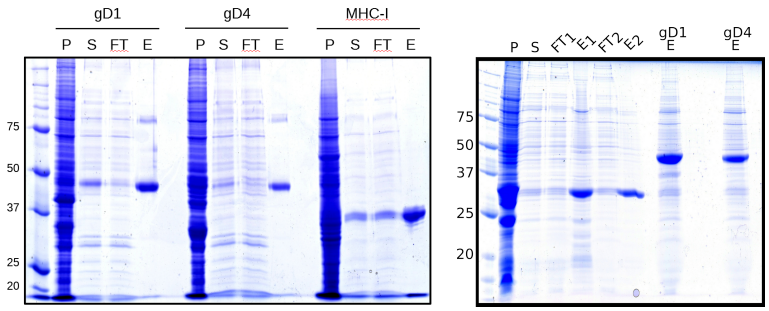


(a) gD1, gD4 and MHC-I (b) $gD4_{36\text{-}280}$

Figure 10: Representative Coomassie stained SDS gels of gD1 (approximately 43 kDa), gD4 (approximately 43 kDa), $gD4_{36\text{-}280}$ (approximately 30 kDa) and MHC-I (comprised of $\alpha$-chain with an approximate size of 38 kDa and $\beta$2m with linker and peptide with an approximate size of 13 kDa) purified by IMAC using Ni-NTA beads. Supernatant of insect cells containing recombinant protein with pH adjusted to 7 was incubated for at least 1 h with Ni-NTA beads. Beads were collected with gravity flow columns and protein detached using imidazole. Procedure was repeated up to three times. Lane 1 = marker, P = cell pellet, S = supernatant from cell pellet, FT = flow through of Ni-NTA beads, E = elution from Ni-NTA beads.

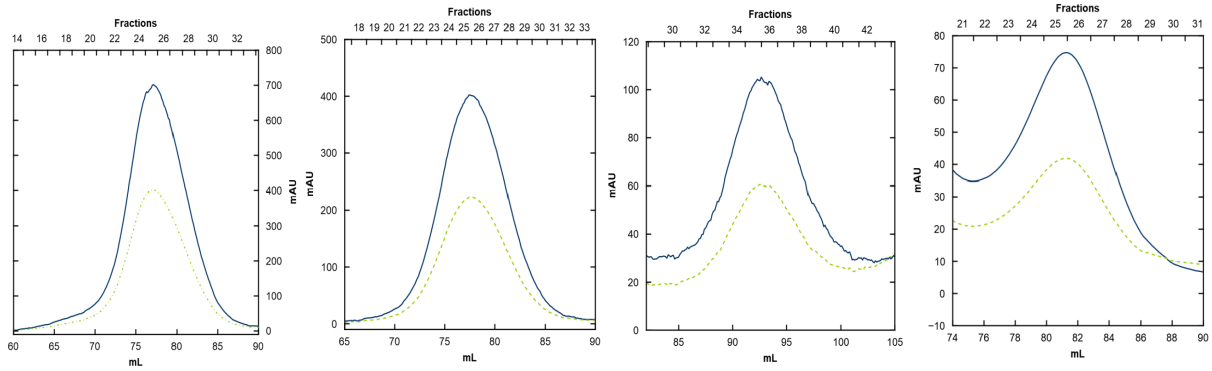


(a) gD1 (b) gD4 (c) $gD4_{36\text{-}280}$ (d) MHC-I

Figure 11: Representative SEC curves of concentrated gD1, gD4, $gD4_{36\text{-}280}$, and MHC-I run on Superdex 200 16/600 after IMAC purification. Solid curves shows UV absorbance at 280 nm, dotted curves at 260 nm.

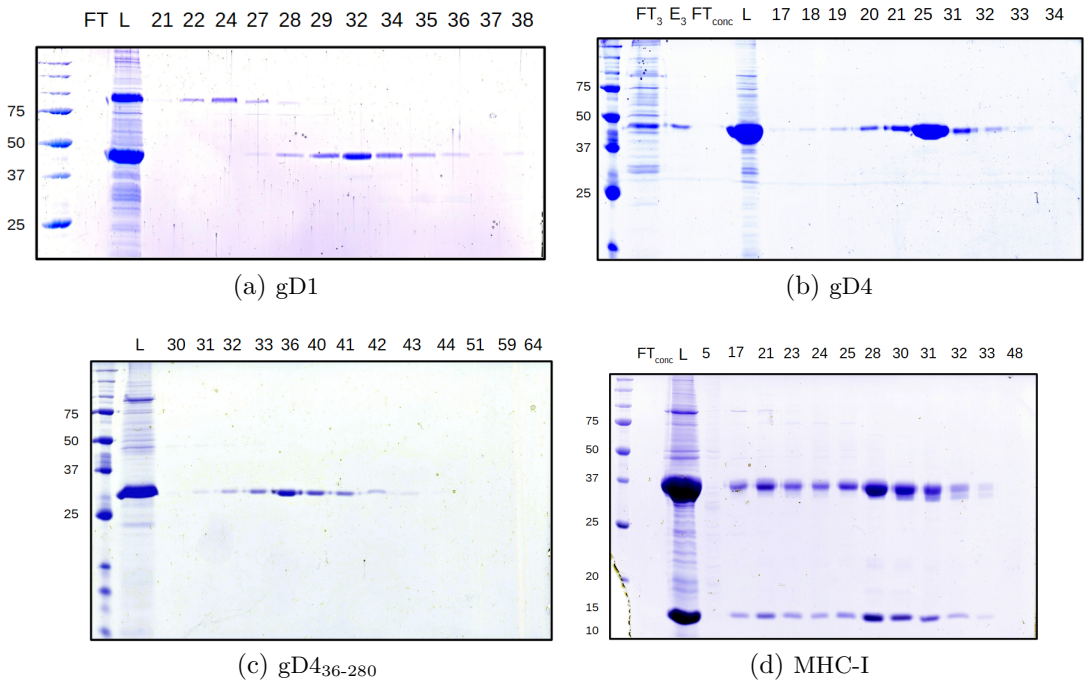


(a) gD1 (b) gD4

(c) $gD4_{36\text{-}280}$ (d) MHC-I

Figure 12: Representative SEC fractions of proteins produced in insect cells on Coomassie stained 12% SDS gels. (a) gD1 (approximately 43 kDa), (b) gD4 (approximately 43 kDa), (c) $gD4_{36\text{-}280}$ (approximately 30 kDa), (d) MHC-I (comprised of $\alpha$-chain with an approximate size of 38 kDa and $\beta$2m with linker and peptide with an approximate size of 13 kDa). FT = flow through, E = elution, L = loaded on SEC column, numbers = fraction number.

## 3.2. Molecular weight analysis of recombinant gD1, gD4, and MHC-I

To evaluate the size of the recombinant proteins gD1, gD4, and MHC-I, mass spectrometry (MS) analysis was conducted. This work was done in line with our collaboration with Dr. Christoph Weise, BioSupraMol Core Facility, Bio-Mass Spectrometry. Diluted recombinant protein was analyzed by matrix-assisted laser desorption ionization-time of flight mass spectrometry (MALDI-TOF-MS). A size of approximately 43,1 kDa for gD1, 43,76 kDa for gD4, 37,8 kDa for the $\alpha$-chain of MHC-I and a clear signal at 13,24 kDa for $\beta$2m with its linker and attached peptide (SDYVKVSNI) were detected (Figure 14a-c). The analysis was repeated with DHB matrix instead of SA matrix and yielded similar results (Figure supplement 33a).
The gDs and $\alpha$-chain contained a TEV cleavage site and a $His_6$-tag (ENLYFQGH$_6$), contributing approximately 1,7 kDa to the molecular weight of the molecules (calculated with `https://web.expasy.org/peptide_mass/`). Additionally the residues EF originating from the Eco-RI restriction site are present in the recombinant proteins. Excluding the molecular weight of the TEV cleavage site and the $His_6$-tag, this translates into a molecular weight of 41,4 and 42,1 kDa for soluble gD1 and 4, respectively (Table 2), and implies an approximate molecular weight of 49,3 kDa for the recombinant MHC-I molecule consisting of $\alpha$-chain (36,1 kDa) and $\beta$2m with linker and peptide (13,24 kDa).
The difference between theoretical and measured molecular masses is due to PTMs like glyco-

sylations and contributes approximately 4 kDa (Table 2). The measured molecular masses are consistent with western blot analysis and SDS-PAGE (Figure 13) when taking into account that the protein size on SDS-PAGE are generally overestimated (Matsumoto et al., 2019).
Further analysis of recombinant gD1, gD4, and MHC-I by in-source decay (ISD) and tandem mass spectrometry (MS/MS) of in-gel digested Coomassie-stained proteins, confirmed protein identity and presence of the correct N-terminus and C-terminus of gD1 and gD4, N-terminus of MHC-I $\alpha$-chain (Figure 14d and e, supplement Figure 33b-d).

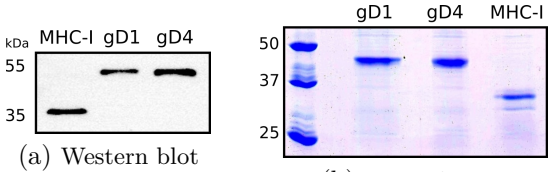


(a) Western blot (b) SDS-PAGE

Figure 13: Western blot and SDS-PAGE of MHC-I, gD1, and gD4. (a) Western blot: MHC-I (50 µg/ml), gD1 (5 µg/ml), and gD4 (5 µg/ml) with 1:1000 rabbit anti-$His_6$ antibody and 1:10000 goat anti-rabbit-HRP antibody. (b) Coomassie stained SDS-PAGE on 12% gel. For MHC-I, only the $\alpha$-chain is visible in (a) and (b).

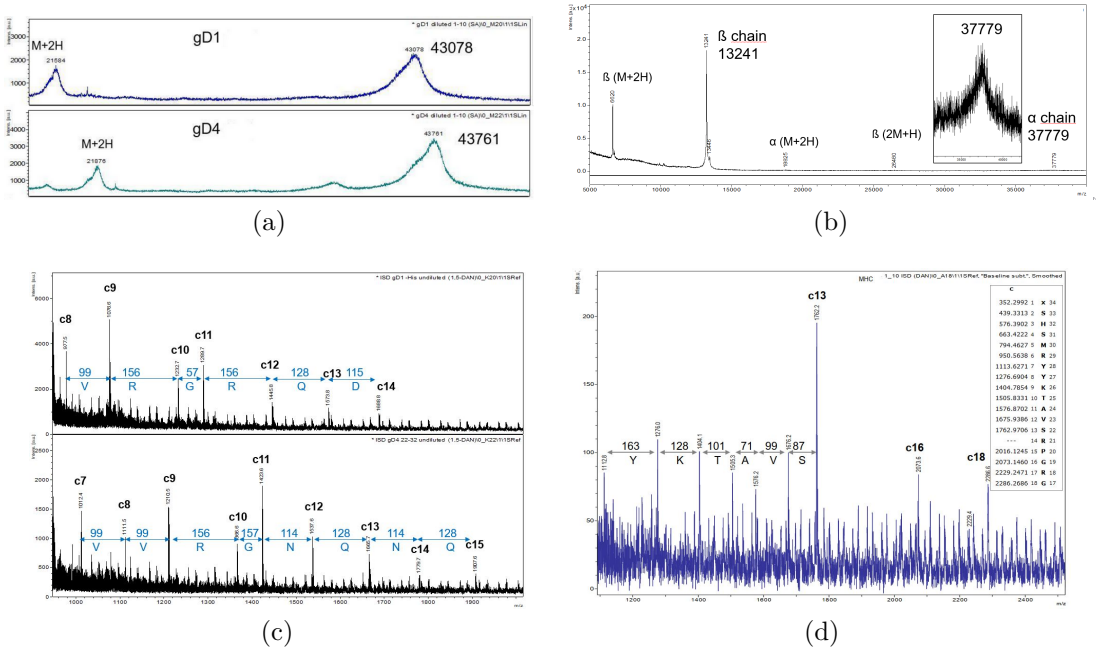


Figure 14: Mass spectrometry analysis. (a) Total mass analysis of recombinant gD1 (top) and gD4 (bottom) including N-terminal residues EF from Eco-RI restriction site, TEV clevage site and $His_6$-tag on SA matrix, (b) Total mass analysis of recombinant MHC-I complex comprised of $\beta$2m and MHC-I-$\alpha$-chain (insert zoom) including the same additional residues as gD1 and gD4 (c) ISD spectrum of recombinant gD1 (top), gD4 (bottom), and (d) MHC-I, insert: Theroretical c-ion series with modified N-terminus (Gly + 277). All samples were diluted 1:10 with water.

Table 2: Predicted and measured molecular mass in kDa of recombinant proteins with the uncleaved TEV site and $His_6$-tag. The prediction was done using `https://web.expasy.org/peptide_mass/` and the actual mass determined by MALDI-TOF-MS. Post-translational modification like glycosylations account for the discrepancies between the predictions and measurements.

| **Molecule** | **predicted** | **measured** | **TEV and $His_6$ subtracted from measured** |
|---|---|---|---|
| $gD1_{31\text{-}349}$ | 38,215 | 43,1 | 41,4 |
| $gD4_{31\text{-}349}$ | 38,251 | 43,76 | 42,1 |
| $\alpha$ 1-3 | 33,399 | 37,8 | 36,1 |
| $\beta$2m (+linker and peptide) | 13,243 | 13,24 | – |

## 3.3. Crystallography

The conditions for successful crystallization of HSV-1, HSV-2 and PrV gDs collectively contained high molecular weight PEG (Krummenacher et al., 2005; Zhang et al., 2011; Di Giovine et al., 2011; Lu et al., 2014; Li et al., 2017). Thus, crystallization experiments of gD1 and 4 focused on screens containing a broad range of PEG (PEGs suite, PEGs suite II, Qigaen, Germany). The crystal quality appears to be dependent on freshly purified protein, since proteins from frozen stocks crystallized but did not diffract. Most crystals of gD were small stars or rod shaped, in some condition eye shaped. A diffracting gD1 crystal was visible after 5 days in a crystallization solution containing 200 mM $MgCl_2$, 100 mM Tris pH 8.5 and 30% (w/v) PEG 4000 and was harvested after three weeks (Figure 15a). Since there were $Mg^{2+}$-ions present in the dimer interface, a crystallization screen containing different buffers with $Mg^{2+}$-ions was conducted. For both proteins, gD1 and 4, no crystals were obtained. A core screen with 384 buffer conditions did not yield further promising results either. Optimization and adaptation to larger volumes of protein solution with PEG buffers similar to the first one resulted in crystals which, however, did not diffract.

For gD4, a truncated version ($gD4_{36\text{-}280}$) was produced after the full length protein initially did not crystallize. Tests with PEG conditions resulted in rod and star shaped crystals of truncated gD4 and the presumably gD1/4-MHC-I complexes. Finally, the structure of gD4 was solved using a small rod shaped crystal grown in a crystallization solution containing 340 µM gD4 and equimolar MHC-I in a mother liquid composed of 200 mM $MgCl_2$, 100 mM MES at pH 6.5 and 30% (v/v) PEG 400 (Figure 15b). The crystals appeared after 7 days and were harvested 8 days later but did not diffract. Crystals harvested a year later from the same well diffracted to 1,9 Å resolution. Although MHC-I molecules were present in the crystallization solution the asymmetric unit contained only a single gD4 molecule suggesting that no complex formation occurred.

An impediment was that the reproducibility of the gD1 and gD4 crystals was challenging and that the crystal growth was rather slow. Due to the low number of crystals available, it was not tested if the C-termini were digested by proteases during crystallization by SDS-PAGE or if they are simply too flexible to be visible and hence could not be resolved in the electron densities.

MHC-I crystals were obtained in a buffer containing 200 mM calcium acetate, 100 mM 4-(2-hydroxyethyl)-1-piperazineethanesulfonic acid (HEPES) pH 7.5 and 10% (w/V) PEG 8000 but did not diffract. All were fragile and shaped like long needles (Figure 15c).

Taken together, the proteins gD1, gD4, the truncated version $gD4_{36\text{-}280}$ and equine MHC-I (Eqca-1*00101) produced in insect cells using the BEVS crystallized in buffers containing high molecular PEGs. Crystals diffracting to high resolutions were obtained for single gD1 and gD4.

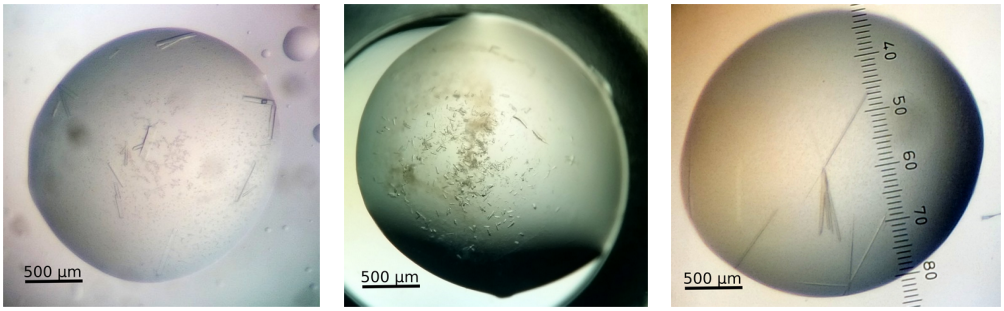


(a) gD1 (b) gD4 (c) MHC-I

Figure 15: Diffracting crystals of gD1 and 4 and needle shaped crystals of MHC-I in a 100 nl drop.

## 3.4. Structure solving of free gD1 and gD4

### 3.4.1. gD1

The EHV-1 gD crystal (Figure 15a) diffracted to a 2,45 Å resolution containing two gD molecules per asymmetric unit (Figure 16a, Table 3, PDB-ID 6SQJ). The structure of gD1 was determined using the HSV-1 gD structure (PDB ID 2C36) for molecular replacement and refined to an $R_{work}$ of 20.3% and $R_{free}$ of 25.7% (Table 3). A clear electron density was present for 477 residues in total, with 242 residues in chain A (G39 to P280) and 236 residues in chain B (Q41 to A276). The terminal residues E32 to R38 and N281 to T348 could not be modeled due to a lack of electron density. The C-termini of gD molecules of other alphaherpesviruses such as HSV and PrV are known to be highly flexible containing disordered loops and can often not be resolved by X-ray crystallography (Li et al., 2017; Carfi et al., 2001; Krummenacher et al., 2005). The C-termini of gD1 and 4 were predicted to be unstructured as well by FoldIndex© (`https://fold.weizmann.ac.il/fldbin/findex`). Partially poorly defined electron density in chain A lead to a gap between the amino acids N71 and N76 (NDQVKN) which was solved in chain B. *N*-acetyl-D-glucosamines (GlcNAcs) are visible at the predicted sites N20 and N28 (Flowers et al., 1991) which are conserved between gD1 and gD4 but not in gDs of other alphaherpesviruses. Six cysteines were found to form three disulfide bonds at sites conserved in members of the gD polypeptide family. The core of the gD structure is composed of a nine-stranded (A', B, C, C', C", D, E, F, and G) $\beta$-barrel, topologically arranged in a typical V-like Ig fold, flanked by N- and C-terminal extensions with loops, $\alpha$-helices ($\alpha$1, $\alpha$2, $\alpha$3', and $\alpha$3), and small $\beta$-strands (str1-4) (Figure 16).

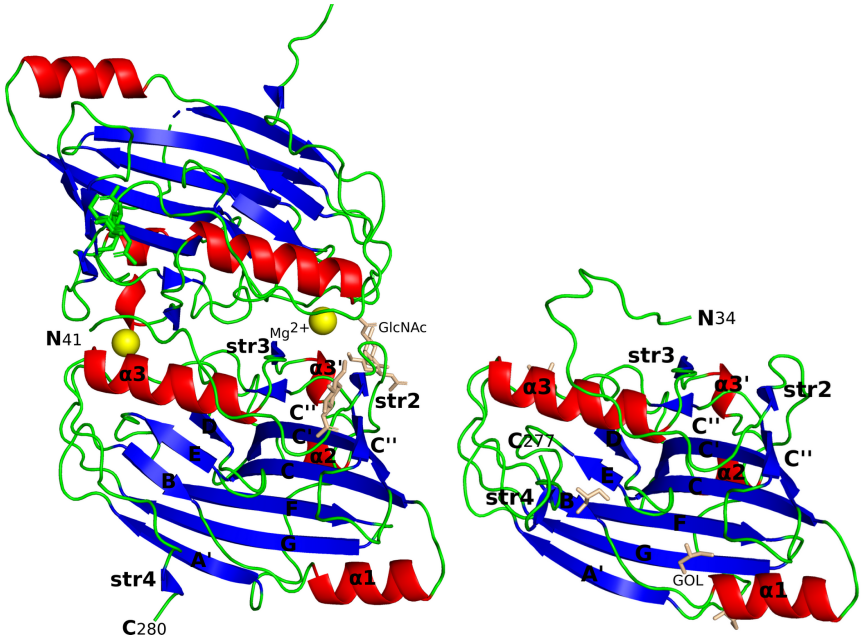


(a) gD1 dimer (b) gD4 monomer

Figure 16: Cartoon representation of (a) gD1 dimer (2,45 Å resolution, PDB ID: 6SQJ) and (b) gD4 (1,9 Å resolution, PDB ID: 6TM8) crystal structure. Molecule orientation is identical and secondary structure assignment was done with hydrogen bond estimation algorithm (dssp) (Kabsch and Sander, 1983). Helices are displayed in red, sheets in blue, loops in green. GlcNAc and glyrecol molecules are shown in stick representation in beige and $Mg^{2+}$-ions in gold balls.

Table 3: Crystallographic data collection and model refinement statistics.

| **Data Collection** | **gD1** | **gD4** |
|---|---|---|
| Wavelength [Å] | 1.0332 | 0.91841 |
| Temperature [°K] | 100 | 100 |
| Space group | $P2_12_12_1$ | $P2_12_12_1$ |
| Unit Cell Parameters a, b, c [Å] | 71.9; 94.5; 101.3 | 73.1; 59.6; 69.7 |
| Resolution Range [Å][a] | 50.00 – 2.24 (2.38 – 2.24) | 50.00 - 1.90 (2.01 - 1.90) |
| Reflections [a] | 218509 (33751) | 138685 (10835) |
| Unique Reflections | 33402 (5140) | 23671 (1810) |
| Completeness [%] | 99.1 (95.8) | 95.6 (78.2) |
| Multiplicity | 6.5 (6.6) | 5.9 (3.5) |
| | | |
| **Data Quality** [a] | | |
| Intensity $[I/\sigma(I)]]$ | 11.71 (0.92) | 8.96 (0.96) |
| $R_{means}$ [%] | 13.5 (199) | 17.4 (126.8) |
| $CC_{1/2}$ | 99.8 (58.6) | 99.5 (40.9) |
| Wilson B value [$Å^2$] | 53.3 | 32.0 |

| **Refinement** | **gD1** | **gD4** |
|---|---|---|
| Resolution Range [Å][a] | 50.00 – 2.24 (2.33 – 2.24) | 50.00 - 1.90 (2.01 - 1.90) |
| **Reflections** [a] | | |
| Number | 33399 (3181) | 23642 (1792) |
| Test Set (0.5%) | 1669 (159) | 1182 (89) |
| $R_{work}$ [%] | 20.3 (33.8) | 17.5 (30.0) |
| $R_{free}$ [%] | 25.7 (34.0) | 21.5 (37.2) |
| **Contents of Asymmetric Unit** | | |
| Protein, Molecules, Residues, Atoms | 1, 2, 477, 4049 | 1, 1, 244, 2037 |
| $Mg^{2+}$, GlcNAc molecules, glycerol | 2, 5, - | -, -, 4 |
| Water molecules | 132 | 174 |
| **Mean Temperature factors** [Å$^2$][b] | | |
| All Atoms | 58.7 | 31.1 |
| Macromelecules | 58.0 | 30.4 |
| Ligands | 106.7 | 49.9 |
| Water Oxygens | 53.5 | 36.0 |
| **RMSD from Target Geometry** | | |
| Bond Length [Å$^2$] | 0.007 | 0.012 |
| Bond Angles [°] | 0.84 | 1.04 |
| **Validation Statistics** [c] | | |
| Ramachandran Plot | | |
| Residues in Allowed Regions [%] | 2.8 | 2.5 |
| Residues in Favored Regions [%] | 97.2 | 97.5 |
| MOLPROBITIY Clashscore [d] | 3.23 | 3.9 |

[a] data for the highest resolution shell in parenthesis
[b] calculated with PHENIX (Adams et al., 2010)
[c] calculated with MOLPROBITY (Williams et al., 2018)
[d] Clashscore is the number of serious steric overlaps (> 0.4 ) per 1,000 atoms.

**The gD1 dimer interface** In the gD1 dimer interface, two ions, interpreted as magnesium originating from the crystallization solution, are interacting by octahedral coordination with the residues E242 and D261 of both protein chains together with water molecules that complete the coordination sphere (Figure 16a). This interaction could be a hint for a biological role of the dimer.
To evaluate whether recombinant gD of EHV-1 has a homodimeric and/or monomeric form in solution, a SEC profile was analyzed using MALS with buffer composed of Tris-HCl at pH 7,5, 200 mM NaCl, 5% glycerol, and 0,02% sodium azide. The presence of the monomer (approximately 44 kDa) was confirmed with no evidence for a dimer (Figure 17).

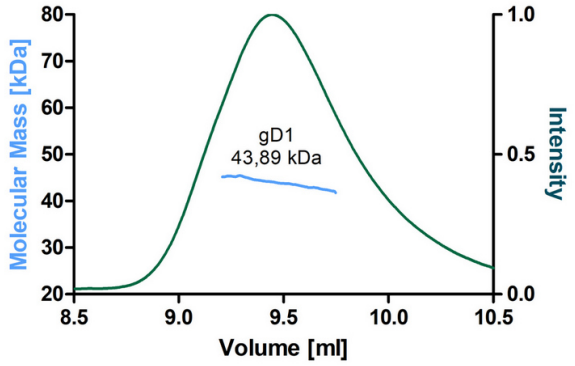


Figure 17: Molecular mass calculations based on SEC combined with MALS analysis for recombinant gD1. Green curve represents the normalized refractive index trace (here named intensity, right y-axis) for gD1 eluted from a Superdex 200 10/300 column. Blue line under the peak corresponds to the averaged molecular mass distribution (left y axis) across the peak.

### 3.4.2. gD4

The structure of the EHV-4 gD monomer was solved with a resolution of 1,9 Å (Figure 16b) using the gD1 structure for molecular replacement and refined to an $R_{work}$ of 17.5% and $R_{free}$ of 21.5% (Table 3, PDB-ID 6TM8). Interestingly, no glycosylations were visible. Instead, electron density was present for four glycerol molecules originating from the cryoprotectant. In total 244 residues could be modeled (R34 to R277) and the protein has the common Ig V-like structure with only small deviations from the gD1 structure.

## 3.5. Comparison of gD1, gD4, and homolog structures

The amino acid sequence identity between EHV-1 and 4 is with 76% very high, whereas the overlap with HSV (25%, GenBank AAK19597.1) and PrV ( 34%, GenBank AEM64108.1) gD is lower. Despite the low sequence identity the overall fold is strikingly similar between these proteins (Figure 19) which becomes apparent in a sequence alignment on the basis of secondary structures (Figure 20). This similarity is also reflected in the root-mean-square deviations (rmsds) when using Secondary Structure Matching (SSM) superposition (Table 4). All of the gD molecules share the IgV-like core wrapped by $\alpha$-helices and loops. The core, comprising A' until G, is structurally very well conserved as visualized by the ConSurf server (Ashkenazy et al., 2016) (Figure 18).
Most $\alpha$-helices and $\beta$-sheets differ slightly between the EHV-1/EHV-4 and PrV/HSV-1/
HSV-2 gDs (PDB ID HSV-2: 4MYV) in length and are shifted. Also the loop regions are mostly comparable in length between the gD structures but not in orientation. The region aa 68 to 77 (numbering based on gD1 aa sequence) in front of A' seems to be generally flexible in all of the compared proteins, except in HSV-1 and 2 gD where it is overlapping in most parts. The loop region aa 54 to 64 resembles the same orientation but is shifted by approximately 2,8 Å between gD1 and gD4, whereas in gD of PrV and HSV-1/2 the orientation is different from gD1/4 but is comparable among themselves.
The number of sheets is the same, however the number of helices differ between gD homologs. In gD1, gD4 and PrV gD an additional $\alpha$3' is visible which is not present in HSV-1 gD. Furthermore,

in PrV gD two helices, termed $\alpha$1' and $\alpha$2', are observed preceding sheet D and $\alpha$2, respectively (Figure 20).
The six disulfide bonds are conserved across EHV-1, EHV-4, PrV, and HSV-1 gD (Figure 20, yellow boxes) while the glycosylation sites, visible in the crystal structure of gD1 and predicted for gD4, are only conserved between EHV-1 and EHV-4 (Figure 20, green dots). Between gD1 and gD4, also the magnesium coordinating residues seen in the gD1 dimer interface are conserved. In HSV-1 and 2 gD, the $\alpha$2' helix is kinked and the $\alpha$3 helix is bent (Figure 19b) (no structural information are available for this region in HSV-2) which is not seen in the other gD structures. The N-termini of EHV-1, EHV-4, and HSV-1 gDs are structurally similar from aa 44 on (no structural information available for HSV-2) but shifted between gD1/4 and HSV-1 gD by approximately 8,5 Å. Notably, in gD1 and gD4 the N-termini ahead of aa 44 point in opposite directions. The N-terminal residues in PrV gD are shifted by approximately 6 Å in the other direction than HSV-1 gD N-terminus based on the position of gD1/4. The C-termini of gD1 and gD4 deviate from Q268 on and move in opposite directions, in a similar manner as the N-termini. PrV and HSV-1 gD C-terminal residues follow the same orientation as in gD1, however, there is a shift of the loop region between aa 266 and 274 of approximately 4,7 Å (based on gD1).

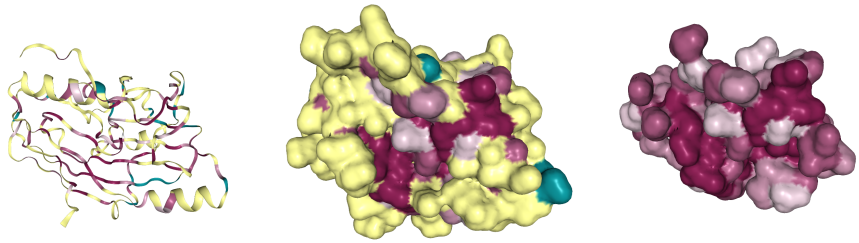

(a) Backbone of gD1 (b) Surface of gD1 (c) Surface of conserved region in gD1

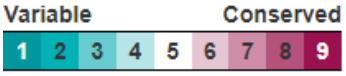


(d) Conservation scale

Figure 18: Conservation of gD1 calculated by the ConSurf server (Ashkenazy et al., 2016) using the structure of gD1 (PDB ID 6SQJ) chain B. (a) orientation of molecule backbone in cartoon representation, (b) surface representation of the whole protein structure, (c) surface representation of the conserved core region with a conservation level >5 according to the legend in (d).

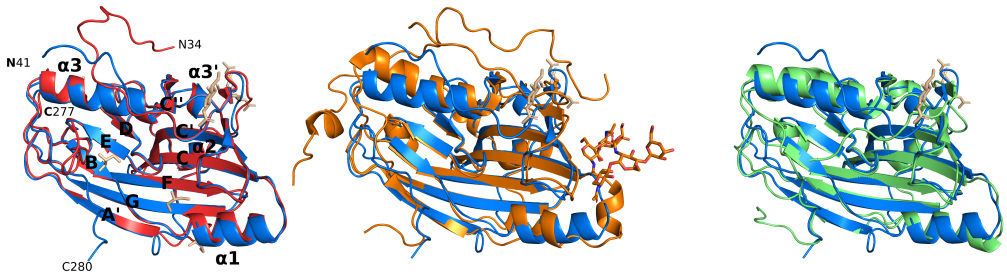


(a) EHV-1 and 4 gD (b) EHV-1 and HSV-1 gD (c) EHV-1 and PrV gD

Figure 19: Superposition of crystal structures of gD from EHV-1 (blue, PDB-ID 6SQJ), EHV-4 (red, PDB-ID 6TM8) HSV-1 (orange, PDB-ID 2C36) and PrV (green, PDB-ID 5X5V) gD.

Table 4: Comparison of rmsd from SSM of all atoms between gD molecules of different alphaherpesviruses.

| gD molecule of | rmsd (Å) | nr. compared residues |
|---|---|---|
| EHV-1 – EHV-4 | 0.71 | 220 |
| EHV-1 – HSV-1 | 2.18 | 238 |
| EHV-1 – PrV | 2.73 | 232 |
| EHV-4 – HSV-1 | 1.79 | 204 |
| EHV-4 – PrV | 2.04 | 211 |
| HSV-1 – PrV | 1.96 | 242 |

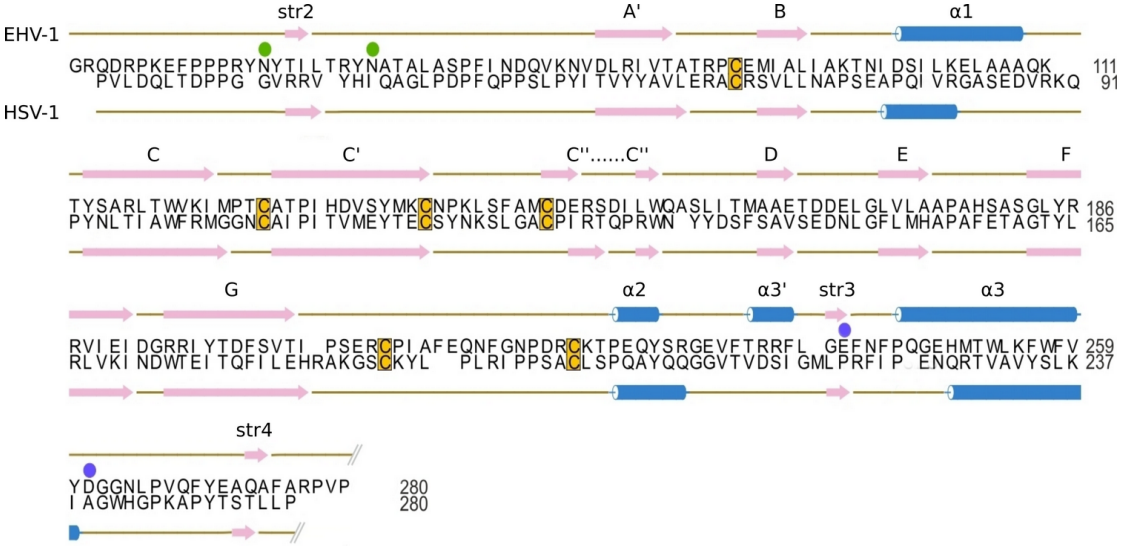


(a) gD of EHV-1 and HSV-1

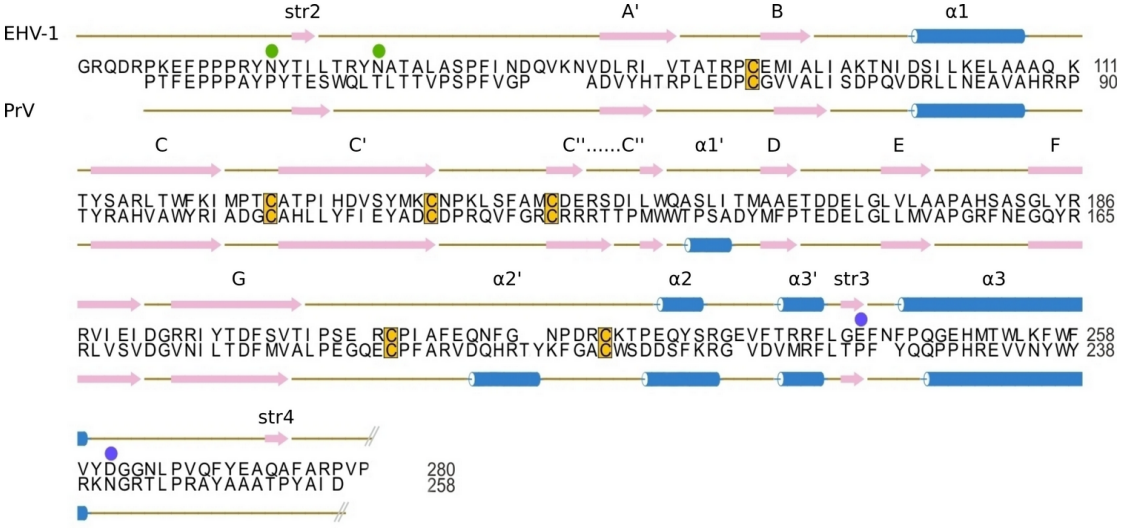


(b) gD of EHV-1 and PrV

Figure 20: Structural alignment of gD1 with HSV-1 (PDB ID 2c3a) and PrV (PDB ID 5x5v) gD according to dssp (Kabsch and Sander, 1983). Sheets are indicated as pink arrows, helices as blue cylinder, disulfide bonds as yellow boxes, glycosylation sites in gD1 as green dots, and magnesium coordinating residues in gD1 as purple dots. Labels are as in Li et al. (2017).

## 3.6. Testing the biological functionality of recombinant gD1, gD4, gD4$_{36\text{-}280}$ and MHC-I

To test whether the recombinant proteins gD1, gD4 and gD4$_{36\text{-}280}$ are functional in terms of their ability to compete with native gD in the virus envelope during entry into ED cells, flow cytometry and plaque assays were performed. Additionally, SPR analysis was conducted to evaluate the binding affinity of the proteins to recombinant MHC-I.

### 3.6.1. Recombinant proteins are correctly folded and functional

To examine the functionality of soluble gDs, ED cells were pre-incubated with proteins in concentrations ranging from 0 to 150 µg, (0 - 3,5 µM). Cells were infected with a MOI of 0,1 for flow cytometry analysis and a range of 60 to 200 plaque forming units (PFU) for plaque reduction assay. Viruses expressing GFP during early infection were used to monitor and analyze the infection levels.
In flow cytometry assay a dose dependent reduction of infection of 50% and 32,67% on average (maximal 67 and 49%) was observed for gD1 and 4, respectively (Figure 21). Plaque numbers decreased on average by 50,8% and maximally by 87% for EHV-1 infection using gD1 to block entry. For EHV-4 the infection was blocked on average by 31,5% and maximally by 53% using gD4 to reduce the infection. Interestingly, gD4 also blocked the entry of EHV-1 by 40,25%. Likewise, gD1 reduced EHV-4 infection by 28,58%. In general, EHV-1 gD proved to be more efficient in blocking infections.
The gD4 variant lacking the C-terminal membrane-proximal residues gD4$_{36\text{-}280}$ exhibits a reduction in EHV-4 infection efficiency of 45,75% (ranging from 39 to 49,5%) and is thus slightly more potent than the full length gD4 (31,5%), which showed a wider range of blocking from 15 to 73% (Figure 22).
To examine whether recombinant MHC-I can be used to block the virus entry into cells, EHV-1 and 4 were incubated for 1 h on ice with 3,5 µM soluble protein, added to ED cells. The infection was analyzed after 24 h incubation by flow cytometry (GFP positive cells) and plaque reduction assay (number of plaques). No decrease in infection was observed.
Taken together, all recombinant gDs compete with native protein from the viral envelope. A dose dependent reduction of infection can be seen for gD1 and gD4. Notably, both recombinant gDs were able to efficiently block the entry of EHV-1 and EHV-4. These results suggest that the proteins are correctly folded and functional in terms of competing with native gD in the viral envelope. Soluble MHC-I seems to be ineffective in blocking the entry of EHV-1 and 4.

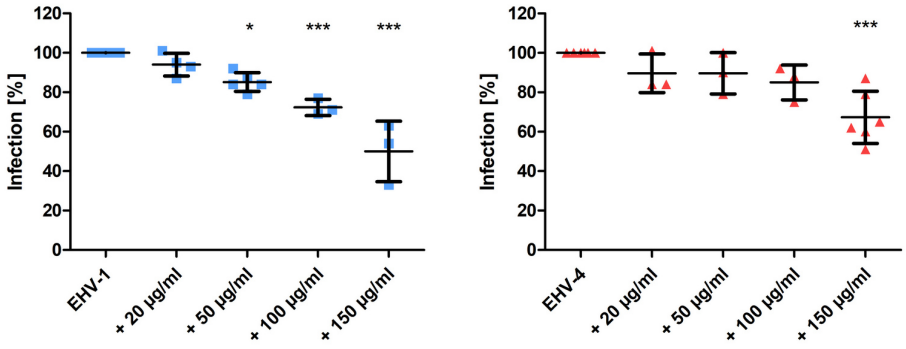


(a) EHV-1 with gD1

(b) EHV-4 with gD4

Figure 21: EHV-1- (strain RacL11) and EHV-4-GFP (strain TH20p) virus entry into ED cells blocked by different concentrations of gD1 and 4 and analyzed by flow cytometry. Cells were incubated with soluble protein for 1 h on ice and infected at MOI 0,1. After 1 h virus on cell surface was removed with citrate buffer and GFP levels were analyzed after 24-48 h by flow cytometry. The experiment was repeated independently at least three times for each concentration. GFP levels were normalized to infection levels without recombinant proteins. Statistical analysis was done using one-way ANOVA Bonferroni's multiple comparison test, * indicates P≤0.05, ** indicates P≤0.01, *** indicates P≤0.001. Error bars represent mean with standard deviation (SD).

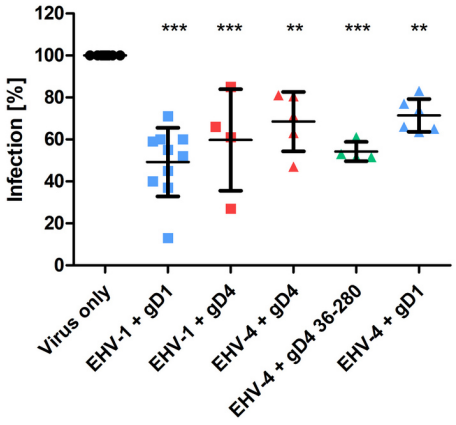


Figure 22: Plaque reduction assay of EHV-1- (strain RacL11) and EHV-4-GFP with recombinant protein. ED cells were incubated for 1 h on ice with 150 µg/ml gD1, gD4 or $gD4_{36\text{-}280}$ and infected with virus at 60-200 PFU. After 1 h virus on cell surface was removed with citrate buffer and cells overlaid with methyl cellulose GFP plaques were counted after 48 h. The experiment was repeated independently at least three times for each protein. Plaque numbers were normalized to infection levels without recombinant proteins. Statistical analysis was done using one-way ANOVA Bonferroni's multiple comparison test, * indicates P≤0.05, ** indicates P≤0.01, *** indicates P≤0.001. Error bars represent mean with SD.

### 3.6.2. Soluble gD1 and gD4 engage recombinant MHC-I with similar binding affinities

To study the interaction of soluble gDs with recombinant MHC-I, surface plasmon resonance (SPR) binding assay was conducted. This work was done in line with our collaboration with Professor Salvatore Chiantia, University of Potsdam, Cell Membrane Biophysics Group. The SPR analysis was done by Ismail Dahmani. Recombinant MHC-I was immobilized on the sensor chip by amine-coupling and soluble gDs were allowed to flow over the chip as analyte. For calculation of the $K_d{}^{app}$ with the Hill-Wand equation, the control sensograms were subtracted from the reaction sensograms. Additionally it was tested whether MHC-I (6000 nM) can bind to amine-coupled gD1. The affinity was determined to be low with 175 RU.
As an initial negative control, gD1 was coupled to the chip and also used as analyte (6980 nM). A signal of 950 RU was obtained, in contrast to 2010 RU for gD1 binding to amine-coupled MHC-I. Second, the binding of gD1 (6980 nM) to a chip coated with poly-L-lysine with positively charged nanogels (size 214 nm) (Dey et al., 2018) was tested and 760 RU were observed, which is a slightly better control and was used as negative control for subsequent experiments (Figure 23a).
Binding kinetics for soluble gDs to coupled MHC-I were characterized using a protein dilution series in a range of 0 to 13 950 nM (Figure 23b). The calculated affinity ($K_d{}^{app}$) for gD1 was determined to be 3996 ± 840 µM, for gD4 4413 ± 1200 µM, and for $gD4_{36\text{-}280}$ 5288 ± 1233 µM (Table 5).
These results show that soluble gDs are interacting with recombinant MHC-I with high specificity but moderate affinity.

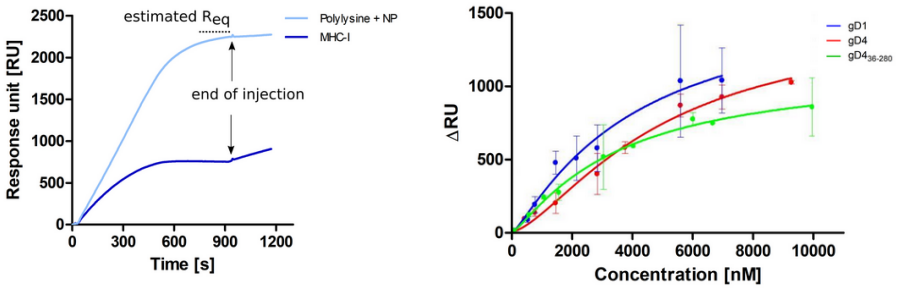


(a) (b)

Figure 23: SPR analysis. (a) SPR sensograms for gD1 flowing over amine-coupled MHC-I (reaction sensogram, dark blue curve) and polylysine with nanogels (Dey et al., 2018) (control sensogram, bright blue curve). (b) $K_d{}^{app}$ calculated with the Hill-Wand equation obtained for different gD concentrations from at least three independent experiments. Displayed are means with SD.

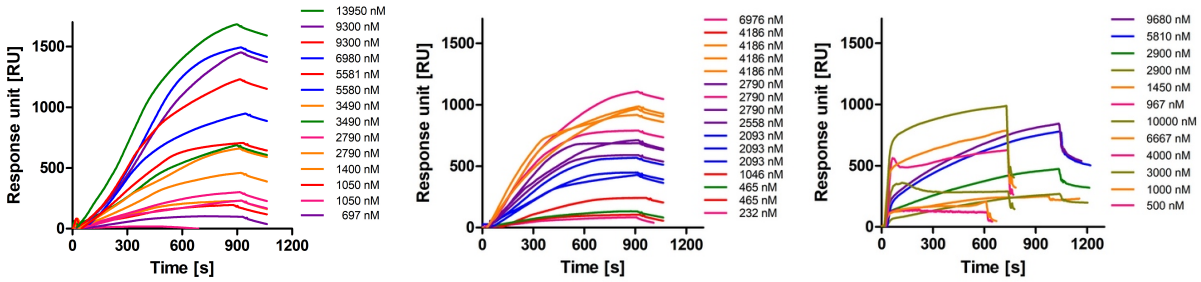


(a) gD1 (b) gD4 (c) $gD4_{36\text{-}280}$

Figure 24: SPR sensogram profiles of recombinant gDs in gradient concentrations flowing through amine-coupled recombinant MHC-I. Data is presented for independent experiments and control sensograms were subtracted from reaction sensograms (a) gD1 n=6, (b) gD4 n=5, (c) $gD4_{36\text{-}280}$ n=3.

Table 5: Parameters obtained from SPR binding curves of gD1, gD4, and $gD4_{36\text{-}280}$. $R_\infty$ is the maximum coverage of bound protein, $K_d{}^{app}$ is the apparent dissociation constant of the protein from the immobilized MHC-I on the sensor chip, $n$ corresponds to the number of independent experiments.

| **Protein** | **$R_\infty$ (RU)** | **$K_d{}^{app}$ (nM)** | ***n*** |
|---|---|---|---|
| gD1 | 1672 ± 286 | 3996 ± 840 | 6 |
| gD4 | 1435 ± 300 | 4413 ± 1200 | 5 |
| $gD4_{36\text{-}280}$ | 1550 ± 180 | 5288 ± 1233 | 3 |

## 3.7. Generation of gD1/4-MHC-I binding hypothesis

While the crystallization trials for the gD-MHC-I complex were ongoing, the structural data of gD1 and gD4 was used by Szymon Pach from the Molecular Design lab at Freie Universität Berlin of Professor Gerhard Wolber to generate binding hypotheses of gD1/4-MHC-I by protein-protein docking and molecular dynamics experiments.
The binding modes of gD1 (Figure 25a) and gD4 to MHC-I (Figure 26a) differ only slightly and show the most stable orientation towards MHC-I in a position that is strikingly similar to HSV and PrV gD–nectin-1 complex (Figure 26b). Further investigation of the gD1/4-MHC-I protein-protein interactions (PPIs) resulted in binding hypotheses with observed stable ionic contacts between R169 of MHC-I and $\pi$-cation interactions D261 and W257 of gD1. Hydrophobic contacts can be found between MHC-I I104/Y108/I166 and gD1 A157/I160/F213 together with an extensive hydrogen bond network between E43 and R103 of MHC-I and gD residues E242

and R59, stabilizing the protein-protein complex (Figure 25b). These main interacting residues are the same in gD4 binding MHC-I, except for the residue N157 that is alanine in gD1, which has only a weak influence on the binding.
The key residues R169 and Y108 of MHC-I implicated in our binding hypothesis are conserved between genotypes allowing the entry of EHV-1 and 4 (Azab et al., 2014) which supports the binding hypothesis. This hypothesis can be further investigated by introducing mutations into MHC-I and EHV-1 and 4 gD. First, point mutations in EHV-1 and 4 gD were generated for evaluation of phenotypic changes.

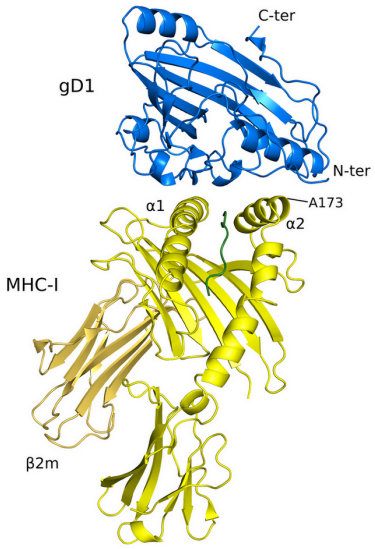


(a) Binding hypothesis gD1-MHC-I

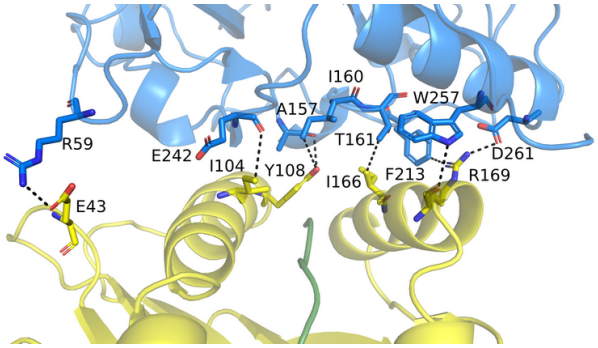


(b) Main interacting residues

Figure 25: Binding hypothesis of gD1 with MHC-I. (a) Backbone in cartoon representation of gD1 (blue) docking pose to MHC-I (gold with green peptide) following MD simulations. (b) Main interacting residues in the gD1-MHC-I interface in stick-model. R169 of MHC-I and D261 and W257 of gD1 form ionic contacts, MHC-I I104/Y108/I166 and gD1 A157/I160/F213 form hydrophobic contacts, and an extensive hydrogen bond network is observed between E43 and R103 of MHC-I and gD residues R59 and E242.

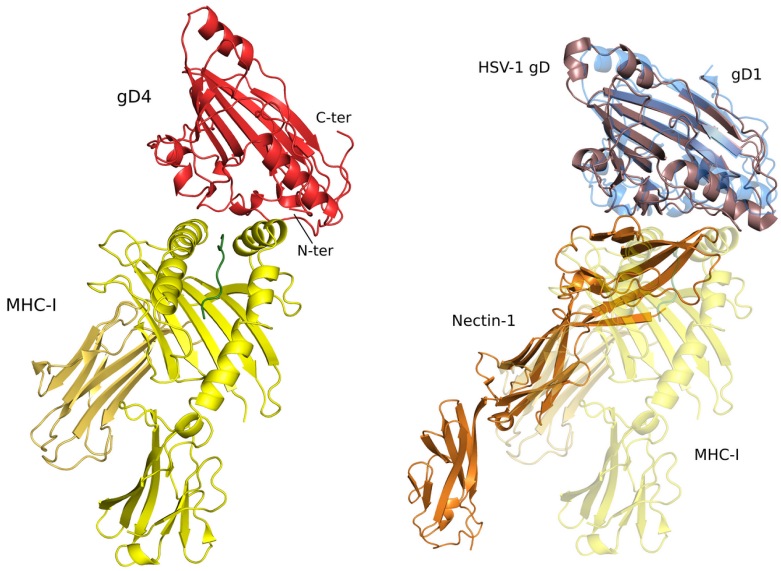


(a) Binding hypothesis gD4-MHC-I

(b) HSV-1 gD-nectin-1

Figure 26: Backbone in cartoon representation of (a) gD4-MHC-I (red and gold, green peptide) binding hypothesis, (b) HSV-1 gD binding nectin-1 (brown and orange, PDB ID: 3U82) aligned with hypothesized docking pose of EHV-1 gD-MHC-I (blue and gold).

## 3.8. Mutating F213A and D261N in EHV-1 and 4 gD leads to growth defects

The gD1/4-MHC-I binding hypotheses (Figure 25) were further investigated by mutating the proposed key residues F213 to alanine and D261 to asparagine in EHV-1 and 4 gD. Two-step Red-mediated mutagenesis (Tischer et al., 2006) was performed on EHV-1 (strain RacL11) and EHV-4 BACs and multi-step growth kinetics used for characterization.
All mutant viruses were successfully reconstituted from mutated BACs (Figure 27) and the modified gD gene sequences confirmed by Sanger sequencing (primer pair WA1/2, see table 2.1.5). However, only EHV-1 $gD_{F213A}$ was evaluated in growth kinetics (Figure 28b) where it displayed a significant 2-log reduction in growth and low titers in cell supernatant compared to wild type. Reverting the mutation rescued the growth.
The virus mutants EHV-1 $gD_{D261N}$, EHV-4 $gD_{D261N}$ and EHV-4 $gD_{F213A}$ did not grow to an extent where growth kinetics could be performed. EHV-1 $gD_{D261N}$ reverted back to wild type twice in the first passage in ED cells. When the mutant did not revert back, it produced very low plaque numbers and was unable to replicate beyond the second passage in ED cells. Reversing the mutation restored the wild type growth (Figure 28a).
The mutants EHV-4 $gD_{D261N}$ and EHV-4 $gD_{F213A}$ could be grown in ED cells over several passages, however, the growth was very slow. Wild type and revertant EHV-4 can be grown after reconstitution from BAC in a 10 cm culture dish to 100% cytopathic effect (CPE) in approximately one week. The mutants were growing under great care for more than two weeks before reaching a CPE of approximately 60%.
Taken together, the mutations $gD_{D261N}$ and $gD_{F213A}$ lead to replication-deficient viruses in EHV-1 and EHV-4.

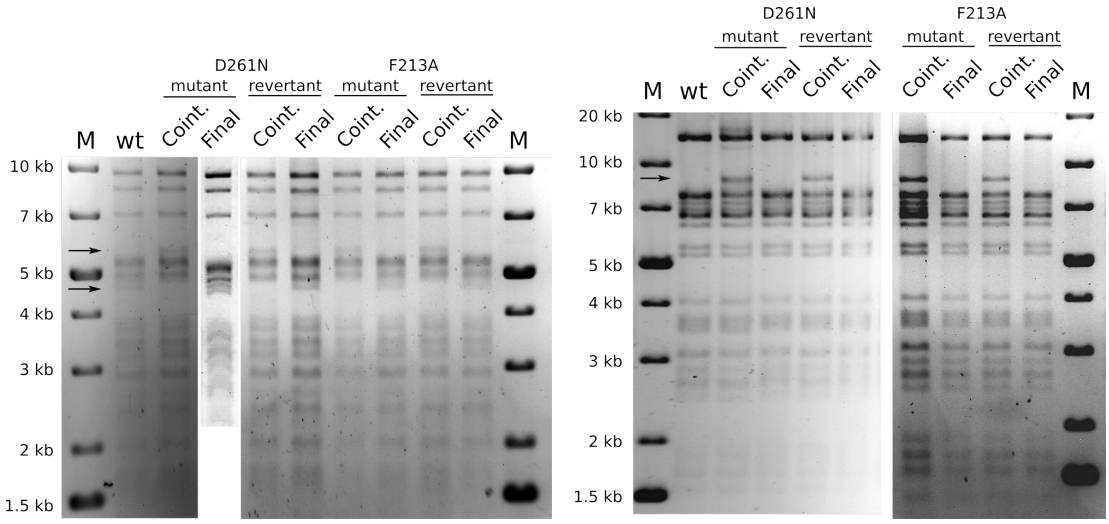


(a) EHV-1 (b) EHV-4

Figure 27: Purified BAC DNA of EHV-1, EHV-4, EHV-1 $gD_{D261N}$, EHV-1 $gD_{F213A}$, EHV-4 $gD_{D261N}$, EHV-4 $gD_{F213A}$ from final clones and intermediate clones with kanamycin cassette was digested using Pst-I HF, loaded onto a 0,8% agarose gel together with a 1 kb DNA ladder and run for approximately 15 h at 55 V. wt = wild type virus, C = Kana-intermediate (Co-integrate), F = final mutant. Arrows indicate band shifts resulting from integration of the Kana-cassette.

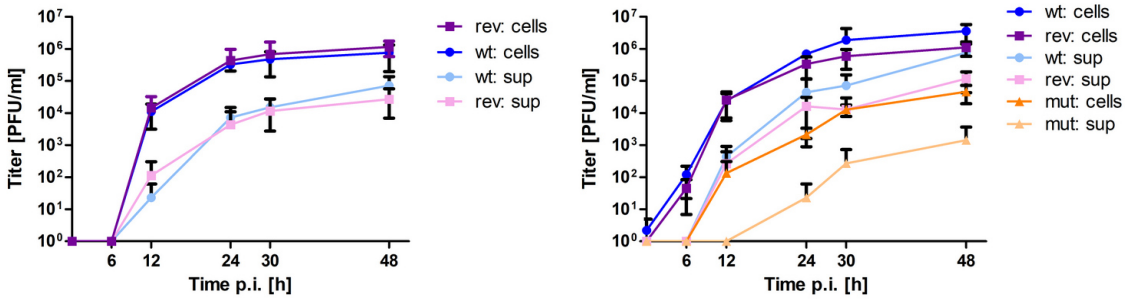


(a) EHV-1 $gD_{D261N}$ revertant (b) EHV-1 $gD_{F213A}$ + revertant

Figure 28: Multi-step growth kinetics of EHV-1-GFP (strain RacL11) wild type and gD mutants. ED cells were infected with an MOI of 0,01, cells and supernatant collected separately at indicated time points post infection and titrated. Represented are means with SD of three independent experiments. (a) EHV-1 wild type (blue colors) and $gD_{D261N}$ revertant (violet colors) viruses. (b) EHV-1 wild type (blue colors), $gD_{F213A}$ (orange colors) and revertant virus (violet colors).

# 4. Discussion

## 4.1. Proteins can be produced in insect cell culture

The proteins gD1, gD4, $gD4_{36\text{-}280}$, $\beta$2m and MHC-I complex were successfully produced in insect cells using recombinant baculoviruses. The $\alpha$-chain of MHC-I alone could not be synthesized in insect cells. The $His_6$-tag and TEV cleavage site might be interfering with the expression. To further investigate the production of the $\alpha$ chain in insect cells, the tag and cleavage site could be swapped to the C-terminus.
A two step purification process using IMAC and SEC (Figure 10, 12) yielded highly pure protein which could be concentrated up to 25 mg/ml for crystallization experiments and further assays after optimization of the purification procedure.

## 4.2. Contribution of glycosylations to the molecular weight of recombinant proteins

The molecular masses of recombinant gD1 measured by SDS-PAGE (Figure 12), Western blot (Figure 13), MS (43,1 kDa), and MALS (approximately 43,9 kDa) are in agreement with predictions when taking into account PTMs like glycosylations and that protein masses on SDS-PAGE are generally overestimated (Matsumoto et al., 2019). The contribution of sugars to the molecular masses for the recombinant proteins produced in this study is yet to be determined exactly but based on the values obtained by mass spectrometry it is expected to be approximately 4 kDa for the four predicted glycosylation sites of gD1 and 4. That value is congruent with glycosylations commonly seen in proteins produced in insect cells where the mass contribution ranges from 700 to 900 Da for one glycosylation site (Wedde et al., 2007). The low signal for gD1 and gD4 in MS analysis may be explained by heterogeneity of glycosylations (Shi and Jarvis, 2007).
In other studies, the contribution of glycosylations to the molecular mass of gD1 has been described to be higher. Full length gD1 with a predicted molecular mass of 41 kDa, including the transmembrane region (TM), has been produced previously using the baculovirus system and yielded protein with sizes of 48, 52, and 56 kDa (IPLB-Sf21-AE cells, 0 to 96 h post infection) (Love et al., 1993), 55 (high mannose-type oligosaccharides) and 58 kDa (complex-type oligosaccharides) (in Sf9 cells, 24 h post infection) (Flowers et al., 1995b), and 58 and 65 kDa (High5 cells, 48 h post infection) (Fuentealba et al., 2014). The unglycosylated full length gD1 has been described to have a mass of 43 kDa (Flowers et al., 1995b), which does conform to a certain extend to the theoretical value for the full length protein. That would translate to a contribution of 5 to 22 kDa to the molecular weight by glycosylation.
Full length gD1 and gD4 from viruses grown in fetal horse kidney (FHK) cells displayed a molecular weight of approximately 55 kDa, with gD1 showing a wider range of glycosylation species than gD4 using SDS-PAGE with specific monoclonal antibodies (Azab and Osterrieder, 2012). Thus, the contribution of glycosylations would be 12 kDa from mammalian cells, based on 43 kDa without glycosylations (Flowers et al., 1995b). This suggests that recombinant gD1 in previous studies was glycosylated to a higher degree than in the current study.
Accounting for that variations could be the different processing of glycosylations in insect and mammalian cells. Insect cell lines add shorter N-glycans with little sialylation to proteins than mammalian cell lines (Betenbaugh et al., 2004; Shi and Jarvis, 2007), which would explain the weight differences between recombinant gDs in the current study and the one conducted by Azab and Osterrieder (2012). However, it does not explain the higher weight contribution of up to 22 kDa in studies where gD1 was produced in insect cells as well (Love et al., 1993; Flowers et al., 1995b; Fuentealba et al., 2014).

Another explanation might be that in previous studies the apparent molecular mass was solely determined by SDS-PAGE, which is known to overestimate protein mass especially in posttranslationally modified proteins (Matsumoto et al., 2019). Also in the present study, protein mass seems to be higher when determined by SDS-PAGE and western blotting.
Notably, in previous studies, recombinant gD1 consisted mainly of a mixture of different glycosylations species present at distinct time points. In the current study, a single clear band was visualized by western blotting and on Coomassie stained SDS-PAGE, suggesting that only one glycosylation species of gD1 and gD4 were present.
Taken together, the here produced recombinant gDs were shown to be functional with short glycosylations added by insect cells and it can be concluded that these PTMs do not interfere greatly with entry into the host cell. To determine the exact size of the here produced recombinant proteins and molecular weight contribution of glycosylations, MS should be repeated with glycosylated and PNGase F deglycosylated protein.
The role of glycosylations in the interaction of alphaherpesvirus gDs with their receptors has not been addressed extensively to date, although glycans are known to affect protein conformation and receptor binding. To assay the impact of gD glycosylations, glycosylated and deglycosylated proteins produced in insect cells along with proteins from mammalian cells could be tested in plaque reduction assays and by SPR. To identify the glycosylation profile, further MS analysis should be conducted. Additionally, virus mutants lacking glycosylation sites could be tested in infection assays.

## 4.3. Proteins produced in *E. coli* are in insoluble form of inclusion bodies

All proteins, except $\beta$2m, could be produced in *E. coli* as well, however, in the insoluble form of inclusion bodies. The $\beta$2m construct failed due to a frame shift after cloning which was not tackled since the focus was on the baculovirus system for protein production. It is possible to isolate the recombinant proteins from inclusion bodies using buffers containing 4 M urea (Figure 8). However, this procedure unfolds the proteins and requires refolding which could lead to misfolding and was not conducted in this study. In earlier work, soluble gD of EHV-1 has been produced successfully using isopropyl-$\beta$-D-thiogalactopyranosid (IPTG) induced HB2151 *E. coli* cultures at 30 °C which were infected with gD1 specific phages (Molinková and Celer, 2006). In the current study, auto-induction with transformed Rosetta cultures at 15-20 °C was employed. For a higher protein yield and a less laborious protocol than needed for insect cell culture, the IPTG induced system should be tested to produce gD1, gD4, $\beta$2m, and the MHC-I $\alpha$-chain. Moreover, the *E. coli* strain could be changed. In this work the Rosetta strain was used for enhanced protein expression. The strain BL21 C41 harbors mutations that provide a higher resistance against toxic proteins and might produce soluble proteins. The functionality of these proteins would need to be tested by blocking assays or SPR since it has been shown that receptor binding of EHV-1 is dependent on glycosaminoglycans (GAGs), although it is not yet clear if the GAGs play a major role on the cellular receptor or virus ligand site. (Osterrieder, 1999; Frampton et al., 2005).

## 4.4. Crystallization

The gD1 and 4 crystals were difficult to reproduce, however, it should be evaluated if the crystals contain the C-terminus of the protein which is not visible in the electron density. It is likely that during the crystal growth, the protein was degraded by proteases. It could be examined by MS since the number of crystals is not sufficient for analysis on Coomassie stained SDS-gels.
Interestingly, 8 days old gD4 crystals did not diffract whereas those mounted a year later lead to a structure of 1,9 Å resolution. Although MHC-I was present in the crystallization solution,

the size for the asymmetric unit is too small to accommodate the MHC-I-gD4 complex. Instead one molecule of gD4 is located in the asymmetric unit. The gD-MHC-I complex formation in the crystal should be tested by MS as well, since no complex is observed in SEC but in SPR analysis.
To optimize and accelerate the crystallization process, micro-seeding with small crystals from previous trials could be employed (Bergfors, 2003). Additionally, the proteins could be deglycolsylated since the complex sugar structures might slow down the crystallization or prevent a well ordered crystal needed for X-ray diffraction experiments. Another reason for the missing electron density of the C-terminus could be a high flexibility, which has been shown for HSV (Krummenacher et al., 2005) and suspected for PrV gDs and is in agreement with flexibility predictions for the EHV-1 and EHV-4 gDs (`https://fold.weizmann.ac.il/fldbin/findex`).
In similar PEG conditions, crystals of $gD4_{36\text{-}280}$ and MHC-I were harvested but did not diffract. Further optimization of the crystallization should focus on micro-seeding to accelerate crystal growth in buffers with a pH ranging from 6 to 8, containing 25 to 30% high molecular weight PEGs.

Other methods aside from crystallization might be suitable to model the structure of single MHC-I and EHV-1 and 4 gD together with the receptor-ligand complexes. Recently, near-atomic-resolution structures were obtained with cryogenic electron microscopy (cryo-EM) of proteins <100 kDa (Merk et al., 2016). To increase the size of the protein from approximately 45 kDa of single molecules and the complexes of 90 kDa to a molecular mass easier to resolve by this technique, antibodies (Wu et al., 2012) or nanobodies (Rasmussen et al., 2011) could be used.

## 4.5. The structure of free gD1 and gD4 alone cannot explain differences in virus tropism

For the first time, the crystal structures of free gD1 and gD4 were obtained. The structures are remarkably similar and display the common V-like Ig fold at their core, surrounded by long termini as in gD homologs of HSV and PrV. Differences between gD1 and 4 are visible as small shifts in loop regions, which could be functional or be caused by the influence of sugar and glycerol molecules, respectively. The N- and C-termini are flexible and, notably, point in opposite directions. The function of the gD4 C-terminus is yet unknown, whose orientation deviates not only from EHV-1 but also from PrV, and HSV-1 gD . The divergence might be an artifact of an interaction of crystal contacts or a glycerol molecule in close proximity, however, it could also play a role in receptor binding or tropism.
Since the C-termini of gD1 and gD4 are missing in the structures (aa 281-347 and aa 277-347, respectively), their role during entry and the orientation of the molecules in the viral envelope cannot be analyzed. This information is also not available for gD homologs, except for the HSV-1 gD C-terminus which has a functional role in the entry mechanism (Krummenacher et al., 2005) and is further discussed in section 4.5.2.
Both proteins are globular and the surface charge is mostly similar with one exceptions in the region $\alpha$3 to str3 where it is reversed. Removing six residues of the flexible gD4 N-terminus that points in the opposite direction than in gD homologs, the surface charge becomes more similar, leaving only a small patch around V249 with a positive charge in contrast to a negative in gD1 (E249). The sequence in the region covered by the N-terminus is rather variable with 60% (aa 235-260, Figure 29) between gD1 and 4 compared to the overall sequence identity of 76% and could be involved in the differing tropism of EHV-1 and 4. This could be tested by swapping this region between the viruses and test the infection in different cell lines.
Based on the crystal structures of free gD1 and 4, there is no clear evidence for the differences

```
Identities:15/25(60%), Positives:18/25(72%), Gaps:0/25(0%)

gD1_235-260    FTRRFLGEFNFPQGEHMTWLKFWFV  25
               +T RFL EFN+ QG H+ W K WFV
gD4_235-260    YTSRFLSEFNYRQGVHLAWVKHWFV  25
```

Figure 29: Amino acid sequence alignment of gD1 and gD4 aa 235 to 260 using `https://blast.ncbi.nlm.nih.gov/Blast.cgi`.

in tropism of EHV-1 and EHV-4 nor for the slower development of EHV-4 infections *in vitro*. The opposite orientation of the termini in both proteins, together with small differences in the structures could give hints but additional data is needed since these observations could be artifacts from protein crystallization. Structural data of the full C-termini and structures of the ligand-receptor complex along with the knowledge of the receptor range used by EHV-1, will give more insights into the entry mechanism of EHV-1 and 4.

### 4.5.1. Insights on EHV-1 and 4 gD mutational study

In an attempt to decipher the region of EHV-1 and 4 gD binding to entry receptors and defining the host cell tropism, mutations were introduced into the gD gene of EHV-1 and 4 using BAC mutagenesis. Parts of the gene were either deleted or replaced by the gene of the other virus (Azab and Osterrieder, 2017) based on HSV-1 and 2 constructs (Carfi et al., 2001; Connolly et al., 2003, 2005).
Mutating Y60 to alanine did not affect viral growth. In HSV-1 gD binding nectin-1, the homolog residue Y38 has been shown to be essential. Mutations to alanine or the formation of a disulfide bridge between Y38C and A3C interfered greatly with receptor binding (Connolly et al., 2005). In the crystal structures, the loop region around Y60 in EHV-1/4 are shifted by 5,1/4,3 Å from the homolog Y38 in HSV-1 gD (PDB ID: 2C36). Responsible for this shift is the C-terminus in HSV-1 gD, locked by cross-linking. According to the gD1/4-MHC-I binding hypothesis , Y60 of gD1 does not play a major role in the receptor interaction and considering the here presented results an essential part of Y60 in EHV-1 and 4 entry into the host cell can be omitted.
The deletion of amino acids 7 to 31 following the signal peptide cleavage site (D42 to A66), lead to a dead virus. Replacing this sequence in EHV-1 with the same region of gD4, did not change tropism and restored the virus growth to wild type level, which is astonishing as the sequences identity in that region is 76%. Nevertheless, the structure is conserved among EHV-1 and EHV-4 and wraps closely around the protein (Figure 30). Interestingly, the truncated version of gD4, $gD4_{45\text{-}276}$, could not be produced in insect cells. Both results suggest that the N-terminal part of gD plays, as previously suggested, an integral part in the structural stability and possibly as well in receptor binding.
EHV-1 and 4 with swapped regions aa 42 to 241 or aa 75 to 212 in the gD gene cannot replicate, demonstrating that the differences between the viruses are too big in that region, to be exchanged (Figure 30). Presumably, the termini cannot be properly structured around the core of a different gD, which underlines the importance of the termini for stability and the entry receptor interaction.
Similarly, replacing aa 212 to 347 or aa 75 to 347 in gD1 with the sequence of gD4, produces replication deficient virus with clear EHV-1 tropism and viruses that only infect ED cells, respectively. Both regions cover large proportions of the gD molecules and an influence of the mutations on the surface and with that on receptor interaction are likely. From this data, a clear conclusion about which domains of gD bind to MHC-I cannot be drawn.

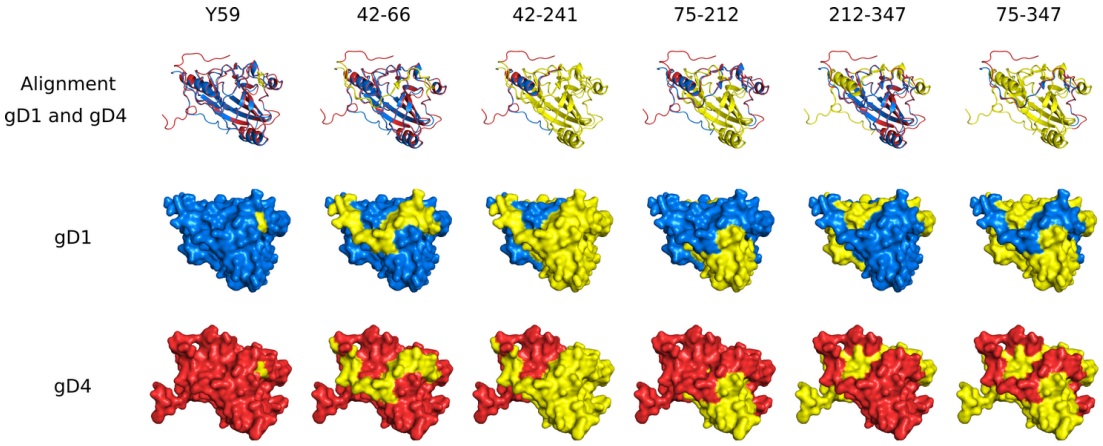


Figure 30: Display of mutated gD1 (blue) and gD4 (red) from a previously conducted study using BAC technology (Azab and Osterrieder, 2017). Each column shows one mutation (yellow), the first row shows the orientation of the gD molecules in cartoon representation. The second and third row show the surface of gD1 and gD4, respectively. GlcNAc and glycerol molecules were removed for clarity.

In summary, structural and functional impacts of all the mutations, even with the structural data of single gD1 and 4 at hand, are generally hard to predict and could be further analyzed using mutated recombinant proteins in blocking assays and SPR analysis. To fully elucidate the receptor interacting residues of gD1 and 4, a structure in complex with MHC-I needs to be solved.

### 4.5.2. Homodimer theory of gD1 and gD4 and the role of the N- and C-terminus in entry

The structure of gD1 was solved as a dimer with two ions in the interface, interpreted as magnesium which are coordinated by conserved residues in EHV-1 and 4 gD. This strong ionic binding and a high Complex Formation Significance Score of 0,765 (PDB Proteins, Interfaces, Structures and Assemblies (PISA) server `https://www.ebi.ac.uk/pdbe/pisa/`) might be a hint that gD1 forms a functional homodimer in the virus envelope.
In HSV-1 a gD homodimer has been observed on the virus envelope by cross-linking experiments (Handler et al., 1996) and in solution by gel filtration (Krummenacher et al., 2005). A functional role of the dimer has been proposed by Krummenacher et al. (2005), when the structure of the C-terminus could be solved for the first time by locking it in the unbound form close to the N-terminus by cross-linking. A structured C-terminus was shown to be essential for efficient entry of the virus into the host cell. However, to allow receptor binding, of HSV-1 gD, the C-terminus needs to be displaced to free the N-terminal binding site. This could be a mechanism to prevent early onset of the fusion machinery before the ligand and receptor are in close proximity.
The dimer is thought to stabilize the C-terminus in the unbound form together with a PxxW site (aa 291- 294 PPNW) in HSV-1 gD. Krummenacher et al. (2013) proposed that all alphaherpesviruses harboring this site, share the same mechanism to control the fusion. EHV-1 and

4 contain PxxW sites (aa 213-216 PFKW) which are not solved in the crystal structures. The HSV-1 gD C-terminus is 14 residues longer ahead of the PxxW site in contrast to EHV-1 and 4 gD. The effect of the shorter distance to the PxxW site in EHV-1 and 4 could be tested by locking the C-terminus using cross-linking similar to what has been done in HSV-1.
The functional and structural role of the HSV gD N-terminus for receptor binding has been elucidated as well. The displacement of the C-terminus upon receptor binding allows the formation of an N-terminal hairpin that is crucial for binding of HVEM which interacts exclusively with N-terminal residues of gD (aa 7-15 and 24-32) (Carfi et al., 2001; Krummenacher et al., 2005; Lazear et al., 2008). The C-terminal displacement is also needed for the complex formation with nectin-1 since the binding sites overlap with those of HVEM with additional C-terminal interactions (aa 35–38, 199–201, 214–217, 219–221, 223) (Di Giovine et al., 2011). The formation of an N-terminal loop is not involved in nectin-1 binding since the deletion of aa 7-32 had little impact on the interaction (Manoj et al., 2004). The hairpin formation is not plausible for EHV-1 and 4 gD as well, since the N-terminus is approximately 20 residues shorter than in HSV gD and would not allow a mode of binding comparable to HSV-1 gD-HVEM. It has been shown experimentally that EHV-1 does not the equine HVEM homolog to enter host cells (Azab and Osterrieder, unpublished data). The same conclusion was reached for PrV gD, which does not bind to HVEM (Li et al., 2017). However, mutational studies of EHV-1 and 4 suggest that the gD N-terminus is involved in the entry (Azab and Osterrieder, 2017) and the binding hypothesis shows the involvement of R59. A crystal structure of the gD-MHC-I complex would reveal more details.
Coming back to the possible function of a gD1 dimer, it has to be noted that the gD1 dimer interface in the crystal structure differs greatly from the HSV-1 gD butterfly shaped dimer. Supposing that the crystal structure of both dimers is the form of the gDs on the virus envelope, the mechanisms for stabilizing and displacing the termini are probably different.
Interestingly, the HSV gD dimer forms a 2:2 complex with nectin-1 and HVEM (Krummenacher et al., 2005). Equine MHC-I, however, is not known to form homodimers on the cell surface, although human MHC-I occasionally does (Campbell et al., 2012). Possibly, gD1 occurs in dimeric and monomoric form to bind different receptors, whereas gD4 may occur only in monomeric form and would, with that, have a more restricted receptor range. However, this theory does not explain the conserved magnesium-coordinating residues in gD1 and 4, but it would explain why the N-terminus of gD4 has a different orientation than seen in homolog structures. Thus, making a dimer as observed in gD1 impossible, providing that the orientation is not an artifact due to the interaction with glycerol or crystal contacts.
One study detected a 102 kDa band from purified EHV-1 strain KyA in western blotting without reducing agents with gD1 specific antibodies which suggested that gD might be a dimer (Elton et al., 1992). For the strain Ab1 no such higher molecular weight band has been detected and it was suggested that an additional cysteine in the C-terminus of KyA gD might be involved in the dimerization. However, the 102 kDa band has not been reproduced to date and might have been an artifact from the purification process or unspecific binding of antibodies.
Contradicting the theory of gD1 forming a functional dimer, are that no dimer was identified by gel filtration, MS, and SEC-MALS (Figure 11, 17) in the current study. However, no $Mg^{2+}$-ions were present in the solution during the experiments except for one SEC experiment which is not further discussed here since no dimer was observed.
The dimer in the crystal structure could have been forced by the dehydration of PEG in the crystallization solution. Although, it is still possible that the affinity between gD monomers is very low, as implicated by the SPR experiments showing an affinity in the µM range and that the protein is being highly diluted on the column in SEC and MALS experiments.
In conclusion, our results point to the dimer rather being an artifact of high protein concentrations

and high molecular weight PEGs in the crystallization buffer than having a biological function. The importance of the N-terminus in binding MHC-I and the role of the C-terminus in activating the membrane fusion need to be evaluated further.
The role of divalent ions in forming the gD1 dimer could be further tested by adding magnesium and in another experiment magnesium plus ethylendiamine tetraacetic acid (EDTA) to the buffer for MALS-SEC, SEC or SPR analysis. If soluble gD dimerizes by ionic contact in the same fashion as seen in the crystal structure, a dimer should be seen in the condition were only magnesium was added. The addition of EDTA in the second condition should complex the ions and prevent dimerization. In the manner, affinity in SPR should increase in the presence of EDTA and a gD–MHC-I be detectable in analytical SEC.

## 4.6. Affinity of soluble gD1 and gD4 to recombinant MHC-I

Characterization of soluble gD1, gD4 and $gD4_{36\text{-}280}$ affinities showed specific binding to amine-coupled recombinant MHC-I in SPR analysis with comparable $K_d{}^{app}$. EHV-1 and 4 gD appear to have lower binding affinities towards MHC-I than gD homologes in HSV and PrV binding nectin-1. However, HSV-1 gD binding HVEM is in the same range (Table 6, upper part).
Interestingly, $gD_{36\text{-}280}$ exhibited a lower affinity to MHC-I contrary to results from C-terminally truncated gD homologs, which display a dramatic increase in receptor affinity (Table 6, lower part). The lowered $K_d$s in the homologs are explained by a faster interaction with the receptors, since the displacement of the C-terminus, which covers the receptor binding site in full length proteins, is not required anymore (Krummenacher et al., 2013). As discussed in the previous section, the C-terminus of EHV-1 and 4 gD seems to function in a different way than in gD homologs and needs further analysis.
The receptor binding affinities of gD1 and gD4 in the µM range are consistent with the observations in the blocking assays, which showed that 150 µg/ml (3,5 µM) soluble gDs block infections efficiently although not completely (Figure 21 and 22). A strong interaction with surface receptors might interfere with efficient fusion at the plasma membrane. However, a stronger interaction has previously been observed where 20 µg/ml (0,3 µM) recombinant gD4-Fc-$His_6$ blocked EHV-4 infection in ED cells by approximately 50% (Azab et al., 2014). Fc-$His_6$ is with 27,5 kDa rather big and could sterically block surrounding binding sites leading to an increased blocking efficiency. Nevertheless, repeating the assay with lower passage cells and 150 µg/ml recombinant protein, lead to a 87% and 53% reduction of EHV-1 and 4 infection, respectively, in contrast to the average of 50,8% and 31,5%. Thus, variability of the primary ED cells might influence the interaction between ligand and receptor which would as well explain the wide spread of data points in blocking assays. To gain comparable results, the here produced recombinant proteins should be used together with gD4-Fc-$His_6$ in blocking assays.
Furthermore, the presence of the TEV cleavage site, $His_6$-tag and the residues EF originating from the Eco-RI restriction site in the recombinant proteins produced in this study might influence the affinity. To evaluate this, the $His_6$-tag could be cleaved by TEV-protease or the cloning strategy for the proteins modified.
Notably, gD1 was able to reduced EHV-4 infection and vice versa, although the blocking was not as potent as in gD1 in EHV-1 and gD4 in EHV-4 infection. It can be concluded, that both gDs use the same receptor binding site, with minor differences in the interacting residues. This theory is supported by the computationally generated binding hypothesis of gD1 binding MHC-I.
The results from blocking assays and SPR analysis show that recombinant gD1 and gD4 can compete at the receptor binding site against native gD in the virus envelope and bind to recombinant, equine MHC-I with affinities in the µM range. These results indicated that all recombinant proteins are properly folded and functional.

Table 6: Comparison of dissociation constants ($K_d{}^{app}s$) of alphaherpesviruses-gDs binding their respective receptors measured by SPR. SW = swine, MHC-I = equine (Eqca-1*00101), nectin-1/HVEM = human. Under 'ligand origin' is the C-terminal truncation of proteins displayed in brackets. The upper part of the table represents full length proteins, the bottom part truncated proteins.

| **Ligand origin** | **Receptor** | **$K_d$ (nM)** | **Reference** |
|---|---|---|---|
| EHV-1 (349) | MHC-I | 3996 ± 840 | |
| EHV-4 (349) | MHC-I | 4413 ± 1200 | |
| HSV-1 (306) | HVEM | 3200 ± 600 | Willis et al. (1998) |
| HSV-1 (306) | HVEM | 4000 | Krummenacher et al. (2005) |
| HSV-1 (306) | nectin-1 | 2700 ± 200 | Whitbeck et al. (1999) |
| HSV-1 (306) | nectin-1 | 1800 | Krummenacher et al. (2005) |
| HSV-2 (306) | HVEM | 1500 | Willis et al. (1998) |
| PrV (354) | nectin-1 | 130 ± 70 | Connolly et al. (2001) |
| PrV (337) | nectin-1 | 191 | Li et al. (2017) |
| PrV (337) | SW-nectin-1 | 301 | Li et al. (2017) |
| EHV-4 (280) | MHC-I | 5288 ± 1233 | |
| HSV-1 (285) | HVEM | 37 | Rux et al. (1998) |
| HSV-1 (285) | HVEM | 110 | Krummenacher et al. (2005) |
| HSV-1 (285) | nectin-1 | 38 | Krummenacher et al. (1999) |
| HSV-1 (285) | nectin-1 | 70 | Krummenacher et al. (2005) |
| HSV-1 (285) | nectin-1 | 17,1 | Zhang et al. (2011) |
| HSV-1 (285) | nectin-1 | 12.5 | Lu et al. (2014) |
| HSV-2 (285) | nectin-1 | 19,1 | Lu et al. (2014) |
| PrV (284) | nectin-1 | 16,1 | Li et al. (2017) |
| PrV (284) | SW-nectin-1 | 18,4 | Li et al. (2017) |

### 4.6.1. Recombinant MHC-I does not reduce EHV-1 and 4 infections

Although the interaction between recombinant gDs and MHC-I was shown in SPR experiments, recombinant MHC-I (150 µg/ml, 3 µM) had no effect on infection levels when incubated with EHV-1 or 4 prior to infection of ED cells. The here used concentrations of soluble protein might have been too low, taking into account that the affinity of recombinant gDs are in a µM range. Experiments with higher protein concentrations should be undertaken.
Another explanation why recombinant MHC-I did not reduce EHV-1 and 4 infections, might be that the linker region (GGGSGGGSGGGS), inserted to tether the peptide to $\beta$2m, interferes with gD binding. By modeling the linker loosely to the MHC-I molecule that binds gD1 in the here hypothesized position, it becomes clear, that it can easily impede the interaction (Figure 31). To investigate this theory, the linker region could be digested or the MHC-I components could be produced separately in insect cells or *E. coli* and assembled to a working complex together

with a synthetic peptide as it has been done for the equine MHC-I molecules Eqca-N*00601 and Eqca-N*00602 (Yao et al., 2016). This recombinant MHC-I should block EHV-1 and 4 infections in ED cells and might even display a higher affinity to soluble gDs in SPR analysis. Additionally, the linker-less MHC-I might crystallize in a more ordered fashion and lead to diffracting crystals as well as crystals of the gD1/4-MHC-I complex.

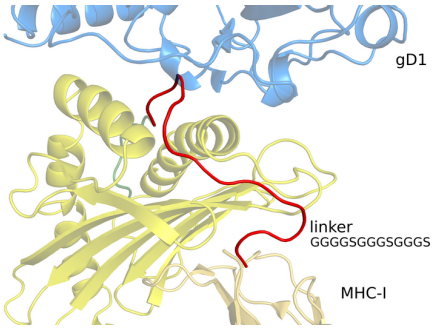


Figure 31: Enlargement of gD1 (blue) interaction with MHC-I (gold) in binding hypothesis in cartoon representation with linker (red) between $\beta$2m and peptide (green) loosely modeled.

## 4.7. Binding hypothesis of gD1/4-MHC-I interaction is plausible

Stable binding hypotheses of gD1/4-MHC-I were generated using molecular modeling that are strikingly similar to HSV and PrV gD binding nectin-1. Preceding structural models, Chiang et al. (1994) identified four distinct functional regions (FRs) for HSV-1 gD by linker insertion mutagenesis, which were later mostly confirmed by structural studies although FR4 has been shown not to be directly involved in the binding and is not solved in any of the gD crystal structures (Krummenacher et al., 2013). FR1 comprises the residues 27-43, FR2 126-131, FR3 225-246, and FR4 277-300. The binding hypotheses of gD1/4-MHC-I can be compared to HSV-1 (PDB ID: 3U82) and PrV (PDB ID: 5X5V) gD binding nectin-1 by using PyMOL and the script "Interface Residues". Focusing on the interacting residues and mapping the FR onto the protein sequences, a high positional similarity can be seen between all gDs binding their receptors and the predicted FRs (Figure 32). The number of interacting residues differs between these four gDs, correlating to some extent with their receptor affinities: 31 in PrV ($K_D$ = 301 nM from Li et al. (2017)), 25 in HSV-1 ($K_d$ = 1800 nM from Krummenacher et al. (2005)), 24 in EHV-1 ($K_d$ = 3996 ± 840 µM), and 21 in EHV-4 ($K_d$ = 4413 ± 1200 nM).
Moreover, the proposed docking position of gD1 to MHC-I explains why MHC-I Eqca-16*00101 (2.16) allows higher infection rates than Eqca-1*00101 (3.1) (Azab et al., 2014). The residue 103 in the 3.1 $\alpha$1 region is an arginine which is more bulky than asparagine in 2.16, thus preventing a closer interaction with gD. A binding hypothesis with MHC-I 2.16 and a crystal structure of this molecule could confirm that theory.

### 4.7.1. Role of MHC-I A173 in EHV-1 and 4 entry

The residue A173 of MHC-I have been shown previously to play a major role in the entry of EHV-1 and 4 by two studies. First, the entry of EHV-1 into usually non-susceptible NIH3T3 cells transfected with altered hamster MHC-I Q173A has been shown together with the negative effect on infection rates of the mutation T173 in equine MHC-I (Sasaki et al., 2011b). Second,

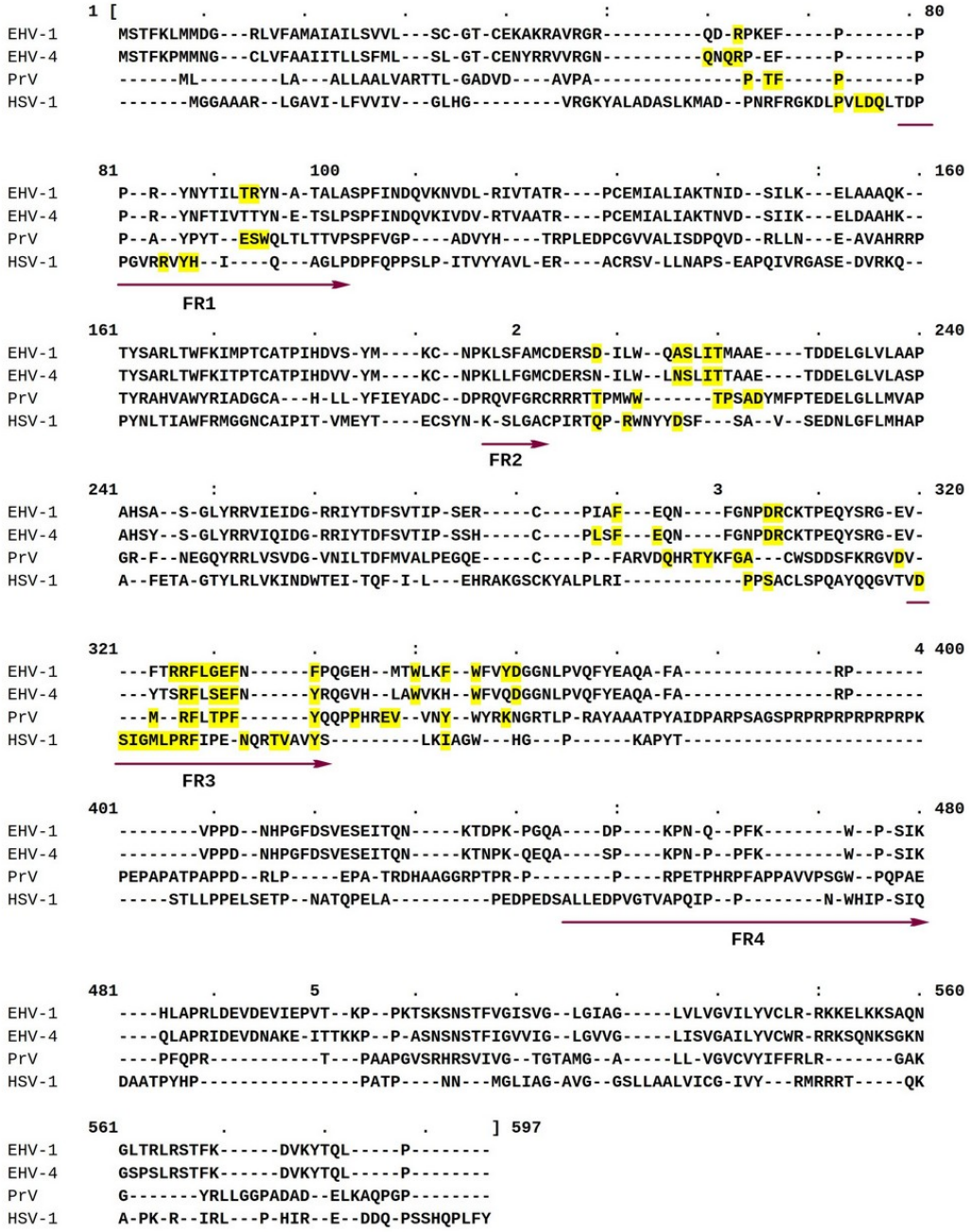


Figure 32: Kalign (2.0) CLUSTAL multiple sequence alignment of EHV-1, EHV-4 , PrV, and HSV-1 gD. Reference sequence is EHV-1 gD, identities are normalized by aligned length, the coverage is 100%, 99.3%, 75.6%, 69.9%, respectively, and identities are 100%, 76.8%, 26.3%, 21.5%, respectively. Receptor interacting residues (for EHV-1/4 MHC-I and PrV/HSV-1 nectin-1) according to PyMOL (script "Interface Residues") are marked yellow. Arrows in dark red mark functional regions (FRs) found by Chiang et al. (1994).

it has been demonstrated that not all equine MHC-I genes support entry of EHV-1 and 4 into equine MHC-I transfected mouse mastocytoma (P815) cells and that MHC-I genes harboring other residues than alanine at position 173 are highly resistant against EHV-1 and 4 infections (Azab et al., 2014).
The gD1/4-MHC-I binding hypotheses explain the role of MHC-I A173 well by showing that bulkier amino acids at that position lead to steric hindrance in the gD binding pocket. This applies to MHC-I allels 3.3 (V173), 3.4 (T173), 3.5 (E173), and 3.6 (V173), which have been shown to not support EHV-1 and 4 entry (Sasaki et al., 2011b; Azab et al., 2014). The model can even explain why the genotype Eqca-7*00201 (3.7), although harboring an alanine at position 173, does not allow entry of EHV-1 and 4 into P815 3.7 (Azab et al., 2014). The glutamine residue at position 174 is assumed to hinder gD binding sterically. The side-chain carboxylate rest would point in the bound state into a hydrophobic residue-patch (W253, F256, W257) of gD, leading to an enthalpic penalty. Strangely, the inability of the viruses to enter via the MHC-I haplotype Eqca-2*00101 (3.2) which harbors A173 and A174 cannot be explained by the binding model. The topology of this MHC-I molecule is predicted to be very similar to those allowing virus entry. A 3D structure of the 3.2 MHC-I gene might give an explanation. Mutations in the gD binding pocket R43, W253, F256, and W257 could prove useful for a more detailed evaluation of the predicted interaction with MHC-I A173.
Another observation by Sasaki et al. (2011b) was that the mutation W171L in equine MHC-I impairs virus entry into NIH3T3 cells transfected with this MHC-I. Although the cell surface expression of this mutant was reduced, this is still interesting since structural data shows that W171 points towards the peptide in the binding groove and should therefore not be directly involved in binding gD. The tryptophan would be able to stabilize some peptides with hydrogen bonds, whereas leucine would not. A leucine at position 171 could therefore lead to a more loosely bound peptide with a higher flexibility, resulting in an interference with the gD-MHC-I binding. This theory would suggest, that the peptide in the MHC-I binding groove itself could play a role in the receptor-ligand interaction which could be tested by using different peptides bound to MHC-I in blocking assays and by testing mutated equine MHC-I W171L in blocking assays with soluble, recombinant gDs.

Taking into account all these results, the question arises whether EHV-1 and 4 can facilitate entry through, so far, unknown non-equine MHC-I molecules. Sasaki et al. (2011b) demonstrated that mutated hamster MHC-I Q173A allowed low EHV-1 infection. Unfortunately, EHV-4 has not been tested in the same manner. A computational approach will be employed to search for non-equine MHC-I molecules that are similar in the binding region that is visible in the gD1/4-MHC-I binding hypothesis and will be used to select promising targets for transfection/infection assays. Experimentally, EHV-1 and 4 infections could be tested in cell lines from susceptible species, e.g. bovine; rabbit; monkey; pig; cat and human (Studdert and Blackney, 1979; Ahn et al., 2010); alpacas; lamas; polar bears (Greenwood et al., 2012) and rhinoceros (Greenwood et al., 2012; Abdelgawad et al., 2014, 2015) cell lines, with and without inhibited MHC-I expression by using $\beta$2m knockdown as in Sasaki et al. (2011a).
Additionally, the entry receptor search for EHV-1 should be pursued further beyond MHC-I by using pull down assays and identification of proteins visualized on SDS-PAGE by MS. Another approach could be the use of c-DNA libraries as in Kurtz et al. (2010) and Sasaki et al. (2011a) but from susceptible cell lines apart from equine cells.

Taken together, the proposed docking position of gD1 and 4 to MHC-I can explain several experimentally obtained results and is therefore plausible.

### 4.8. EHV-1 and EHV-4 mutants $gD_{F213A}$ and $gD_{D261N}$

To test the relevance of gD key residues F213 and D261 observed in the gD-MHC-I binding hypothesis, EHV-1 and 4 mutants were generated by using BAC mutagenesis and characterized by growth kinetics. All tested viruses harboring point mutations in gD exhibited an impaired growth. EHV-1 $gD_{D261N}$ showed a reduced replication rate, however, repaired the mutation several times and no stable mutant could be tested in growth kinetics. To examine whether the point mutation was repaired due to the importance to the virus or coincidentally, reconstitution of the mutant virus from the BAC should be repeated. Mutating $gD_{F213A}$ in EHV-1 lead to a 2-fold reduction in growth, which was rescued by repairing the mutation. EHV-4 $gD_{D261N}$ and $gD_{F213A}$ could not be subjected to growth kinetics due to their slow replication. Repair of point mutations rescued the growth, however, these viruses were not tested in growth kinetics yet since laboratories had to be closed to slow down the SARS-CoV-2 outbreak.
Taken together, these results demonstrate, that the gD residues F213 and D261 play an important role during entry of EHV-1 and 4 and imply that the gD-MHC-I binding hypothesis is correct.
To further investigate their role, plaque size assays should be performed, different cell lines infected with the mutant viruses, and double mutants might be generated. To examine key residues in MHC-I, point mutations could be introduced into equine MHC-I as well, transfected into non-susceptible cells, and infected with wild type virus and mutant virus. To determine the impact on the receptor-ligand affinity, recombinant gDs harboring the mutations F213A and D261N could be produced and tested by SPR and in blocking assays. To verify the binding hypothesis, the structures of gD1/4 binding MHC-I need to be solved.

## 5. Outlook

The here presented work contributes new insights into the interaction of two alphaherpesviruses, EHV-1 and EHV-4, with their host cells. Future work should concentrate on investigating the interaction of gD1 and gD4 with the atypical entry receptor equine MHC-I further. A crystal structure of the ligand-receptor complex would give detailed insights into which residues interact and would lead to even more targeted mutational studies. Preceding structural data of the complex, further mutations could be introduced in the gD1 and 4 region 234-261, predicted here to interact with MHC-I, with the focus on R237 (interaction with MHC-I R103), W253 and W257.
Furthermore, a crystal structure of the gD1/4-MHC-I complex may reveal why EHV-1 has such a broad host cell tropism in comparison to EHV-4, which is restricted mainly to equines and equine derived cells. The differences in tropisms can additionally be addressed by searching for other receptors used by EHV-1. Affinity- or immunoprecipitation of membrane proteins bound or cross-linked to soluble gD1 could be employed, followed by SDS-PAGE and single band identification by mass spectrometry analysis. The search could as well focus on nectin-1 by transfecting non-susceptible cells with nectin-1 and test the EHV-1 and 4 infectivity. Even more promising might be a computational search for MHC-I molecules similar to equine MHC-I genes allowing entry of EHV-1 and 4. These molecules could be tested with transfected non-susceptible cells as well.
Moreover, the role of gD glycosylations should be pursued further. Producing soluble, recombinant protein in *E. coli* and usage in blocking assays with EHV-1 and 4, might be a simple way to examine this, tested together with recombinant gDs from insect cell culture in glycosylated and deglycosylated form. A better way would be to test protein produced in mammalian cells in glycosylated and deglycosylated form in blocking assays. If gD glycans play a major role in infection, attenuated viruses might be produced with unglycosylated gDs.

Finally, the now available crystal structure of single gD1 and gD4 will prove useful to search for small molecule inhibitors that could be administered as therapeutics during acute EHV-1 and 4 infections, not only in equines, and might lead to an improvement of current vaccines.

# 6. References


Abdelgawad, A., Azab, W., Damiani, A. M., Baumgartner, K., Will, H., Osterrieder, N. and Greenwood, A. D. (2014). Zebra-borne equine herpesvirus type 1 (ehv-1) infection in non-african captive mammals. *Veterinary microbiology*, 169(1-2):102–106.

Abdelgawad, A., Hermes, R., Damiani, A., Lamglait, B., Czirják, G. Á., East, M., Aschenborn, O., Wenker, C., Kasem, S., Osterrieder, N. et al. (2015). Comprehensive serology based on a peptide elisa to assess the prevalence of closely related equine herpesviruses in zoo and wild animals. *PLoS One*, 10(9):e0138370.

Adams, P. D., Afonine, P. V., Bunkóczi, G., Chen, V. B., Davis, I. W., Echols, N., Headd, J. J., Hung, L.-W., Kapral, G. J., Grosse-Kunstleve, R. W. et al. (2010). Phenix: a comprehensive python-based system for macromolecular structure solution. *Acta Crystallographica Section D: Biological Crystallography*, 66(2):213–221.

Afonine, P. V., Grosse-Kunstleve, R. W., Echols, N., Headd, J. J., Moriarty, N. W., Mustyakimov, M., Terwilliger, T. C., Urzhumtsev, A., Zwart, P. H. and Adams, P. D. (2012). Towards automated crystallographic structure refinement with phenix. refine. *Acta Crystallographica Section D: Biological Crystallography*, 68(4):352–367.

Aharonson-Raz, K., Davidson, I., Porat, Y., Altory, A., Klement, E. and Steinman, A. (2014). Seroprevalence and rate of infection of equine influenza virus (h3n8 and h7n7) and equine herpesvirus (1 and 4) in the horse population in israel. *Journal of Equine Veterinary Science*, 34(6):828–832.

Ahn, B. C., Zhang, Y. and O'Callaghan, D. J. (2010). The equine herpesvirus-1 (ehv-1) ir3 transcript downregulates expression of the ie gene and the absence of ir3 gene expression alters ehv-1 biological properties and virulence. *Virology*, 402(2):327–337.

Albrecht, R. A., Kim, S. K. and O'Callaghan, D. J. (2005). The eicp27 protein of equine herpesvirus 1 is recruited to viral promoters by its interaction with the immediate-early protein. *Virology*, 333(1):74–87.

Allen, G. (1986). Molecular epizootiology, pathogenesis, and prophylaxis of equine herpesvirus-1 infections. *Prog. Vet. Microbiol. Immunol.*, 2:78–144.

Allen, G., Yeargan, M., Costa, L. and Cross, R. (1995). Major histocompatibility complex class i-restricted cytotoxic t-lymphocyte responses in horses infected with equine herpesvirus 1. *Journal of virology*, 69(1):606–612.

Allen, G. P. (2007). Development of a real-time polymerase chain reaction assay for rapid diagnosis of neuropathogenic strains of equine herpesvirus-1. *Journal of Veterinary Diagnostic Investigation*, 19(1):69–72.

Ansari, H. A., Hediger, R., Fries, R. and Stranzinger, G. (1988). Chromosomal localization of the major histocompatibility complex of the horse (ela) by in situ hybridization. *Immunogenetics*, 28(5):362–364.

Arvin, A., Campadelli-Fiume, G., Mocarski, E., Moore, P. S., Roizman, B., Whitley, R. and Yamanishi, K. (2007). *Human herpesviruses: biology, therapy, and immunoprophylaxis*. Cambridge University Press.

Ashkenazy, H., Abadi, S., Martz, E., Chay, O., Mayrose, I., Pupko, T. and Ben-Tal, N. (2016). Consurf 2016: an improved methodology to estimate and visualize evolutionary conservation in macromolecules. *Nucleic acids research*, 44(W1):W344–W350.

Atwood, W. J. and Norkin, L. C. (1989). Class i major histocompatibility proteins as cell surface receptors for simian virus 40. *Journal of virology*, 63(10):4474–4477.

Awan, A. R., Chong, Y.-C. and Field, H. J. (1990). The pathogenesis of equine herpesvirus type 1 in the mouse: a new model for studying host responses to the infection. *Journal of General Virology*, 71(5):1131–1140.

Azab, W., Bedair, S., Abdelgawad, A., Eschke, K., Farag, G. K., Abdel-Raheim, A., Greenwood, A. D., Osterrieder, N. and Ali, A. A. (2019). Detection of equid herpesviruses among different arabian horse populations in egypt. *Veterinary medicine and science*.

Azab, W., Dayaram, A., Greenwood, A. D. and Osterrieder, N. (2018). How host specific are herpesviruses? lessons from herpesviruses infecting wild and endangered mammals. *Annual review of virology*, 5:53–68.

Azab, W., Gramatica, A., Herrmann, A. and Osterrieder, N. (2015). Binding of alphaherpesvirus glycoprotein h to surface $\alpha 4\beta 1$-integrins activates calcium-signaling pathways and induces phosphatidylserine exposure on the plasma membrane. *MBio*, 6(5):e01552–15.

Azab, W., Harman, R., Miller, D., Tallmadge, R., Frampton Jr, A. R., Antczak, D. F. and Osterrieder, N. (2014). Equid herpesvirus type 4 uses a restricted set of equine major histocompatibility complex class i proteins as entry receptors. *J Gen Virol*, 95:1554–63.

Azab, W., Kato, K., Abdel-Gawad, A., Tohya, Y. and Akashi, H. (2011). Equine herpesvirus 4: Recent advances using bac technology. *Veterinary microbiology*, 150(1-2):1–14.

Azab, W., Kato, K., Arii, J., Tsujimura, K., Yamane, D., Tohya, Y., Matsumura, T. and Akashi, H. (2009). Cloning of the genome of equine herpesvirus 4 strain th20p as an infectious bacterial artificial chromosome. *Archives of virology*, 154(5):833–842.

Azab, W., Lehmann, M. J. and Osterrieder, N. (2013). Glycoprotein h and $\alpha 4\beta 1$ integrins determine the entry pathway of alphaherpesviruses. *Journal of virology*, 87(10):5937–5948.

Azab, W. and Osterrieder, K. (2017). Initial contact: the first steps in herpesvirus entry. In *Cell Biology of Herpes Viruses*, pages 1–27. Springer.

Azab, W. and Osterrieder, N. (2012). Glycoproteins d of equine herpesvirus type 1 (ehv-1) and ehv-4 determine cellular tropism independently of integrins. *Journal of virology*, 86(4):2031–2044.

Azab, W., Tsujimura, K., Maeda, K., Kobayashi, K., Mohamed, Y. M., Kato, K., Matsumura, T. and Akashi, H. (2010). Glycoprotein c of equine herpesvirus 4 plays a role in viral binding to cell surface heparan sulfate. *Virus research*, 151(1):1–9.

Azab, W., Zajic, L. and Osterrieder, N. (2012). The role of glycoprotein h of equine herpesviruses 1 and 4 (ehv-1 and ehv-4) in cellular host range and integrin binding. *Veterinary research*, 43(1):61.

Banfield, B. W., Leduc, Y., Esford, L., Visalli, R. J., Brandt, C. R. and Tufaro, F. (1995). Evidence for an interaction of herpes simplex virus with chondroitin sulfate proteoglycans during infection. *Virology*, 208(2):531–539.

Barton, G. J. et al. (1993). Alscript: a tool to format multiple sequence alignments. *Protein Engineering Design and Selection*, 6(1):37–40.

Battye, T. G. G., Kontogiannis, L., Johnson, O., Powell, H. R. and Leslie, A. G. (2011). imosflm: a new graphical interface for diffraction-image processing with mosflm. *Acta Crystallographica Section D: Biological Crystallography*, 67(4):271–281.

Baxi, M., Borchers, K., Bartels, T., Schellenbach, A., Baxi, S. and Field, H. (1996). Molecular studies of the acute infection, latency and reactivation of equine herpesvirus-1 (ehv-1) in the mouse model. *Virus research*, 40(1):33–45.

Bergfors, T. (2003). Seeds to crystals. *Journal of structural biology*, 142(1):66–76.

Bergmann, T., Moore, C., Sidney, J., Miller, D., Tallmadge, R., Harman, R. M., Oseroff, C., Wriston, A., Shabanowitz, J., Hunt, D. F. et al. (2015). The common equine class i molecule eqca-1* 00101 (ela-a3. 1) is characterized by narrow peptide binding and t cell epitope repertoires. *Immunogenetics*, 67(11-12):675–689.

Betenbaugh, M. J., Tomiya, N., Narang, S., Hsu, J. T. and Lee, Y. C. (2004). Biosynthesis of human-type n-glycans in heterologous systems. *Current opinion in structural biology*, 14(5):601–606.

Bjorkman, P. J. and Parham, P. (1990). Structure, function, and diversity of class i major histocompatibility complex molecules. *Annual review of biochemistry*, 59(1):253–288.

Blacklaws, B., Krishna, S., Minson, A. t. and Nash, A. (1990). Immunogenicity of herpes simplex virus type 1 glycoproteins expressed in vaccinia virus recombinants. *Virology*, 177(2):727–736.

Boehmer, P. and Nimonkar, A. (2003). Herpes virus replication. *IUBMB life*, 55(1):13–22.

Boehmer, P. E. and Lehman, I. (1997). Herpes simplex virus dna replication. *Annual review of biochemistry*, 66(1):347–384.

Bogan, A. A. and Thorn, K. S. (1998). Anatomy of hot spots in protein interfaces. *Journal of molecular biology*, 280(1):1–9.

Brandtzaeg, P., Berstad, A., Farstad, I., Haraldsen, G., Helgeland, L., Jahnsen, F., Johansen, F., Natvig, I., Nilsen, E. and Rugtveit, J. (1997). Mucosal immunity–a major adaptive defence mechanism. *Behring Institute Mitteilungen*, (98):1–23.

Bryans, J. and Prickett, M. (1970). Consideration of the pathogenesis of abortigenic disease caused by equine herpesvirus 1. In *Int Conf Equine Infec Dis Proc*.

Bunkóczi, G., Echols, N., McCoy, A. J., Oeffner, R. D., Adams, P. D. and Read, R. J. (2013). Phaser. mrage: automated molecular replacement. *Acta Crystallographica Section D: Biological Crystallography*, 69(11):2276–2286.

Burrows, R. and Goodridge, D. (1974). In vivo and in vitro studies of equine rhinopneumonitis virus strains. In *Equine Infectious Diseases*, pages 306–321. Karger Publishers.

Campadelli-Fiume, G., Amasio, M., Avitabile, E., Cerretani, A., Forghieri, C., Gianni, T. and Menotti, L. (2007). The multipartite system that mediates entry of herpes simplex virus into the cell. *Reviews in medical virology*, 17(5):313–326.

Campbell, E. C., Antoniou, A. N. and Powis, S. J. (2012). The multi-faceted nature of hla class i dimer molecules. *Immunology*, 136(4):380–384.

Carfi, A., Willis, S. H., Whitbeck, J. C., Krummenacher, C., Cohen, G. H., Eisenberg, R. J. and Wiley, D. C. (2001). Herpes simplex virus glycoprotein d bound to the human receptor hvea. *Molecular cell*, 8(1):169–179.

Carpenter, S., Baker, J. M., Bacon, S. J., Hopman, T., Maher, J., Ellis, S. A. and Antczak, D. F. (2001). Molecular and functional characterization of genes encoding horse mhc class i antigens. *Immunogenetics*, 53(9):802–809.

Caughman, G. B., Staczek, J. and O'Callaghan, D. J. (1985). Equine herpesvirus type 1 infected cell polypeptides: evidence for immediate early/early/late regulation of viral gene expression. *Virology*, 145(1):49–61.

Chiang, H.-Y., Cohen, G. and Eisenberg, R. (1994). Identification of functional regions of herpes simplex virus glycoprotein gd by using linker-insertion mutagenesis. *Journal of virology*, 68(4):2529–2543.

Chowdhury, S., Ludwig, H. and Buhk, H.-J. (1988). Molecular biological characterization of equine herpesvirus type 1 (ehv-1) isolates from ruminant hosts. *Virus research*, 11(2):127–139.

Cole, N. L. and Grose, C. (2003). Membrane fusion mediated by herpesvirus glycoproteins: the paradigm of varicella-zoster virus. *Reviews in medical virology*, 13(4):207–222.

Connolly, S. A., Landsburg, D. J., Carfi, A., Whitbeck, J. C., Zuo, Y., Wiley, D. C., Cohen, G. H. and Eisenberg, R. J. (2005). Potential nectin-1 binding site on herpes simplex virus glycoprotein d. *Journal of virology*, 79(2):1282–1295.

Connolly, S. A., Landsburg, D. J., Carfi, A., Wiley, D. C., Cohen, G. H. and Eisenberg, R. J. (2003). Structure-based mutagenesis of herpes simplex virus glycoprotein d defines three critical regions at the gd-hvea/hvem binding interface. *Journal of Virology*, 77(14):8127–8140.

Connolly, S. A., Landsburg, D. J., Carfi, A., Wiley, D. C., Eisenberg, R. J. and Cohen, G. H. (2002). Structure-based analysis of the herpes simplex virus glycoprotein d binding site present on herpesvirus entry mediator hvea (hvem). *Journal of virology*, 76(21):10894–10904.

Connolly, S. A., Whitbeck, J. C., Rux, A. H., Krummenacher, C., Cohen, G. H., Eisenberg, R. J. et al. (2001). Glycoprotein d homologs in herpes simplex virus type 1, pseudorabies virus, and bovine herpes virus type 1 bind directly to human hvec (nectin-1) with different affinities. *Virology*, 280(1):7–18.

Crabb, B. S., Nagesha, H. S. and Studdert, M. J. (1992). Identification of equine herpesvirus 4 glycoprotein g: a type-specific, secreted glycoprotein. *Virology*, 190(1):143–154.

Crabb, B. S. and Studdert, M. J. (1993). Epitopes of glycoprotein g of equine herpesviruses 4 and 1 located near the c termini elicit type-specific antibody responses in the natural host. *Journal of virology*, 67(10):6332–6338.

Crowe, J., Dobeli, H., Gentz, R., Hochuli, E., Stiiber, D. and Henco, K. (1994). 6xffis-ni-nta chromatography as a superior technique in recombinant protein expression/purification. In *Protocols for gene analysis*, pages 371–387. Springer.

Csellner, H., Walker, C., Wellington, J., McLure, L., Love, D. and Whalley, J. (2000). Ehv-1 glycoprotein d (ehv-1 gd) is required for virus entry and cell-cell fusion, and an ehv-1 gd deletion mutant induces a protective immune response in mice. *Archives of virology*, 145(11):2371–2385.

David-Watine, B., Israël, A. and Kourilsky, P. (1990). The regulation and expression of mhc class i genes. *Immunology today*, 11:286–292.

Davison, A. J., Eberle, R., Ehlers, B., Hayward, G. S., McGeoch, D. J., Minson, A. C., Pellett, P. E., Roizman, B., Studdert, M. J. and Thiry, E. (2009). The order herpesvirales. *Archives of virology*, 154(1):171–177.

Davison, A. J. and Scott, J. E. (1986). The complete dna sequence of varicella-zoster virus. *Journal of General Virology*, 67(9):1759–1816.

Dayaram, A., Franz, M., Schattschneider, A., Damiani, A. M., Bischofberger, S., Osterrieder, N. and Greenwood, A. D. (2017). Long term stability and infectivity of herpesviruses in water. *Scientific reports*, 7:46559.

DeLano, W. L. (2002). Pymol.

Dey, P., Bergmann, T., Cuellar-Camacho, J. L., Ehrmann, S., Chowdhury, M. S., Zhang, M., Dahmani, I., Haag, R. and Azab, W. (2018). Multivalent flexible nanogels exhibit broad-spectrum antiviral activity by blocking virus entry. *ACS nano*, 12(7):6429–6442.

Di Giovine, P., Settembre, E. C., Bhargava, A. K., Luftig, M. A., Lou, H., Cohen, G. H., Eisenberg, R. J., Krummenacher, C. and Carfi, A. (2011). Structure of herpes simplex virus glycoprotein d bound to the human receptor nectin-1. *PLoS pathogens*, 7(9):e1002277.

Domingo, E., Parrish, C. R. and Holland, J. J. (2008). *Origin and evolution of viruses*. Elsevier.

Donald, J. J. (1998). *Epidemiology and diagnosis of Equid herpesviruses 1 and 4 in horses in New Zealand: a thesis presented in partial fulfilment of the requirements for the degree of Doctor of Philosophy at Massey University*. PhD thesis, Massey University.

Donaldson, W., Crump, A., Zhang, C., Kornbluth, J., Kamoun, M., Davis, W. and Antczak, D. (1988). At least two loci encode polymorphic class i mhc antigens in the horse. *Animal genetics*, 19(4):379–390.

DuBois, R. M., Vaney, M.-C., Tortorici, M. A., Al Kurdi, R., Barba-Spaeth, G., Krey, T. and Rey, F. A. (2013). Functional and evolutionary insight from the crystal structure of rubella virus protein e1. *Nature*, 493(7433):552.

Dummer, L. A., Leite, F. P. L. et al. (2014). Bovine herpesvirus glycoprotein d: a review of its structural characteristics and applications in vaccinology. *Veterinary Research*, 45(1):111.

Edington, N., Bridges, C. and Patel, J. (1986). Endothelial cell infection and thrombosis in paralysis caused by equid herpesvirus-1: equine stroke. *Archives of virology*, 90(1-2):111–124.

Edington, N., Smyth, B. and Griffiths, L. (1991). The role of endothelial cell infection in the endometrium, placenta and foetus of equid herpesvirus 1 (ehv-1) abortions. *Journal of comparative pathology*, 104(4):379–387.

Ellis, S., Martin, A., Holmes, E. and Morrison, W. (1995). At least four mhc class i genes are transcribed in the horse: phylogenetic analysis suggests an unusual evolutionary history for the mhc in this species. *International Journal of Immunogenetics*, 22(3):249–260.

Elton, D. M., Halliburton, I. W., Killington, R. A., Meredith, D. M. and Bonass, W. A. (1992). Identification of the equine herpesvirus type 1 glycoprotein 17/18 as a homologue of herpes simplex virus glycoprotein d. *Journal of general virology*, 73(5):1227–1233.

Emsley, P., Lohkamp, B., Scott, W. G. and Cowtan, K. (2010). Features and development of coot. *Acta Crystallographica Section D: Biological Crystallography*, 66(4):486–501.

Ferrera, A. et al. (1950). Virus abortion of mares in spain. *Trabajos del Instituto de Biologia Animal*, 9.

Flowers, C. C., Eastman, E. M. and O'Callaghan, D. J. (1991). Sequence analysis of a glycoprotein d gene homolog within the unique short segment of the ehv-1 genome. *Virology*, 180(1):175–184.

Flowers, C. C., Flowers, S. P., Jennings, S. R. and O'Callaghan, D. J. (1995a). Synthesis and processing of equine herpesvirus 1 glycoprotein d. *Virology*, 208(1):9–18.

Flowers, C. C., Flowers, S. P., Sheng, Y., Tarbet, E. B., Jennings, S. R. and O'Callaghan, D. J. (1995b). Expression of membrane-bound and secreted forms of equine herpesvirus 1 glycoprotein d by recombinant baculovirus. *Virus research*, 35(1):17–34.

Flowers, C. C. and O'Callaghan, D. J. (1992). The equine herpesvirus type 1 (ehv-1) homolog of herpes simplex virus type 1 us9 and the nature of a major deletion within the unique short segment of the ehv-1 kya strain genome. *Virology*, 190(1):307–315.

Foote, C., Gilkerson, J., Whalley, J. M. and Love, D. (2003). Seroprevalence of equine herpesvirus 1 in mares and foals on a large hunter valley stud farm in years pre-and postvaccination. *Australian veterinary journal*, 81(5):283–288.

Frampton, A. R., Goins, W. F., Cohen, J. B., Von Einem, J., Osterrieder, N., O'Callaghan, D. J. and Glorioso, J. C. (2005). Equine herpesvirus 1 utilizes a novel herpesvirus entry receptor. *Journal of virology*, 79(5):3169–3173.

Frampton, A. R., Stolz, D. B., Uchida, H., Goins, W. F., Cohen, J. B. and Glorioso, J. C. (2007). Equine herpesvirus 1 enters cells by two different pathways, and infection requires the activation of the cellular kinase rock1. *Journal of virology*, 81(20):10879–10889.

Frampton Jr, A. R., Uchida, H., Von Einem, J., Goins, W. F., Grandi, P., Cohen, J. B., Osterrieder, N. and Glorioso, J. C. (2010). Equine herpesvirus type 1 (ehv-1) utilizes microtubules, dynein, and rock1 to productively infect cells. *Veterinary microbiology*, 141(1-2):12–21.

Fuentealba, N., Sguazza, G., Scrochi, M., Bravi, M., Zanuzzi, C., Corva, S., Gimeno, E., Pecoraro, M. and Galosi, C. (2014). Production of equine herpesvirus 1 recombinant glycoprotein d and development of an agar gel immunodiffusion test for serological diagnosis. *Journal of virological methods*, 202:15–18.

Gabev, E., Tobler, K., Abril, C., Hilbe, M., Senn, C., Franchini, M., Campadelli-Fiume, G., Fraefel, C. and Ackermann, M. (2010). Glycoprotein d of bovine herpesvirus 5 (bohv-5) confers an extended host range to bohv-1 but does not contribute to invasion of the brain. *Journal of virology*, 84(11):5583–5593.

Geraghty, R. J., Krummenacher, C., Cohen, G. H., Eisenberg, R. J. and Spear, P. G. (1998). Entry of alphaherpesviruses mediated by poliovirus receptor-related protein 1 and poliovirus receptor. *Science*, 280(5369):1618–1620.

Germain, R. N. and Margulies, D. H. (1993). The biochemistry and cell biology of antigen processing and presentation. *Annual review of immunology*, 11(1):403–450.

Gilcrease, M. Z. (2007). Integrin signaling in epithelial cells. *Cancer letters*, 247(1):1–25.

Gilkerson, J., Jorm, L. R., Love, D. N., Lawrence, G. L. and Whalley, J. M. (1994). Epidemiological investigation of equid herpesvirus-4 (ehv-4) excretion assessed by nasal swabs taken from thoroughbred foals. *Veterinary microbiology*, 39(3-4):275–283.

Gilkerson, J., Love, D. and Whalley, J. (1997). A review of equine herpesvirus vaccines: from the traditional to the experimental. *Aust. Equine Vet.*, 15:27–32.

Gilkerson, J., Whalley, J., Drummer, H., Studdert, M. and Love, D. (1999). Epidemiology of ehv-1 and ehv-4 in the mare and foal populations on a hunter valley stud farm: are mares the source of ehv-1 for unweaned foals. *Veterinary microbiology*, 68(1-2):27–34.

Goehring, L., Wagner, B., Bigbie, R., Hussey, S., Rao, S., Morley, P. and Lunn, D. (2010). Control of ehv-1 viremia and nasal shedding by commercial vaccines. *Vaccine*, 28(32):5203–5211.

Goodman, L. B., Wimer, C., Dubovi, E. J., Gold, C. and Wagner, B. (2012). Immunological correlates of vaccination and infection for equine herpesvirus 1. *Clin. Vaccine Immunol.*, 19(2):235–241.

Granzow, H., Klupp, B. G., Fuchs, W., Veits, J., Osterrieder, N. and Mettenleiter, T. C. (2001). Egress of alphaherpesviruses: comparative ultrastructural study. *Journal of virology*, 75(8):3675–3684.

Granzow, H., Weiland, F., Jöns, A., Klupp, B. G., Karger, A. and Mettenleiter, T. C. (1997). Ultrastructural analysis of the replication cycle of pseudorabies virus in cell culture: a reassessment. *Journal of virology*, 71(3):2072–2082.

Greenwood, A. D., Tsangaras, K., Ho, S. Y., Szentiks, C. A., Nikolin, V. M., Ma, G., Damiani, A., East, M. L., Lawrenz, A., Hofer, H. et al. (2012). A potentially fatal mix of herpes in zoos. *Current Biology*, 22(18):1727–1731.

Gryspeerdt, A. C., Vandekerckhove, A., Garré, B., Barbé, F., Van de Walle, G. and Nauwynck, H. (2010). Differences in replication kinetics and cell tropism between neurovirulent and non-neurovirulent ehv1 strains during the acute phase of infection in horses. *Veterinary microbiology*, 142(3-4):242–253.

Handler, C. G., Cohen, G. H. and Eisenberg, R. J. (1996). Cross-linking of glycoprotein oligomers during herpes simplex virus type 1 entry. *Journal of virology*, 70(9):6076–6082.

Harless, W. and Pusterla, N. (2006). Equine herpesvirus 1 and 4 respiratory disease in the horse. *Clinical Techniques in Equine Practice*, 5(3):197–202.

Hasebe, R., Sasaki, M., Sawa, H., Wada, R., Umemura, T. and Kimura, T. (2009). Infectious entry of equine herpesvirus-1 into host cells through different endocytic pathways. *Virology*, 393(2):198–209.

Heldwein, E. and Krummenacher, C. (2008). Entry of herpesviruses into mammalian cells. *Cellular and molecular life sciences*, 65(11):1653–1668.

Heldwein, E. E., Lou, H., Bender, F. C., Cohen, G. H., Eisenberg, R. J. and Harrison, S. C. (2006). Crystal structure of glycoprotein b from herpes simplex virus 1. *Science*, 313(5784):217–220.

Henry, B. E., Robinson, R. A., Dauenhauer, S. A., Atherton, S. S., Hayward, G. S. and O'Callaghan, D. J. (1981). Structure of the genome of equine herpesvirus type 1. *Virology*, 115(1):97–114.

Hong, S. S., Karayan, L., Tournier, J., Curiel, D. T. and Boulanger, P. A. (1997). Adenovirus type 5 fiber knob binds to mhc class i $\alpha$2 domain at the surface of human epithelial and b lymphoblastoid cells. *The EMBO journal*, 16(9):2294–2306.

Hübert, P., Birkenmaier, S., Rziha, H.-J. and Osterrieder, N. (1996). Alterations in the equine herpesvirus type-1 (ehv-1) strain rach during attenuation. *Journal of Veterinary Medicine, Series B*, 43(1-10):1–14.

Israel, B. A., Herber, R., Gao, Y. and Letchworth III, G. J. (1992). Induction of a mucosal barrier to bovine herpesvirus 1 replication in cattle. *Virology*, 188(1):256–264.

Jarvis, D. and Garcia, J. A. (1994). Long-term stability of baculoviruses stored under various conditions. *Biotechniques*, 16(3):508–513.

Jarvis, D. L. (2003). Developing baculovirus-insect cell expression systems for humanized recombinant glycoprotein production. *Virology*, 310(1):1–7.

Kabsch, W. (2010). Xds. *Acta Crystallographica Section D: Biological Crystallography*, 66(2):125–132.

Kabsch, W. and Sander, C. (1983). Dssp: definition of secondary structure of proteins given a set of 3d coordinates. *Biopolymers*, 22:2577–2637.

Kamel, M., Pavulraj, S., Osterrieder, K. and Azab, W. (2020). Ehv-1 pathogenesis: Current in vitro models and future perspectives. *Frontiers in veterinary science*, 6:251.

Kaminski, G. A., Friesner, R. A., Tirado-Rives, J. and Jorgensen, W. L. (2001). Evaluation and reparametrization of the opls-aa force field for proteins via comparison with accurate quantum chemical calculations on peptides. *The Journal of Physical Chemistry B*, 105(28):6474–6487.

Kanitz, F. A., Cargnelutti, J. F., Anziliero, D., Gonçalves, K. V., Masuda, E. K., Weiblen, R. and Flores, E. F. (2015). Respiratory and neurological disease in rabbits experimentally infected with equid herpesvirus 1. *Microbial pathogenesis*, 87:45–50.

Krishna, S., Blacklaws, B. A., Overton, H. A., Bishop, D. H. and Nash, A. A. (1989). Expression of glycoprotein d of herpes simplex virus type 1 in a recombinant baculovirus: protective responses and t cell recognition of the recombinant-infected cell extracts. *Journal of general virology*, 70(7):1805–1814.

Krummenacher, C., Carfí, A., Eisenberg, R. J. and Cohen, G. H. (2013). Entry of herpesviruses into cells: the enigma variations. In *Viral entry into host cells*, pages 178–195. Springer.

Krummenacher, C., Rux, A. H., Whitbeck, J. C., Ponce-de Leon, M., Lou, H., Baribaud, I., Hou, W., Zou, C., Geraghty, R. J., Spear, P. G. et al. (1999). The first immunoglobulin-like domain of hvec is sufficient to bind herpes simplex virus gd with full affinity, while the third domain is involved in oligomerization of hvec. *Journal of virology*, 73(10):8127–8137.

Krummenacher, C., Supekar, V. M., Whitbeck, J. C., Lazear, E., Connolly, S. A., Eisenberg, R. J., Cohen, G. H., Wiley, D. C. and Carfí, A. (2005). Structure of unliganded hsv gd reveals a mechanism for receptor-mediated activation of virus entry. *The EMBO journal*, 24(23):4144–4153.

Kurtz, B. M., Singletary, L. B., Kelly, S. D. and Frampton, A. R. (2010). Equus caballus major histocompatibility complex class i is an entry receptor for equine herpesvirus type 1. *Journal of virology*, 84(18):9027–9034.

Kydd, J., Slater, J., Osterrieder, N., Lunn, D., Antczak, D., Azab, W., Balasuriya, U., Barnett, C., Brosnahan, M., Cook, C. et al. (2012). Third international havemeyer workshop on equine herpesvirus type 1. *Equine veterinary journal*, 44(5):513–517.

Kydd, J. H., Smith, K., Hannant, D., Livesay, G. J. and Mumford, J. A. (1994). Distribution of equid herpesvirus-1 (ehv-1) in respiratory tract associated lymphoid tissue: implications for cellular immunity. *Equine veterinary journal*, 26(6):470–473.

Kydd, J. H., Townsend, H. G. and Hannant, D. (2006). The equine immune response to equine herpesvirus-1: the virus and its vaccines. *Veterinary immunology and immunopathology*, 111(1-2):15–30.

Lang, A., de Vries, M., Feineis, S., Müller, E., Osterrieder, N. and Damiani, A. M. (2013). Development of a peptide elisa for discrimination between serological responses to equine herpesvirus type 1 and 4. *Journal of virological methods*, 193(2):667–673.

Lazear, E., Carfi, A., Whitbeck, J. C., Cairns, T. M., Krummenacher, C., Cohen, G. H. and Eisenberg, R. J. (2008). Engineered disulfide bonds in herpes simplex virus type 1 gd separate receptor binding from fusion initiation and viral entry. *Journal of virology*, 82(2):700–709.

Leutenegger, C., Madigan, J. E., Mapes, S., Thao, M., Estrada, M. and Pusterla, N. (2008). Detection of ehv-1 neuropathogenic strains using real-time pcr in the neural tissue of horses with myeloencephalopathy.

Li, A., Lu, G., Qi, J., Wu, L., Tian, K., Luo, T., Shi, Y., Yan, J. and Gao, G. F. (2017). Structural basis of nectin-1 recognition by pseudorabies virus glycoprotein d. *PLoS pathogens*, 13(5):e1006314.

Lopez, M., Cocchi, F., Menotti, L., Avitabile, E., Dubreuil, P. and Campadelli-Fiume, G. (2000). Nectin2$\alpha$ (prr2$\alpha$ or hveb) and nectin2$\delta$ are low-efficiency mediators for entry of herpes simplex virus mutants carrying the leu25pro substitution in glycoprotein d. *Journal of virology*, 74(3):1267–1274.

Love, D., Bell, C., Pye, D., Edwards, S., Hayden, M., Lawrence, G., Boyle, D., Pye, T. and Whalley, J. (1993). Expression of equine herpesvirus 1 glycoprotein d by using a recombinant baculovirus. *Journal of virology*, 67(11):6820–6823.

Love, D. N., Bell, C. W. and Whalley, J. M. (1992). Characterization of the glycoprotein d gene products of equine herpesvirus 1 using a prokaryotic cell expression vector. *Veterinary microbiology*, 30(4):387–394.

Lu, G., Zhang, N., Qi, J., Li, Y., Chen, Z., Zheng, C., Gao, G. F. and Yan, J. (2014). Crystal structure of herpes simplex virus 2 gd bound to nectin-1 reveals a conserved mode of receptor recognition. *Journal of virology*, 88(23):13678–13688.

Lunn, D., Davis-Poynter, N., Flaminio, M., Horohov, D., Osterrieder, K., Pusterla, N. and Townsend, H. (2009). Equine herpesvirus-1 consensus statement. *Journal of Veterinary Internal Medicine*, 23(3):450–461.

Lyman, M. G. and Enquist, L. W. (2009). Herpesvirus interactions with the host cytoskeleton. *Journal of virology*, 83(5):2058–2066.

Ma, G., Azab, W. and Osterrieder, N. (2013). Equine herpesviruses type 1 (ehv-1) and 4 (ehv-4)–masters of co-evolution and a constant threat to equids and beyond. *Veterinary microbiology*, 167(1):123–134.

Makinen, A., Chowdhary, B., Mahdy, E., Andersson, L. and Gustavsson, I. (1989). Localization of the equine major histocompatibility complex (ela) to chromosome 20 by in situ hybridization. *Hereditas*, 110(1):93–96.

Manoj, S., Jogger, C. R., Myscofski, D., Yoon, M. and Spear, P. G. (2004). Mutations in herpes simplex virus glycoprotein d that prevent cell entry via nectins and alter cell tropism. *Proceedings of the National Academy of Sciences*, 101(34):12414–12421.

Matsumoto, H., Haniu, H. and Komori, N. (2019). Determination of protein molecular weights on sds-page. In *Electrophoretic Separation of Proteins*, pages 101–105. Springer.

Mayr, A., Pette, J., Petzoldt, K. and Wagener, K. (1968). Untersuchungen zur entwicklung eines lebendimpfstoffes gegen die rhinopneumonitis (stutenabort) der pferde 1. *Zentralblatt für Veterinärmedizin Reihe B*, 15(6):406–418.

McCoy, A. J., Grosse-Kunstleve, R. W., Adams, P. D., Winn, M. D., Storoni, L. C. and Read, R. J. (2007). Phaser crystallographic software. *Journal of applied crystallography*, 40(4):658–674.

Merk, A., Bartesaghi, A., Banerjee, S., Falconieri, V., Rao, P., Davis, M. I., Pragani, R., Boxer, M. B., Earl, L. A., Milne, J. L. et al. (2016). Breaking cryo-em resolution barriers to facilitate drug discovery. *Cell*, 165(7):1698–1707.

Molinková, D. and Celer, V. (2006). Recombinant single chain fv antibodies specific for glycoprotein d of equid herpesvirus 1. *Folia microbiologica*, 51(5):492–496.

Montgomery, R. I., Warner, M. S., Lum, B. J. and Spear, P. G. (1996). Herpes simplex virus-1 entry into cells mediated by a novel member of the tnf/ngf receptor family. *Cell*, 87(3):427–436.

Mori, C. M. C., Mori, E., Favaro, L. L., Santos, C., Lara, M., Villalobos, E., Cunha, E., Brandao, P., Richtzenhain, L. and Maiorka, P. (2012). Equid herpesvirus type-1 exhibits neurotropism and neurovirulence in a mouse model. *Journal of comparative pathology*, 146(2-3):202–210.

Mullen, M. M., Haan, K. M., Longnecker, R. and Jardetzky, T. S. (2002). Structure of the epstein-barr virus gp42 protein bound to the mhc class ii receptor hla-dr1. *Molecular cell*, 9(2):375–385.

Neubauer, A., Braun, B., Brandmüller, C., Kaaden, O.-R. and Osterrieder, N. (1997). Analysis of the contributions of the equine herpesvirus 1 glycoprotein gb homolog to virus entry and direct cell-to-cell spread. *Virology*, 227(2):281–294.

Nie, Y., Chaillet, M., Becke, C., Haffke, M., Pelosse, M., Fitzgerald, D., Collinson, I., Schaffitzel, C. and Berger, I. (2016). Acembl tool-kits for high-throughput multigene delivery and expression in prokaryotic and eukaryotic hosts. In *Advanced Technologies for Protein Complex Production and Characterization*, pages 27–42. Springer.

Nii, S. (1992). Electron microscopic study on the development of herpesviruses. *Microscopy*, 41(6):414–423.

Norkin, L. C. (1999). Simian virus 40 infection via mhc class i molecules and caveolae. *Immunological reviews*, 168(1):13–22.

Nugent, J., Birch-Machin, I., Smith, K., Mumford, J., Swann, Z., Newton, J., Bowden, R., Allen, G. and Davis-Poynter, N. (2006). Analysis of equid herpesvirus 1 strain variation reveals a point mutation of the dna polymerase strongly associated with neuropathogenic versus nonneuropathogenic disease outbreaks. *Journal of virology*, 80(8):4047–4060.

Osterrieder, N. (1999). Construction and characterization of an equine herpesvirus 1 glycoprotein c negative mutant. *Virus research*, 59(2):165–177.

Osterrieder, N. and Van de Walle, G. R. (2010). Pathogenic potential of equine alphaherpesviruses: the importance of the mononuclear cell compartment in disease outcome. *Veterinary microbiology*, 143(1):21–28.

Osterrieder, N., Wagner, R., Brandmüller, C., Schmidt, P., Wolf, H. and Kaaden, O.-R. (1995). Protection against ehv-1 challenge infection in the murine model after vaccination with various formulations of recombinant glycoprotein gp14 (gb). *Virology*, 208(2):500–510.

Ostlund, E. N. (1993). The equine herpesviruses. *Veterinary Clinics of North America: Equine Practice*, 9(2):283 – 294. Update on Infectious Diseases.

Packiarajah, P., Walker, C., Gilkerson, J., Whalley, J. M. and Love, D. N. (1998). Immune responses and protective efficacy of recombinant baculovirus-expressed glycoproteins of equine herpesvirus 1 (ehv-1) gb, gc and gd alone or in combinations in balb/c mice. *Veterinary microbiology*, 61(4):261–278.

Patel, J., Edington, N. and Mumford, J. (1982). Variation in cellular tropism between isolates of equine herpesvirus-1 in foals. *Archives of virology*, 74(1):41–51.

Patel, J. and Heldens, J. (2005). Equine herpesviruses 1 (ehv-1) and 4 (ehv-4)–epidemiology, disease and immunoprophylaxis: a brief review. *The Veterinary Journal*, 170(1):14–23.

Perelygina, L., Patrusheva, I., Vasireddi, M., Brock, N. and Hilliard, J. (2015). B virus (macacine herpesvirus 1) glycoprotein d is functional but dispensable for virus entry into macaque and human skin cells. *Journal of virology*, 89(10):5515–5524.

Perkins, G., Goodman, L., Tsujimura, K., Van de Walle, G., Kim, S., Dubovi, E. and Osterrieder, N. (2008). Investigation of neurologic equine herpes virus 1 epidemiology from 1984-2007. In *Research Abstract Program of the 26th Annual ACVIM Forum*, volume 22, pages 819–820.

Potterton, E., McNicholas, S., Krissinel, E., Cowtan, K. and Noble, M. (2002). The ccp4 molecular-graphics project. *Acta Crystallographica Section D: Biological Crystallography*, 58(11):1955–1957.

Pusterla, N., Leutenegger, C. M., Wilson, W. D., Watson, J. L., Ferraro, G. L. and Madigan, J. E. (2005). Equine herpesvirus-4 kinetics in peripheral blood leukocytes and nasopharyngeal secretions in foals using quantitative real-time taqman pcr. *Journal of Veterinary Diagnostic Investigation*, 17(6):578–581.

Rasmussen, S. G., DeVree, B. T., Zou, Y., Kruse, A. C., Chung, K. Y., Kobilka, T. S., Thian, F. S., Chae, P. S., Pardon, E., Calinski, D. et al. (2011). Crystal structure of the $\beta$ 2 adrenergic receptor–gs protein complex. *Nature*, 477(7366):549–555.

Reed, S. M. and Toribio, R. E. (2004). Equine herpesvirus 1 and 4. *Veterinary Clinics: Equine Practice*, 20(3):631–642.

Roizman, B. (1996). Herpes simplex viruses and their replication. *Virology*, pages 2231–2295.

Rudolph, J., O'CALLAGHAN, D. and Osterrieder, N. (2002). Cloning of the genomes of equine herpesvirus type 1 (ehv-1) strains kya and racl11 as bacterial artificial chromosomes (bac). *Journal of Veterinary Medicine, Series B*, 49(1):31–36.

Ruitenberg, K., Walker, C., Wellington, J., Love, D. and Whalley, J. (1999a). Dna-mediated immunization with glycoprotein d of equine herpesvirus 1 (ehv-1) in a murine model of ehv-1 respiratory infection. *Vaccine*, 17(3):237–244.

Ruitenberg, K., Walker, C., Wellington, J., Love, D. and Whalley, J. (1999b). Potential of dna-mediated vaccination for equine herpesvirus 1. *Veterinary microbiology*, 68(1-2):35–48.

Ruitenberg, K. M., Gilkerson, J. R., Wellington, J. E., Love, D. N. and Whalley, J. M. (2001). Equine herpesvirus 1 glycoprotein d expressed in pichia pastoris is hyperglycosylated and elicits a protective immune response in the mouse model of ehv-1 disease. *Virus research*, 79(1-2):125–135.

Rux, A. H., Willis, S. H., Nicola, A. V., Hou, W., Peng, C., Lou, H., Cohen, G. H. and Eisenberg, R. J. (1998). Functional region iv of glycoprotein d from herpes simplex virus modulates glycoprotein binding to the herpesvirus entry mediator. *Journal of Virology*, 72(9):7091–7098.

Sarrazin, S., Lamanna, W. C. and Esko, J. D. (2011). Heparan sulfate proteoglycans. *Cold Spring Harbor perspectives in biology*, 3(7):a004952.

Sasaki, M., Hasebe, R., Makino, Y., Suzuki, T., Fukushi, H., Okamoto, M., Matsuda, K., Taniyama, H., Sawa, H. and Kimura, T. (2011a). Equine major histocompatibility complex class i molecules act as entry receptors that bind to equine herpesvirus-1 glycoprotein d. *Genes to Cells*, 16(4):343–357.

Sasaki, M., Kim, E., Igarashi, M., Ito, K., Hasebe, R., Fukushi, H., Sawa, H. and Kimura, T. (2011b). Single amino acid residue in the a2 domain of major histocompatibility complex class i is involved in the efficiency of equine herpesvirus-1 entry. *Journal of Biological Chemistry*, 286(45):39370–39378.

Schasfoort, R. B. (2017). *Handbook of surface plasmon resonance*. Royal Society of Chemistry.

Schnabel, C. L., Babasyan, S., Rollins, A., Freer, H., Wimer, C. L., Perkins, G. A., Raza, F., Osterrieder, N. and Wagner, B. (2019). An equine herpesvirus type 1 (ehv-1) ab4 open reading frame 2 deletion mutant provides immunity and protection from ehv-1 infection and disease. *Journal of virology*, 93(22).

Shakya, A. K., O'Callaghan, D. J. and Kim, S. K. (2017). Comparative genomic sequencing and pathogenic properties of equine herpesvirus 1 kya and racl11. *Frontiers in Veterinary Science*, 4:211.

Shi, X. and Jarvis, D. L. (2007). Protein n-glycosylation in the baculovirus-insect cell system. *Current drug targets*, 8(10):1116–1125.

Shukla, D., Liu, J., Blaiklock, P., Shworak, N. W., Bai, X., Esko, J. D., Cohen, G. H., Eisenberg, R. J., Rosenberg, R. D. and Spear, P. G. (1999). A novel role for 3-o-sulfated heparan sulfate in herpes simplex virus 1 entry. *Cell*, 99(1):13–22.

Sievers, F., Wilm, A., Dineen, D., Gibson, T. J., Karplus, K., Li, W., Lopez, R., McWilliam, H., Remmert, M., Söding, J. et al. (2011). Fast, scalable generation of high-quality protein multiple sequence alignments using clustal omega. *Molecular systems biology*, 7(1).

Slater, J., Borchers, K., Thackray, A. and Field, H. (1994). The trigeminal ganglion is a location for equine herpesvirus 1 latency and reactivation in the horse. *Journal of General Virology*, 75(8):2007–2016.

Smith, K., WHITWELL, K. E., Binns, M., DOLBY, C. A., Hannant, D. and MUMFORD, J. A. (1992). Abortion of virologically negative foetuses following experimental challenge of pregnant pony mares with equid herpesvirus 1. *Equine veterinary journal*, 24(4):256–259.

Smith, K., WHITWELL, K. E., MUMFORD, J. A., GOWER, S. M., Hannant, D. and Tearle, J. (1993). An immunohistological study of the uterus of mares following experimental infection by equid herpesvirus 1. *Equine Veterinary Journal*, 25(1):36–40.

Spear, P. (1993). Entry of alphaherpesviruses into cells. In *Seminars in virology*, volume 4, pages 167–180. Elsevier.

Spear, P. G. and Longnecker, R. (2003). Herpesvirus entry: an update. *Journal of virology*, 77(19):10179–10185.

Stewart, L. M., Hirst, M., Ferber, M. L., Merryweather, A. T., Cayley, P. J. and Possee, R. D. (1991). Construction of an improved baculovirus insecticide containing an insect-specific toxin gene. *Nature*, 352(6330):85–88.

Stokes, A., Allen, G., Pullen, L. and Murray, P. K. (1989). A hamster model of equine herpesvirus type 1 (ehv-1) infection; passive protection by monoclonal antibodies to ehv-1 glycoproteins 13, 14 and 17/18. *Journal of General Virology*, 70(5):1173–1183.

Stokes, A., Cameron, R., Marshall, R. and Killington, R. (1997). High level expression of equine herpesvirus 1 glycoproteins d and h and their role in protection against virus challenge in the c3h (h-2kk) murine model. *Virus research*, 50(2):159–173.

Studdert, M. and Blackney, M. (1979). Equine herpesviruses: on the differentiation of respiratory from foetal strains of type 1. *Australian Veterinary Journal*, 55(10):488–492.

Taddeo, B. and Roizman, B. (2006). The virion host shutoff protein (ul41) of herpes simplex virus 1 is an endoribonuclease with a substrate specificity similar to that of rnase a. *Journal of Virology*, 80(18):9341–9345.

Tallmadge, R. L., Campbell, J. A., Miller, D. C. and Antczak, D. F. (2010). Analysis of mhc class i genes across horse mhc haplotypes. *Immunogenetics*, 62(3):159–172.

Tallmadge, R. L., Lear, T. L. and Antczak, D. F. (2005). Genomic characterization of mhc class i genes of the horse. *Immunogenetics*, 57(10):763–774.

Tan, X., Brunovskis, P. and Velicer, L. F. (2001). Transcriptional analysis of marek's disease virus glycoprotein d, i, and e genes: gd expression is undetectable in cell culture. *Journal of virology*, 75(5):2067–2075.

Telford, E., Watson, M. S., Perry, J., Cullinane, A. A. and Davison, A. J. (1998). The dna sequence of equine herpesvirus-4. *Journal of General Virology*, 79(5):1197–1203.

Telford, E. A., Watson, M. S., McBride, K. and Davison, A. J. (1992). The dna sequence of equine herpesvirus-1. *Virology*, 189(1):304–316.

Tewari, D., Whalley, J., Love, D. and Field, H. (1994). Characterization of immune responses to baculovirus-expressed equine herpesvirus type 1 glycoproteins d and h in a murine model. *Journal of General Virology*, 75(7):1735–1741.

Thomson, G., Numford, J. and Smith, I. (1979). Experimental immunization against respiratory disease due to equid herpesvirus 1 infection (rhinopneumonitis) using formalin-inactivated virus with various adjuvants. *Veterinary Microbiology*, 4(3):209–222.

Tischer, K. B., von Einem, J., Kaufer, B. and Osterrieder, N. (2006). Two-step red-mediated recombination for versatile high-efficiency markerless dna manipulation in escherichia coli. *Biotechniques*, 40(2):191–197.

Triantafilou, K., Fradelizi, D., Wilson, K. and Triantafilou, M. (2002). Grp78, a coreceptor for coxsackievirus a9, interacts with major histocompatibility complex class i molecules which mediate virus internalization. *Journal of virology*, 76(2):633–643.

Vaiman, M., Chardon, P. and Cohen, D. (1986). Dna polymorphism in the major histocompatibility complex of man and various farm animals. *Animal genetics*, 17(4):113–133.

Van de Walle, G. R., Kaufer, B. B., Chbab, N. and Osterrieder, N. (2009). Analysis of the herpesvirus chemokine-binding glycoprotein g residues essential for chemokine binding and biological activity. *Journal of Biological Chemistry*, 284(9):5968–5976.

Van de Walle, G. R., Peters, S. T., VanderVen, B. C., O'Callaghan, D. J. and Osterrieder, N. (2008). Equine herpesvirus 1 entry via endocytosis is facilitated by $\alpha$v integrins and an rsd motif in glycoprotein d. *Journal of virology*, 82(23):11859–11868.

Van Maanen, C., Willink, D., Smeenk, L., Brinkhof, J. and Terpstra, C. (2000). An equine herpesvirus 1 (ehv1) abortion storm at a riding school. *Veterinary Quarterly*, 22(2):83–87.

Vandekerckhove, A., Glorieux, S., Gryspeerdt, A., Steukers, L., Duchateau, L., Osterrieder, N., Van de Walle, G. and Nauwynck, H. (2010). Replication kinetics of neurovirulent versus non-neurovirulent equine herpesvirus type 1 strains in equine nasal mucosal explants. *Journal of General Virology*, 91(8):2019–2028.

Vaughn, J., Goodwin, R., Tompkins, G. and McCawley, P. (1977). The establishment of two cell lines from the insectspodoptera frugiperda (lepidoptera; noctuidae). *In vitro*, 13(4):213–217.

Warner, M. S., Geraghty, R. J., Martinez, W. M., Montgomery, R. I., Whitbeck, J. C., Xu, R., Eisenberg, R. J., Cohen, G. H. and Spear, P. G. (1998). A cell surface protein with herpesvirus entry activity (hveb) confers susceptibility to infection by mutants of herpes simplex virus type 1, herpes simplex virus type 2, and pseudorabies virus. *Virology*, 246(1):179–189.

Wedde, M., Weise, C., Nuck, R., Altincicek, B. and Vilcinskas, A. (2007). The insect metalloproteinase inhibitor gene of the lepidopteran galleria mellonella encodes two distinct inhibitors. *Biological chemistry*, 388(1):119–127.

Welch, H. M., Bridges, C. G., Lyon, A. M., Griffiths, L. and Edington, N. (1992). Latent equid herpesviruses 1 and 4: detection and distinction using the polymerase chain reaction and co-cultivation from lymphoid tissues. *Journal of General Virology*, 73(2):261–268.

Whalley, J., Ruitenberg, K., Sullivan, K., Seshadri, L., Hansen, K., Birch, D., Gilkerson, J. and Wellington, J. (2007). Host cell tropism of equine herpesviruses: glycoprotein d of ehv-1 enables ehv-4 to infect a non-permissive cell line. *Archives of virology*, 152(4):717–725.

Whitbeck, J. C., Muggeridge, M. I., Rux, A. H., Hou, W., Krummenacher, C., Lou, H., Van Geelen, A., Eisenberg, R. J. and Cohen, G. H. (1999). The major neutralizing antigenic site on herpes simplex virus glycoprotein d overlaps a receptor-binding domain. *Journal of Virology*, 73(12):9879–9890.

White, J., Crawford, F., Fremont, D., Marrack, P. and Kappler, J. (1999). Soluble class i mhc with $\beta$2-microglobulin covalently linked peptides: specific binding to a t cell hybridoma. *The Journal of Immunology*, 162(5):2671–2676.

Whitford, M., Stewart, S., Kuzio, J. and Faulkner, P. (1989). Identification and sequence analysis of a gene encoding gp67, an abundant envelope glycoprotein of the baculovirus autographa californica nuclear polyhedrosis virus. *Journal of virology*, 63(3):1393–1399.

Whittaker, G. R., Taylor, L. A., Elton, D. M., Giles, L. E., Bonass, W. A., Halliburton, I. W., Killington, R. A. and Meredith, D. M. (1992). Glycoprotein 60 of equine herpesvirus type 1 is a homologue of herpes simplex virus glycoprotein d and plays a major role in penetration of cells. *Journal of General Virology*, 73(4):801–809.

Whitwell, K. E. and Blunden, A. (1992). Pathological findings in horses dying during an outbreak of the paralytic form of equid herpesvirus type 1 (ehv-1) infection. *Equine Veterinary Journal*, 24(1):13–19.

Wickham, T., Davis, T., Granados, R., Shuler, M. and Wood, H. (1992). Screening of insect cell lines for the production of recombinant proteins and infectious virus in the baculovirus expression system. *Biotechnology progress*, 8(5):391–396.

Wilkie, B. (1982). Respiratory tract immune response to microbial pathogens. *Journal of the American Veterinary Medical Association*, 181(10):1074–1079.

Williams, C. J., Headd, J. J., Moriarty, N. W., Prisant, M. G., Videau, L. L., Deis, L. N., Verma, V., Keedy, D. A., Hintze, B. J., Chen, V. B. et al. (2018). Molprobity: More and better reference data for improved all-atom structure validation. *Protein Science*, 27(1):293–315.

Willis, S. H., Rux, A. H., Peng, C., Whitbeck, J. C., Nicola, A. V., Lou, H., Hou, W., Salvador, L., Eisenberg, R. J. and Cohen, G. H. (1998). Examination of the kinetics of herpes simplex virus glycoprotein d binding to the herpesvirus entry mediator, using surface plasmon resonance. *Journal of virology*, 72(7):5937–5947.

Wilson, W. D. (1997). Equine herpesvirus 1 myeloencephalopathy. *Veterinary Clinics of North America: Equine Practice*, 13(1):53–72.

Wohlsein, P., Lehmbecker, A., Spitzbarth, I., Algermissen, D., Baumgärtner, W., Böer, M., Kummrow, M., Haas, L. and Grummer, B. (2011). Fatal epizootic equine herpesvirus 1 infections in new and unnatural hosts. *Veterinary microbiology*, 149(3):456–460.

Wu, S., Avila-Sakar, A., Kim, J., Booth, D. S., Greenberg, C. H., Rossi, A., Liao, M., Li, X., Alian, A., Griner, S. L. et al. (2012). Fabs enable single particle cryoem studies of small proteins. *Structure*, 20(4):582–592.

Yang, H., Guranovic, V., Dutta, S., Feng, Z., Berman, H. M. and Westbrook, J. D. (2004). Automated and accurate deposition of structures solved by x-ray diffraction to the protein data bank. *Acta Crystallographica Section D: Biological Crystallography*, 60(10):1833–1839.

Yao, S., Liu, J., Qi, J., Chen, R., Zhang, N., Liu, Y., Wang, J., Wu, Y., Gao, G. F. and Xia, C. (2016). Structural illumination of equine mhc class i molecules highlights unconventional epitope presentation manner that is evolved in equine leukocyte antigen alleles. *The Journal of Immunology*, 196(4):1943–1954.

Yewdell, J. W. and Bennink, J. R. (1992). Cell biology of antigen processing and presentation to major histocompatibility complex class i molecule-restricted t lymphocytes. In *Advances in immunology*, volume 52, pages 1–123. Elsevier.

Zhang, N., Yan, J., Lu, G., Guo, Z., Fan, Z., Wang, J., Shi, Y., Qi, J. and Gao, G. F. (2011). Binding of herpes simplex virus glycoprotein d to nectin-1 exploits host cell adhesion. *Nature communications*, 2:577.

Zhang, Y., Smith, P. M., Tarbet, E. B., Osterrieder, N., Jennings, S. R. and O'Callaghan, D. J. (1998). Protective immunity against equine herpesvirus type-1 (ehv-1) infection in mice induced by recombinant ehv-1 gd. *Virus research*, 56(1):11–24.

## Acknowledgements

First of all, I would like to thank Prof. Nikolaus Osterrieder for giving me the opportunity to work in his lab and supervising my thesis. I would also like to thank Prof. Dr. Markus Wahl for welcoming me in his lab and for evaluating my thesis. A special thanks goes to Dr. Walid Azab for his close support even beyond his employment at the university.
My thanks goes also to Dr. Bernhard Loll for his close support and help in solving the protein structures of gD1 and gD4. I also want to thank my collaborators Prof. Dr. Gerhard Wolber and Szymon Pach for the *in silico* work as well as Prof. Dr. Salvatore Chiantia and Ismail Dahmani for SPR analysis and Dr. Chirstoph Weise for MS analysis. Without all those collaborations, this work would have been impossible.
I am also grateful for access to and support from beamlines at the DESY (Hamburg, Germany) and the BESSY II (Berliner Elektronenspeicherring-Gesellschaft für Synchrotronstrahlung II) storage ring (Berlin, Germany) via the Joint Berlin MX-Laboratory sponsored by the Helmholtz Zentrum Berlin für Materialien und Energie, the Freie Universität Berlin, the Humboldt-Universität zu Berlin, the Max-Delbrück Centrum, and the Leibniz-Institut für Molekulare Pharmakologie.
Thanks to Michaela Zeitlow, who supported and helped me with mutagenesis, Nicole Holton, who trained me in protein production in bacteria and protein purification, Claudia Aligns, giving away the secrets of crystallography, Ursula Neu, for insights into the sweet parts of proteins and fruitful discussions, Ann Reum and Anette Neubert who where always there to help me and our interns and students.
And certainly I want to thanks all lab members from the virology and biochemistry lab as well as all members of ZIBI for their professional and moral support and for making the time worthwhile.
Last but not least I want to thank my friends and family who reminded me constantly that I have a life outside of the lab too, particularly Yo, Hannah, Bekka, Clara, my mum Nina, and my sister Marayke.

# A. Supplement

## A.1. Mass spectrometry analysis

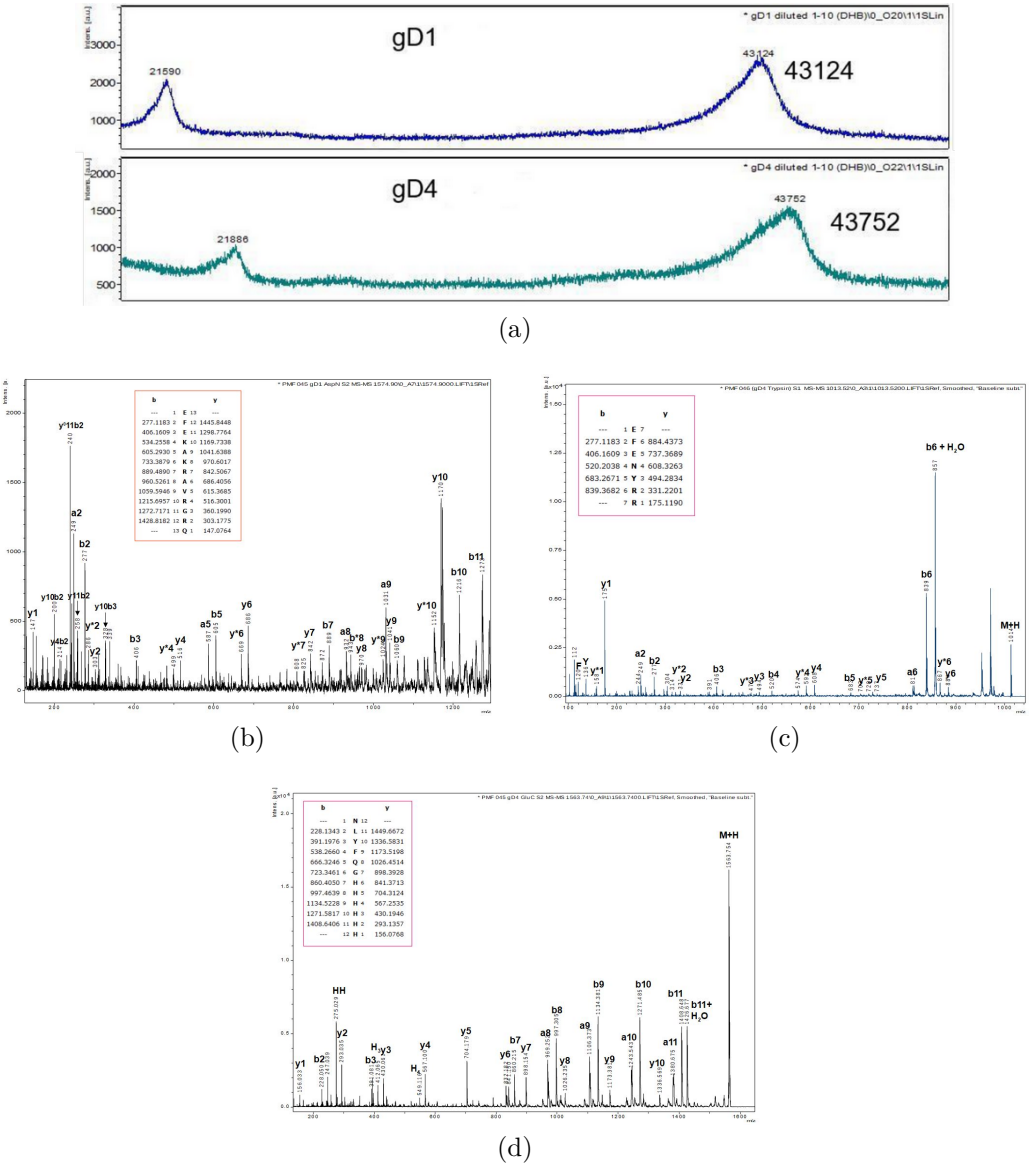


Figure 33: Mass spectrometry analysis.(a) Total mass analysis of gD1 (top) and gD4 (bottom) on DHB matrix. (b) tandem mass spectrometry (MS/MS) of in-gel digested Coomassie-stained gD1 with Asp-N endoproteinase and (c) gD4 with Trypsin and (d) Glu-C endoproteinase. All samples were diluted 1:10 with water.

## A.2. Protocols

# Protein production in insect cells and purifcation

## Bacmid Preparation from Bacteria Culture

- 5 ml o/N culture with antibiotics of recombinant DH10 MultiBac
- spin down 4500 rcf for 10 min, discard supernatant
- resuspend pellet in 250 µl P1 (Qiagen, Mini-prep), transfer to 1,5 ml tube
- add 250 µl P2, mix
- add 350 µl P3, mix immediately
- spin down 13 000 rcf for 10 min
- transfer supernatant to fresh tube, spin down 13 000 rcf for 20 min
- transfer supernatant to 2 ml tube
- add 800 µl Isopropanol
- (if you want to store Bacmid, put this in -20°C)
- spin down 13 000 rcf for 20 min
- discard supernatant, wash pellet with 500 µl 70% EtOH
- spin down 13 000 rcf for 10 min
- dry pellet until it becomes white
- dilute pellet in 30-50 µl sterile milliQ water, leave for ~10 min (no pipetting up and down!)

## Transfection of SF9 cells with Bacmid - V0 production

- dilute pellet in 30-50 µl sterile milliQ water, leave for ~10 min (no pipetting up and down!)
- in the meantime prepare master mix:

  for each sample: **2x 100 µl medium** (Gibco, SF9 900 III SF1)

  **2x 10 µl x-treme Gene9 DNA Transfection Reagent**

  (Roche, REF 06 365 779 001)

- pipette transfection reagent directly into the medium since it reacts with plastic
- add **110 µl of the master mix** to each Bacmid, incubate at RT for **30 min to 2 h**
- in the meantime plate **3 ml** of SF9 cells with **0,3x10$^6$ cells/ml** (for each Bacmid 2 wells), take along a control without DNA
- count cells, need to be >95% viable
  - press Menu, select Setup, press Enter, press Next to change program (for SF9 program 03, press twice Enter
  - dilute **50 µl of SF9** cells in **10 ml Casyton buffer**

  - put the tube into the counter, press Start (three mesurements with 400 µl)
  - note cell number, viability, aggregation, mean diameter, and peak diameter
  - clean 3x with 10 ml buffer, check by pressing Start (ok if cell number < $10^3$)
- after incubation of Bacmid with master mix add **~140 µl of Bacmid mix** to the cells in a dropwise manner
- incubate at **27°C for 60-72 h**

- on day 2 prepare cells if you want to grow V1 on day 3
  - infect **25 ml of 1x$10^6$ cells/ml** with **3-6 ml of V0** depending on the infection (good infection = 3 ml, not so good infection = 6 ml)

## Production of V1 Baculovirus in SF9 cells

- Prepare a **250 ml flask containing 25 ml of SF9 cells at 0,5x$10^6$ cells/ml** one day before infection with V0 virus (cell count + microscope)
- the next day split the cells to **0,5x$10^6$ cells/ml (in 25 ml)**, cells should be **>95% viable** (cell count + microscope)
- check cells producing V0 under the microscope
- spin down
- take off the medium, maybe filter with siringe, collect in 15 ml falcon
- add **3-6 ml of the V0 virus** to the cells depending on how strong the virus is
- incubate at 27°C and 220 rpm, check the proliferation after **24 h**
  - take a sample containing **1x$10^6$ cells/ml** (**optional**)
  - if they are proliferating, add medium to a cell density of **0,5x$10^6$ cells/ml**
  - repeat until they stop proliferating, you may need to transfer the culture into a bigger flask
- when cells stop proliferating collect V1 after **60 h**
  - take samples every **12 h** after cells stopped proliferating
- spin down at **2000 rcf for 10 min**, collect supernatant and store at **4°C**

# Purification of secreted His tagged protein from H5

## Harvest supernatant of infected H5 cells

- spin down cell suspensions at 2000 rcf for 10 min
- adjust pH if you use Ni-NTA beads at least to pH 7 with 1 M Tris-HCl buffer
- centrifuge again to get rid of precipitated salts
- collect supernatant in fresh bottle
- take a 20 µl sample for the gel, add 10 µl loading SDS LD

Prepare IMAC buffer

| **Concentration** | **Stock solutions** | **Use for 800 mL** |
|---|---|---|
| 20 mM MES pH6 /Tris-HCl pH7.5 on ice | | 8,53 g |
| 200 mM NaCl | 5 M | 32 ml |
| 5% Glycerol | 86% | 46,4 ml |

Fill with 4°C MilliQ to 800 ml, filter with 0,22 µm filter

Prepare Ni-NTA beads:

- use ca. 5 ml beads per 800 ml supernatant
- Discard EtOH used for storage (over column).
- Wash beads with MilliQ.
- Spin down at 4°C at 500 rcf for 4 min.
- Discard supernatant.
- Repeat washing step with MilliQ.
- Repeat washing step with IMAC buffer.
- Add fresh buffer (for ~50% solution).

## IMAC

- transfer the beads into the supernatant, incubate for about an hour at 4°C with occasional mixing
- set up a 200 ml glas gravity flow column in the cold room (test flow with water), get beaker, tube for collecting 20 µl flow through for gel, 10 eppis for collecting elution fractions
- prepare Elution buffer as IMAC buffer but with 400 mM Imidazol
- transfer supernatant and beads into the gravity flow column, take a 20 µl sample for the gel (FT)
- rinse the bottles with IMAC buffer, transfer as well
- wash columns with approx. 300 ml IMAC buffer
- transfer beads into small column with IMAC buffer
- you can collect a 20 µl sample of the wash if you like for the gel (W)
- elute the protein with the elution buffer in 1 ml steps, collect fractions
- measure all fractions by Nano-Drop

- pool the fractions that look good
- take 10 µl sample for the gel
- run all samples on SDS gel

## Concentrate protein

- cut-off of 10 kDa (for 38 kDa protein), 15 ml concentrator better than 50 ml (less interaction surface due to smaller membrane)
- wash concentrator once with elution buffer and spin down for 4-5 min at 3800 rcf
- maximal 10 min centrifugation, invert sample
- check flow through and concentrated protein always by Nano-Drop

## SEC

Pre-cool centrifuges to 4°C, get ice bucket, book Äkta few days in advance (Äkta 2 or 4)

**Prepare Äkta**

Prepare buffer for SEC

| **Reagent concentration** | **Stock solutions** | **Use for 500 ml** |
|---|---|---|
| 20 -50 mM MES pH6 /Tris-HCl pH7.5 on ice | | 5.3 g |
| 20-50 mM NaCl | 5 M | 20 ml |
| 5% Glycerol | 86% | 29 ml |

Fill with 4°C MilliQ to 500 ml, filter with 0,22 µm filter, degas

- equilibrate a 16/600 Superdex 200 column with the GeFi buffer at a flow speed of 0,1 ml/min (aprrox. 1 h)
- spin down sample before loading for 5 min at max speed
- wash loop with GeFi buffer
- load the fraction collector with glass tubes and eppis (fraction 15-40)
- load the loop with the protein solution, run with flow speed of 0.4 ml/min and collect fractions with a volume of 250 µl in eppis (fraction 15-40)
- collect eppis after approx. 30 min
- analyse fractions by Nano-Drop and SDS-PAGE gel electrophoresis, take pooled sample from IMAC along as a control
- pool fractions containing the protein

## Concentrate protein

- as before
- concentrate the protein using a Millipore concentrator to a concentration of approx. 15 mg/ml or higher
- **aliquot in 10 and 20 µl, shock freeze and keep at -80°C, for crystallization use fresh protein! You might wanna cleave the $His_6$-tag using TEV protease**

# Prodcution and purification of His-tagged Proteins from *E. coli*

Transformation:
Day 1:

- Transform expression plasmid into Rosetta2.
- Plate on LB plates with antibiotics.

Growth and induction:
Day 2:

- Start 50 ml over night culture in LB with antibiotics.

Day 3:

- Dilute culture 1:100 into 1000 ml ZYM-5052 medium.
- Let grow at 37°C at 200 rpm until $OD_{600}$ 0.6.
- Take a 2 ml aliquot of culture for SDS-PAGE.
- At A600 between 0.4-0.5 (do not overgrow!!) transfer culture to 15-20°C.
- Grow over night.

Purification (all procedures at 4°C!):
Day 4:

- Take a 2 ml aliquot of culture for SDS-PAGE.
- Pellet cells at 6,000 rpm, 5 min.
- Discard supernatant, dip a tip into pellet for SDS-PAGE.
- (you can freeze the pellet at -80°C and use later)
- Resuspend cells completely (!) in 25 ml ice cold Tris-HCl pH7.5 (at 4°C) with 1mM DTT and 5% Glycerol.
- Add Lysozym and DNAse1.
- Sonicate 1 s on, 2 s off, 20 min at 70% amplitude on ice.
- Save 50 µl for analysis (or 2 µl in 20 µl 2x loading buffer).
- Spin 21,500 rpm, 45 min. (55,914 *g*)
- Collect supernatant (lysate), save 50 µl for analysis (or 2 µl in 20 µl 2x loading buffer).

Prepare Ni-NTA beads:

- Discard EtOH used for storage (over column).
- Wash beads with MilliQ.
- Spin down at 4°C at 500 *g* for 5 min.
- Discard supernatant (over column to recycle beads).
- Repeat washing step with MilliQ.
- Repeat washing step with Binding buffer A.

- Add fresh buffer (for ~50% solution).

Prepare Elution buffer:

- Use 80 ml of Binding buffer A and 20 ml of 2 M Imidazol for 400 mM.
- (prepare fresh if buffer components get diluted too much)

Column purification:

- Mix lysate and beads and invert for 30-60 min.
- Place lysate mix on gravity flow column, collect sample from flow through for SDS-PAGE.
- Wash tubes with Binding buffer A and place on column too.
- Wash column 3x with binding buffer A.
- Prepare 10 1.5 ml tubes for each sample for fraction collection.
- Place 1 ml Elution buffer over colum, collect flow through in eppi. Repeat 10x.
- Measure protein concentration with Nano Drop.

Run samples on SDS gel:

| | |
|---|---|
| Uninduced cells | U |
| Cell pellet | P |
| Whole cell (after sonication) | WC |
| Supernatant (of cell lysate) | S |
| Flow through (column) | FT |
| Eluate (pooled fractions) | E |
| Washed beads only | B |

Viviane Kremling, 2018, Thermofluor

# Thermofluor

Initial screens for optimization pH, buffer and salt
Screens:

- pHat buffer
- Custom „FU“
- PACT

- tell Claudia at least **3 days in advance** that you need compound plates for thermofluor
- book thermofluor (approx. 2 h for 1 plate, one run takes 1 h 12 min)

- start computer, login
- turn on Mx3005P Q-PCR machine
- start program MxPro
- warm up xenon lamp for **20 min**:
  if ‚Turn on lamp for warm up‘ option has been selected previously it‘s on already,
  if not, select ‚Instrument/Lamp On‘ from the menu, check at the right lower corner
- prepare **1,1 ml** (or a little more) **purification buffer** with 1:500 **SYPRO organge** (**2,2 µl**, light sensitive!!!) and add **protein** (minimum use 0,165 mg, use **0,2 mg** for better signal), mix carefully
- aliquot **135 µl of the protein mix** into a 8 tubes PCR-strip
- take the compound plate from 4°C, spin briefly at **200 g for 1 min**
- remove the aluminium foil
- remove water for **10 µl purification buffer** from H10, H11 and H12 as references
- add **10 µl protein mix** to each well using a 8-channel pipette, do not mix, avoid bubbles by emptying tips at the sides of the wells
- cover the plate with optical foil
- place the plate in the machine and start program **25-95°C at 1°C min$^{-1}$** (any on the desktop should be ok, template from Jan W. in Karen‘s folder)
  - you can save the template in your own folder
  - the program will ask you to save the data elsewhere, click yes and save it to your folder
- when the run is done it takes a bit longer than a minute before the program is actually finished

## Data processing

- export data

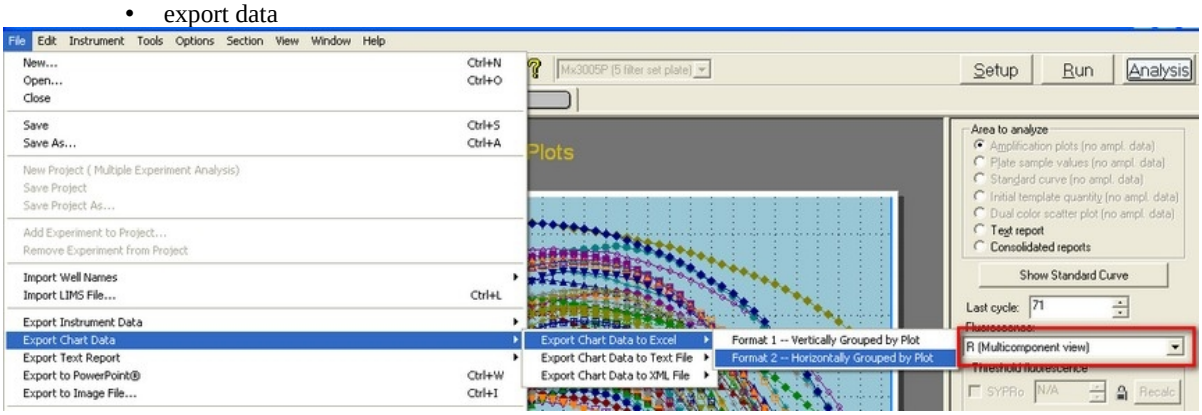

- save in the format „Excel-Arbeitsmappe“
- open this file on a computer which has Origin or Graphpad installed
- select the whole table and copy it
- open the table „Transform Agilent Mx3005p data for DSF Analysis v3.0“
- do not click somewhere, paste in the exported data
- go to the table sheet „Output“, select all and copy the transformed data
- open the table „DSF Analysis v3.0.1_FU_screen“
- paste in the transformed data into the table sheet „Paste in transformed data“
- go to the table sheet „Processed Data“ and copy the table „Paste this table into Graphpad or similar software, to perform fitting to Boltzman equation:“
- open Origin Pro, paste in the transformed data
- select all, run Boltzmann Function

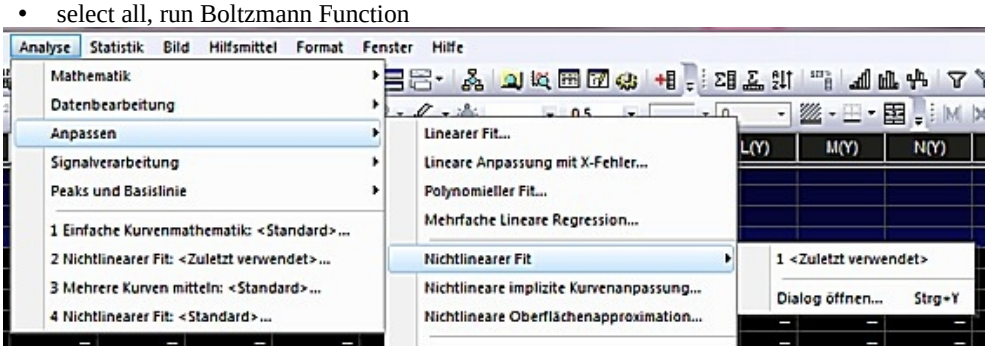


- copy values from table „Zusammenfassung“ $x_0$ Wert

Zusammenfas

| | A1 | | A2 | | x0 | | dx | | span | EC50 | Statistik | |
|---|---|---|---|---|---|---|---|---|---|---|---|---|
| | Wert | Standardfehler | Wert | Standardfehler | Wert | Standardfehler | Wert | Standardfehler | Wert | | Chi-Quadr Reduziert | Kor. R-Quadrat |
| B | 15181.25722 | 162.23379 | 31052.02065 | 155.08364 | 43.70932 | 0.11453 | 2.0463 | 0.10401 | 15870.76343 | 9.60982E18 | 147256.08025 | 0.99678 |
| C | 17914.15847 | 184.00421 | 27874.16326 | 258.12796 | 43.4358 | 0.19448 | 1.43959 | 0.17247 | 9960.00479 | 7.3102E18 | 252525.97482 | 0.98643 |
| D | 14642.84489 | 244.71029 | 29630.60141 | 233.66516 | 48.25498 | 0.12986 | 1.32097 | 0.11575 | 14987.75652 | 9.05462E20 | 288657.85376 | 0.9934 |
| E | 13215.64922 | 158.43985 | 26475.04209 | 187.81552 | 50.40815 | 0.10512 | 1.29731 | 0.09344 | 13259.39287 | 7.79798E21 | 150914.82701 | 0.99556 |
| F | 12329.22687 | 82.96981 | 27906.27322 | 62.48386 | 51.50518 | 0.04203 | 1.32396 | 0.03687 | 15577.04636 | 2.33568E22 | 35150.44877 | 0.99926 |
| G | 14062.45234 | 81.57637 | 25162.19895 | 63.74665 | 52.26518 | 0.05526 | 1.19128 | 0.04835 | 11099.74661 | 4.99434E22 | 35594.18386 | 0.99857 |

- open a new excel sheet, transpose values, copy them
- go back to the table „DSF Analysis v3.0.1_FU_screen“
- paste in the processed data into the table sheet „Processed Data“ into the table „Paste in here the results from Boltzman fitting (Paste special/values):“
- save the excel sheet under a name you recognize
- check for analysis the graphs in the table sheet „All graphs“ and for the best buffer conditions in table sheet „Results at a Glance“ the values in the column „For graph: delta Tm ok“

## A.2.4.

Novermber 28 2017

# MALS Protocol

## Starting the machine, equilibrating column

- **prepare fresh buffer with 0.02% sodium azide, if necessary new MilliQ water has to be prepared with 0.04% sodium azide**
- switch on the cisco switch first, then the HPLC (incl. fraction collector) and the computer
- switch on the Refractomax press the "**Purge**" button of the Refractomax
- connect the buffer bottles with the pump (buffer goes at position A, MilliQ water at B and EtOH at C)
- open the ChemStation software („**Rosinante online**") and click "**Upload from instrument**"
- in the box "**Quat. Pump**" right-click on the bottles and go to → "**Bottle fillings**", enter the right volume for each bottle
- click the large green "**On**" button
- switch off the UV lamp by right-click on the lamp → "**Switch off**" as long as you don't start a sample run
- go the "**Quat. Pump**" box again, right-click in the box and open the "**Method**" window
- set the pump to 100% C (EtOH), adjust the flow to 0.2ml/min, set the min. pressure limit to 0.0bar, the max. pressure limit to **17 bar** and the max. flow gradient to 5 ml/min$^2$
- now open the purge valve of the HPLC by twisting the black knob to the left
- go to the "**Method**" window again and set the flow to 5ml/min
- wait until all air bubbles are gone and set the pump to 100% B (MilliQ water) and wait again for about 2min, do the same for the buffer and in the end switch back to water
- set the flow to **0.8 ml/min** and close the purge valve
- to connect the column go to the "**Method**" window and set the flow to **0.15ml/min**, set the max. pressure limit to **25.0bar** for the S75 column and **35.0bar** for the S200 column or Superose6 column. Set the min. pressure limit to 0.0bar
- now connect the column and put it upside down (do not run it reverse) and check if nothing is leaking
- in the advanced tab of the "**Method**" window:

  set the **max. flow gradient** to **0.1ml/min$^2$** **(CRUCIAL !!)**
- set the flow rate to **0.6ml/min** and equilibrate with 2-3 column volumes of buffer (100% A) (in case the column is in 25 % EtOH, run one column volume water first)
- **DO NOT CHANGE THE FLOW RATE DURING THE EQUILIBRATION OR THE RUNS, THE FLOW HAS TO STAY CONSTANT ALL THE TIME!**
- switch on the WYATT machine
  (at least 30 min before the experiment, as the laser needs 30min to warm up)
- equilibration is done when the light scattering baseline is precise as 10-30µV

## Running a sample

- spin down your sample for 10min (13,000xg) at RT and keep it at RT until loading it to the column
- go to the ASTRA software and click "**File**" → "**New**" → "**Experiment from Method...**" (use normalization run from BSA)
- adjust all the parameters of the method to your current run, such as UV extinction coefficient, injection volume, flow rate, sample name etc.
- when done right-click on the experiment and click "**Save as...**"
- then start by clicking on the run button on top (small green triangle, do not press the green circle!)
- now go back to the ChemStation software and go to "**Method**" → "**Edit entire method**" (empty the time-table if there are entries)
- check all the parameters for your run and set the draw speed to 150µl/min and the draw position to 1mm, then click OK and save the method with "**File**" → "**Save as**" → "**Method**"
- now go to "**Sequence**" → "**Sequence table**" and enter sample name, injection volume, number of injection etc. and make sure that the current method is selected
- click OK and save the sequence table with "**File**" → "**Save as**" → "**Sequence template**"
- now open the sequence table again and click "**Run**"

## Washing the column to water, together with water injection

- Go to the ChemStation software (**Rosinate online**) and in the **Quant. Pump** box, right-click and open the **Method** window
- Set the pump to 100% B ($H_2O$) and
- Fill a vial with 500 µL water containing 0.04% sodium azide and place it in the sample tray
- go to "**Method**" → "**Edit entire method**" and change the stop-time to 1min
- To turn off the UV light during water wash, uncheck the box "Lamp required during acquisition", in the UV tab. Turn off the UV lamp manually by clicking on the lamp icon in the VWD module.
- Go to Sequence table, select this method, choose the position of your injection vial, the injection volume and the number of injections/loci (3x90 µL injections are enough), **save the table!**
- run the sequence table you saved and flow at least 1.2 column volumes of H2O (with Azide!)
- after the injections are done: press the Purge button on the Refractometer

## Disconnecting, system shut-down

- make sure the Purge button of the Refractomax is pressed.
- **systematically lower the flow rate** going down **in steps of 0.04 mL/min**. to 0.15 ml/min
- disconnect the column
- **change the pressure limit to 17 bar (CRUCIAL !!)**
- increase the flow-rate to **0.8 ml/min** and flush the system for 5 more minutes (until pressure steady) with 25% EtOH
- decrease flow in 0.3 ml/min steps to zero.
- close ChemStation software,
- switch of the computer, the HPLC (incl. fraction collector), WYATT machine (if not already done earlier), Refractoctomax and the Cisco Switch.

## Analysis of MALS data (briefly)

- Click on **Baselines** (located in the side-bar)
- Start with analyzing the LS2 scattering curve (measured at 90 degrees to laser)
- Ctrl-click and zoom. You really need to zoom in well into the peak to fit the baseline correctly
- use Snap-Y to fit the baseline (recommended)
- Click set-all. The same base-line is then applied to all the traces. (does not work well with manually set baselines)
- Check all the other traces to see if the base-line fits, re-fit if necessary
- Press OK
- Go to **Peaks**
- Select the range you want to analyze, spanning your peak
- Click on EasyGraph and look at plots of LS and molar mass. Hovering around the peak holding the Shift button will give you the molar mass. A straight line through the LS curve peak denotes a homogeneous species of defined molar mass.

# EHV blocking assay with soluble gD1 and gD4, FACS

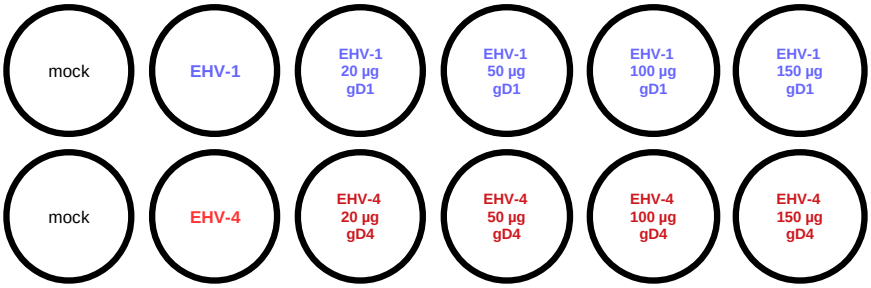


## Reagents

- Citrate Buffer
  - 40 mM citric acid, 10 mM Potassium chloride, 135 mM Sodium chloride, pH 3, store at 4°C

Viruses

| | **FACS** | **Volume needed** |
|---|---|---|
| **EHV-1** | MOI 0.1 | |
| | *180 µl of $10^{-2}$ dilution of 1,1 x $10^{7}$ virus (7.2.19)* | *1000 µl for 5 wells* |
| **EHV-4** | MOI 0.1 | |
| | *76 µl of 2,6 x $10^{5}$ virus (26.2.19)* | *500 µl for 5 wells* |

Protein

for both, gD1 and gD4, **22,5 µg per well** → 12 µl of 2 mg/ml in 138 µl media

## Protocol

prepare citrate buffer, book FACS machine

- plate **1,5-2 x $10^{5}$ ED cells per 24-well** one day before starting the assay
- chill cells and reagents for the first incubation with the protein on ice for 10 min
- incubate gDs with NBL-6 cells for **1 h on ice**
- take out the citrate buffer from the fridge to warm to room temeperature
- add the virus to the cells and incubate for **1 h at 37°C**
- tilt the plate after infection every 2 min in the first 10 min, later every 10 min
- wash cells with **PBS**
- add a few drops of **citrate buffer** to cover the cells for **max. 30 seconds!** (pH 3)

- neutralize with a few drops of **media**, take off media
- wash cells **2x with PBS**
- add **500 ul medium** to the cells and incubate for **24-48 h at 37°C**
- harvest cells with **trypsin**, spin down, wash with **PBS**, add **300 µl PBS**
- transfer **200 µl of cells in 96-well** palte round bottom, keep rest on ice

## A.2.6.



### EHV blocking assay with soluble gD1 and gD4, plaque numbers

## Reagents

- Citrate Buffer
  - 40 mM citric acid, 10 mM Potassium chloride, 135 mM Sodium chloride, pH 3, store at 4°C
- Methylcellusose
  - 3 mgMethylcellusose (viscosit 400 pC) in 300 ml dest. H2O, 4,75 mg DMEM in 100 ml H2O, 25 ml FCS, 5 ml NaHCO3 (7,5%), 1% P/S
- Crystal violet

Viruses

| | **Plaque assay (duplicates)** | **Volume needed** |
|---|---|---|
| **EHV-4** | 100 PFU/**well** | |
| | *20 µl of of $10^{-1}$ dilution of 2,6 x $10^{5}$ virus (26.2.19)* | *400 µl for 8 wells (40 µl in 360 µl media)* |

## Protein

all **22,5 µg per well → 12 µl of 2 mg/ml,** add 138 µl media

## Protocol

prepare citrate buffer and Methylcellusose if neccessary

- plate **1,5-2x10^5 ED cells per 24-well** one day before starting the assay
- chill cells and reagents on ice for **10 min**
- prepare protein dilutions
- add gDs to NBL-6 cells, incubate for **1 h on ice**
- prepare virus dilutions
- take out the citrate buffer and methylcellulose from the fridge to warm to room temeperature
- add the virus to the cells and incubate for **1 h at 37°C**
- tilt the plate after infection every 2 min in the first 10 min, later every 10 min
- wash cells with **PBS**
- add a few drops of **citrate buffer** to cover the cells for **max. 30 seconds!** (pH 3)
- neutralize with a few drops of **media**, take off media
- wash cells **2x with PBS**
- add **500 ul methylcellulose** medium and incubate for **48 h at 37°C**
- count GFP plaques after 24 and 48 h
- stain with crystal violet **when plaques are visible**

# BAC Mutagenesis

Takes ~2 weeks if everything works well until you have recombinant virus.

## Design Primers

- Kana start (aggatgacgacgataagtag) and end (cagaattggttaattggttg) sequence
- get the sequences for the block 1-4
- get the gene position in the BAC
- add blocks to primers, for reverse primer make reverse complement
- check if the sequence length is correct (83)
- check primers in pEP KanS plasmid and check annealing temperatures
- insert disired mutation into original gene sequence, translate to amino acids and run a blast to check if mutation is correct
- order primers

### Example: gD1 D261N (Gat to Aat)

**Fwd :** block 1 + block 2 + block 3 + Kana start
aggagagcatatgacatggttgaagttctggttcgtctacAatggtggaaacctaccagtgcaaggatgacgacgataagtag (83 b)

Rev: Kana end + block 2 + block 3 + block 4
cagaattggttaattggttgtgaagttctggttcgtctacAatggtggaaacctaccagtgcagttttatgaagcccaggcat
make reverse complement -->
**Rev final**
atgcctgggcttcataaaactgcactggtaggtttccaccatTgtagacgaaccagaacttcacaaccaattaaccaattctg (83 b)

| | |
|---|---|
| Kana start | aggatgacgacgataagtag |
| Kana end | cagaattggttaattggttg |
| gD1 block one (40 before 261) | aggagagcatatgacatggt |
| gD1 block two (20 before 261) | tgaagttctggttcgtctac |
| gD1 block three (23 after and including 261) | Gat change to Aatggtggaaacctaccagtgca |
| gD1 block three (43 after 261) | gttttatgaagcccaggcat |

**gD1 nucleotide sequence**

| | |
|---|---|
| **in EHV-1** | 131583-132791 |
| **in BAC** | 13905-140303 |

atgtctaccttcaagcttatgatggatggacgtttggtttttgccatggcaatcgcgatcttgagcgttgtgctctcttgtggaacatgcgagaaagccaagcgtgcggttcgagga
cgccaggataggccaaaggagtttccaccaccccgctataactatacaattttaacaagatacaacgcgactgcgctagcatcaccgtttattaacgaccaagtaaaaaatgttg
acttgcggattgttactgctacgcgcccatgtgaaatgatagcgctgatcgctaagacaaacatagactcaatcctgaaggagctggccgctgcccaaaaaacttattccgcca
gactcacctggtttaaaattatgccaacgtgtgcaacgcctatacacgatgttagttatatgaaatgcaacccgaagctatcatttgcaatgtgtgatgagagatcagacatactat
ggcaagctagtttaattactatggctgctgaaactgacgatgaacttggacttgtactggcagcccctgcacattctgcctcgggactgtatcgccgtgttatagaaatcgacgga
aggcgaatttacacggacttttctgtaactattcccagtgaacggtgtccgattgcctttgagcaaaactttggcaatccggatcggtgtaaaactccagagcagtactcgcggg
gagaagtttttacacgtcggtttcttggtgaattcaacttcccacaaggagagcatatgacatggttgaagttctggttcgtctacGatggtggaaacctaccagtgcagttttatga
agcccaggcattcgcaagacccgtgcctccggataaccaccctggatttgattctgttgagtcggagattacacaaaataaaacagacccgaaaccaggccaggcggaccc
caaacccaatcagccttttaagtggcccagcatcaaacacttggccccaagactcgatgaggtggatgaggtcatagagcccgtaacaaagccccccaaaaacgtctaagagc
aactctacgtttgtgggcatcagcgtcggtttgggtatcgccggcctagtattggtgggcgtcattctatacgtctgcttgcgtcggaagaaggaactgaaaaagtctgcacaga
acggcttgactcgcctacgctcgacctttaaggatgttaaatatacccagcttccgtaa

**Checking for frame shift in old an new sequences**

```
Query  1    MSTFKLMMDGRLVFAMAIAILSVVLSCGTCEKAKRAVRGRQDRPKEFPPPRYNYTILTRY  60
            MSTFKLMMDGRLVFAMAIAILSVVLSCGTCEKAKRAVRGRQDRPKEFPPPRYNYTILTRY
Sbjct  1    MSTFKLMMDGRLVFAMAIAILSVVLSCGTCEKAKRAVRGRQDRPKEFPPPRYNYTILTRY  60

Query  61   NATALASPFINDQVKNVDLRIVTATRPCEMIALIAKTNIDSILKELAAAQKTYSARLTWF  120
            NATALASPFINDQVKNVDLRIVTATRPCEMIALIAKTNIDSILKELAAAQKTYSARLTWF
Sbjct  61   NATALASPFINDQVKNVDLRIVTATRPCEMIALIAKTNIDSILKELAAAQKTYSARLTWF  120

Query  121  KIMPTCATPIHDVSYMKCNPKLSFAMCDERSDILWQASLITMAAETDDELGLVLAAPAHS  180
            KIMPTCATPIHDVSYMKCNPKLSFAMCDERSDILWQASLITMAAETDDELGLVLAAPAHS
Sbjct  121  KIMPTCATPIHDVSYMKCNPKLSFAMCDERSDILWQASLITMAAETDDELGLVLAAPAHS  180

Query  181  ASGLYRRVIEIDGRRIYTDFSVTIPSERCPIAFEQNFGNPDRCKTPEQYSRGEVFTRRFL  240
            ASGLYRRVIEIDGRRIYTDFSVTIPSERCPIAFEQNFGNPDRCKTPEQYSRGEVFTRRFL
Sbjct  181  ASGLYRRVIEIDGRRIYTDFSVTIPSERCPIAFEQNFGNPDRCKTPEQYSRGEVFTRRFL  240

Query  241  GEFNFPQGEHMTWLKFWFVYDGGNLPVQFYEAQAFARPVPPDNHPGFDSVESEITQNKTD  300
               GEFNFPQGEHMTWLKFWFVY+GGNLPVQFYEAQAFARPVPPDNHPGFDSVESEITQNKTD
Sbjct  241  GEFNFPQGEHMTWLKFWFVYNGGNLPVQFYEAQAFARPVPPDNHPGFDSVESEITQNKTD  300

Query  301  PKPGQADPKPNQPFKWPSIKHLAPRLDEVDEVIEPVTKPPKTSKSNSTFVGISVGLGIAG  360
            PKPGQADPKPNQPFKWPSIKHLAPRLDEVDEVIEPVTKPPKTSKSNSTFVGISVGLGIAG
Sbjct  301  PKPGQADPKPNQPFKWPSIKHLAPRLDEVDEVIEPVTKPPKTSKSNSTFVGISVGLGIAG  360

Query  361  LVLVGVILYVCLRRKKELKKSAQNGLTRLRSTFKDVKYTQLP  402
            LVLVGVILYVCLRRKKELKKSAQNGLTRLRSTFKDVKYTQLP
Sbjct  361  LVLVGVILYVCLRRKKELKKSAQNGLTRLRSTFKDVKYTQLP  402
```

# Prepare liphosilated Primers

- spin down
- add dd$H_2O$ to a final concentration of 100 µM
- vortex
- leave for 15-20 min
- vortex
- make a working stock with a 1:10 dilution (90 µl dd$H_2O$ + 10 µl oligos)

## Run PCR on pEP KanS plasmid

- This will give you a PCR construct with your gene of interest including the Kana-casette
- 2-step PCR, adjust Tm if needed

50 µl reaction

| | µl |
|---|---|
| 5x Phusion Buffer | 10 |
| dNTPs | 1 |
| Primer 1 | 2,5 |
| Primer 2 | 2,5 |
| pEP KanS 1:10 from Mini-prep | 1 |
| S7 Phusion polymerase | 1 |
| H2O | 32 |

| **Temp. [°C]** | **Zeit [s]** | **Zyklen** |
|---|---|---|
| 98 | 120 | |
| 98 | 15 | 10 |
| **55** | 45 | |
| 72 | 120 | |
| 98 | 30 | |
| **63** | 45 | 25 |
| 72 | 120 | |
| 72 | 600 | |
| 4 | pause | |

- Gel purify PCR product, elute in 30 µl (optional, you can also go directly for the Dpn-I digest if you verifyied the PCR product on a gel, that saves time and DNA)

## Dpn-I digest 1-3 h at 37°C

| | |
|---|---|
| PCR product | 30 µl |
| Cut Smart buffer | 4 µl |
| Dpn-I enzyme | 1 µl |
| H2O | 5 µl |

- Column purify digested PCR product, elute in 30 µl H2O or elution buffer
- check on gel and measure by nano drop

## Preparation of recombination- and electrocompetent GS1783

Prepare 3-5 ml LB overnight culture containing 30 µg/ml chloramphenicol of the E.coli containing the target BAC the night prior to the preparation of competent cells. (Method adapted from Lee *et al*.)
You can prepare several aliquots (store at -80°C) or prepare only a 5 ml o/N culture and use it directly (adjust volumes)

1. Inoculate 100 ml pre-warmed LB broth with 30 µg/ml chloramphenicol and 3-4 ml of the overnight culture. Shake at 32°C, 220 rpm until $OD_{600}$ reaches 0.5 – 0.7 (approx. 3h).
2. Turn on 42°C water bath.
3. Transfer culture **immediately** into water bath shaker at 42°C, 220 rpm for 15 min.
4. Chill bacteria culture for 20-30 min in ice bath.
5. Transfer bacteria into two pre cooled 50 ml falcon.
6. Spin bacteria for 5-10 min at ≤4°C, 4,500 x g. Discard supernatant.
7. Resuspend pellet in 5 ml sterile 10% ice-cold glycerol in ddH2O.
8. Fill up the tube with ice cold glycerol to 40 ml and invert the tube

9. Spin bacteria for 5-15 min at ≤4°C, 4,500 x g. Discard supernatant.
10. Repeat washing steps 7 to 9.
11. Resuspend bacteria with 10% glycerol in a total volume of 500 µl (1:100 of culture volume).
12. Make 100 µl aliquots and freeze in liquid N2. Store at -80°C or use directely.

## Electroporation and 1st Red recombination

1. Thaw electrocompetent bacteria (if from -80°C) for 10 min on ice, chill electroporation cuvette on ice
2. Add approx. 100 ng of PCR product to 100 µl of electrocompetent bacteria.
3. Transfer DNA / bacteria mix to chilled electroporation cuvette. Electroporate immediately with 18 kV/cm (1.8 kV with 1 mm cuvettes) using settings of 25 µF and 200 Ω.
4. Remove bacteria immediately from cuvette with 1 ml LB broth without antibiotics.
5. Shake bacteria 1-2 h at 32°C.
6. Spin at 6.000 rcf for 2 min, discard supernatant and plate on LB agar plate with 30 µg/ml chloramphenicol and 30 µg/ml kanamycin.
7. Incubate plates for 24-48 h at 32°C. These bacteria are very slow.
8. Inoculate 3 ml LB media containing CAM and Kana with clones picked from the trafo plates (make replica plate), also inoculate original BAC as control for RFLP
9. incubate overnight at 32°C

## Miniprep DNA isolation

**(Protocol from Darren Weight)**

**Solutions and equipment:**

**P1:** Dissolve 6.06 g Tris base, 3,72 g Na2EDTA.2H2O in 800 ml distilled water. Adjust the pH to 8.0 with HCl (DO IT UNDER THE HOOD!). Adjust the volume to 1 L with distilled water. Leave it at 4°C. If it has RNAse to it, ist must gewain at 4°C.
RNase- prepare fresh, ~1 mg/ml (1:1000 of our stock should do)

**P2:** Dissolve 8 g of NaOH pellets in 950 ml distilled water, 50 ml 20% SDS (w/V) solution. The final volume should be 1 L. Must leave it at RT! If you see SDS precipitate, warm it up until they dissolve.

**P3:** Dissolve 147.1 g potassium acetate in 500 ml distilled water. Adjust the pH to 5.5 with glacial acetic acid (~110 ml). Adjust the volume to 1 L with distilled water. Must leave it at 4°C.

**Isopropanol**- placed at -20°C before starting

**EtOH** 70 %

**Centrifuge** at 4°C

- Materials and Reagents Needed:
- P1 (Store at 4°C)
- P2 (Store at RT)

- P3 (Store at 4°C)
- TE + RNAse Mix (200X)
- Buffered Phenol:Chloroform.

- Methods:
- Start 5 ml overnight culture of bacteria in appropriate antibiotics.
- Spin bacteria down at 5000 rpm for 10 min.
- Take off supernatant.
- Resupsend pellet in 300 **µl P1** by vortexing.
- Transfer to a 2 ml Eppendorf tube.
- Add **300 µl P2** to lyse the cells and mix by inverting.
- Incubate **in RT** for **5 min**.
- Add 300 **µl P3** to neutralize the solution and mix by inverting.
- Incubate on **ice** for 10 **min**.
- Spin at top speed (**14,000 rpm**) for 10 **min**.
- transfer supernatant into 2 ml eppi
- (Add 9**00 µl Buffered phenol:chloroform** and mix by vortexing.
- Spin for 10 min at RT as before.
- Collect aqueous (top) phase from phenol:chloroform extraction with cut-off pipette tips, and place in the new tube) optional
- Add **700 µl 100% isopropanol** and mix by inverting.
- Put in -20°C for 20 min
- Spin on top speed (**14,000 rpm**) for 1**0 min** at 4°C and pour off alcohol.
- Wash 1-2X with **1 ml 70% ethanol**.
- On final spin, pour off ethanol, then pellet residual liquid in centrifuge for a few seconds.
- Remove residual liquid without disturbing the DNA/RNA pellet using suction.
- Let stand at RT until pellet gets trasparent.
- Resuspend pellet in **30 µl TE plus RNAse mix (1:200)**.
- Incubate for 10-20 **min** at **37°C**.

## Restriction Fragment Length Polymorphisms (RFLP) Analysis

Check what enzyme works for your sequence. SmaI, XmaI, AvaI, HindIII and ClaI cut in Kana sequence. However, it might be better to choose something outsite the Kana sequence. Best thing is to have a fragment of the gene which is bigger if Kana sequence is inserted. The fragment should be bigger than 7 kb to be seen clear on the gel.

**Pst-I digest ~3 h at 37°C**
(1 h with HF enzyme is enough)

| | |
|---|---|
| BAC DNA | 10-15 µl |
| Cut Smart buffer | 4 µl |
| Pst-I enzyme | 1 µl |
| H2O | 15-20 µl |

- Prepare 0,8% agarose gel (2 g agarose in 250 ml buffer), let dry for ~20 min
- book gel chamber (maybe one day in advance)
- run at 45-60 V overnight

- soak gel for 30 min in ethidium bromide, wash for 15 min in water, take gel picture
- make glycerol stocks of correct intermidate (Co-integrates) clones

## Resolution of integrates

- grow 5 ml LB culture **o/N** with appropriate antibiotics (Cam/Kana) at 32°C
- prepare 2 ml LB media with appropriate antibiotics (Cam), warm to 32°C
- add 100 µl o/N culture to the 2 ml warm LB, shake at 220 rpm for **2 ½ h (2-4 h)** at 32°C until bacteria reach early logarithmic phase
- add 2 ml 32°C LB with Cam and 1% L-arabinose (make always fresh 10% stock in LB, use 1:10 dilution, you also need some for the agar plates later)
- shake for another **45 min (30-60 min)** at 220 rpm
- transfer culture into 42°C water bath, shake 220 rpm for **30 min (15-30 min)** (Induction of Expression of Red recombination system)
- return culture to 32°C for **2-3 h (1-4 h)** (2 h is fine, there are a lot of colonies)
- plate $10^{-3}$ and $10^{-5}$ dilutions on Cam/arabinose plates, incubate at 32°C for one or two days
- pick replica plates (Cam only, Kana only)
- select colonies growing on Cam only (these are your final clones) and check by RFLP and sequencing (PCR for gD gene), check Kana-plates after 3-4 days, sometimes a clone grows there late
- make glycerol stocks of correct clones

## DNA-prep for transfection of BACs

For EHV-1:

- inoculate 100 ml LB with CAM with the correct clone, picked from replica plate, incubate o/N at 32°C
- use midi-prep kit (takes ~ 4 h)

For EHV-4:

- inoculate 2 ml LB with CAM with correct clone, picked from replica plate, incubate o/N at 32°C
- add the 2 ml culture to 500 ml LB with CAM, incubate o/N at 32°C
- use large construct kit (takes ~ 6-7 h, can be paused o/N after step 12)

## Transfection of 293T to reconstitute viruses

(Protocol from Darren Weight)

- 293T should be 60-70% confluent at the day of transfection
- if you let them grow o/n before infection, change media 1 h prior to transfection
- Remove PEI, Opti-MEM and the BACs about 10 mins before starting, so that they can get to room temperature.
- Add Opti-MEM into 1.5 ml eppendorf tubes (100 ul for a 6wp and 50ul for a 12wp).
- Add the BAC DNA in as small a volume as is possible. NOTE- for cells in a 6wp; total DNA should not exceed 1-3ug (based on U20S). For cells in a 12wp; total DNA must not exceed 500 ng (based on U20S).
- Add the PEI into each tube (40 ul for 6wp and 20 ul for a 12wp). NOTE- do not vortex the PEI as it will produce compounds which will kill the cells. Just flick the tube to mix.

- Incubate the tubes at room temperature for 20mins.
- Add to the cells in a dropwise motion.
- Check GFP fluorescence of EHV-1 mutants after 48 h and EHV-4 mutants after 72 h
- if good, harvest supernatant plus cells (1 ml for stock, 1 ml for infection), put in 80°C for freeze-thawing

## Infection of NBL-6 to passage mutant viruses

- prepare 90% confluent 6-well of NBL-6 cells (if you know already that you have a slow virus, use less cells or work with later passage of NBL-6, but take care they are not too old and dying already)
- spin down thawed 1 ml stock of transfected 293T culture at 6000 rcf for 6 min
- take supernatant to infect NBL-6 cells
- passage virus by trypsinising and adding new cells until a CPE of 100%, avoid thawing, this reduces the titer

## Make Methylcellulose

for 500 ml

**Day 1:**

- 3 g Methylcellulose, fill to 300 ml with MilliQ
- add magnetic bar, autoclave

- 4.75 g DMEM-powder, fill to 100 ml with MilliQ
- mix well, autoclave

**Day 2:** work steril

- dissolve Methylcellulose at 4°C by stirring for 3-5 h (room temperature works too but slower)
- add the 100 ml DMEM, 25 ml FCS, 4 ml P/S, 5 ml NaHCO3 (7.5%)
- stirr again for 1-2 h

## Make PFA

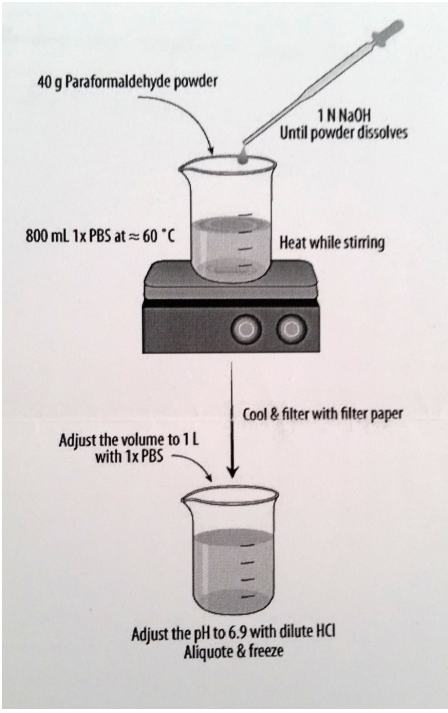


## Virus-Titration

**Day 1:** Prepare NBL-6 in 24 well plate with a volume of 500 µl 1-1,5 * $10^5$ cells per well depending on the passage), 2 x 6 wells per virus

- for EHV-1 ~90% confluent the next day
- for EHV-4 ~95% confluent the next day

**Day 2:** Preparation of 10-fold serial dilution series to $10^{-7}$ (360µl Medium + 40 µl virus = 400 µl total volume)

Work on ice, store thawed virus on ice too, move the vortex close to the hood if you prepare many samples

- thaw virus and store on ice
- Prepare 360µl medium (IMDM for NBL-6) in each tube
- Vortex virus suspension, add 40 µl in the first eppi (1:10)
- Start the dilution (add 40 µl from the first eppi in the next eppi)
- discard $10^1$ dilution

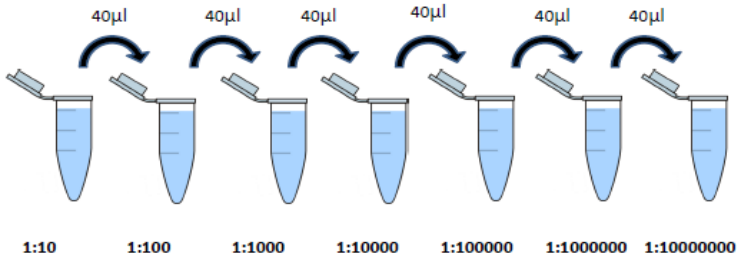


1. Take off medium from NBL-6 (if you are fast, take it off from all, otherwise do it stepwise)
2. add 150 µl of the right dilution step, start with $1:10^2$
3. Incubate for 1 h at 37°C, tilt the plate 5 times in the first 10 min and than every 10 min
4. Discard the supernatant
5. Add 500 µl Methylcellulose-medium in each well
6. incubate for 72 h at 37°C
7. you can count GFP the next day already

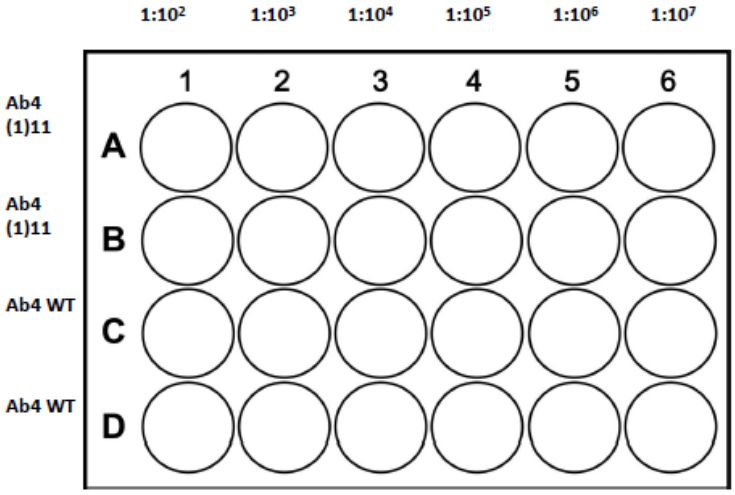


8. fix cells with 100% EtOH for 15-20 min, wash with tab water (if GFP needs to be visible after fixation use 4% PFA)
9. stain cells with crystal violet
10. count plaques

Since we use 150 µl for the infection the calculation for plaque forming units per ml (PFU/ml) would be: # plaques * dilution / 0,15 ml
For example, if there are 55 plaques in the $10^{-5}$ dilution well the titer would be $3,7 * 10^7$ PFU/ml.
A 24 well has an approximate growth area of 1,9 cm² which would be covered by approximately $1,9x10^5$ cells at 100% confluency. I assume I have $1,9x10^5$ cells per 24 well with approx. 90%

confluency for the calculation of the Multiplicity of Infection (MOI). The calculation for the above sample would be 3,7 * $10^7$ PFU/ml / 1,9x$10^5$ cells = MOI 195

### Make citrate buffer

40 mM citric acid, 10 mM Potassium chloride, 135 mM Sodium chloride, pH 3, store at 4°C

## Growth kinetics

For statistics repeat at least 3 independ times.

**Day 1**

- seed NBL-6 cells (6 wells per virus) not older than P 33, 80-90% confluent for EHV-1, 90-100% confluent for EHV-4 (1 conflunt 10 cm plate ok for 1 24-well plate)

Timepoints: EHV-1 → 0, 6, 12, 24, 30 h, supernatant and cells seprate samples

EHV-4 → 0, 6, 12, 24, 48, 72 h, supernatant and cells together

**Day 2**

**Important: plan infection according to timepoints** (realistic working hours)

- calculate virus volumes (MOI 0.01-1), control wild type virus
- thaw viruses, vortex
- take off supernatant from NBL-6 cells, add 150 µl virus-media mix
- incubate 1 h at 37°C, tilt every 10 min
- take off virus-media mix, wash with 500 µl PBS
- add a few drops of citrate buffer to cover the cells, not for longer than 30 s!
- Neutralize with 500 µl media
- remove citrate buffer, wash 3 x with PBS
- add 500 µl fresh media, collect timepoint 0 h right away
    - supernatant → pipette up and down 2 x with 1 ml pipette tip, transfer into 1,5 ml eppi
    - cells → add 500 µl fresh media, cut 13 mm cell sraper with sterile scissors, scrape cells throroughly, use 1 ml pipette tip to reach the edges, pipette 2 x up and down, transfer into 1,5 ml eppi
- collect rest of the timepoints accordingly:
    - start → 8:00 a.m.<br>0 h → 9:30 a.m.<br>6 h → 3:30 p.m.<br>12 h → 9:30 p.m.<br>24 h → 9:30 a.m.<br>72 h → 9:30 a.m.

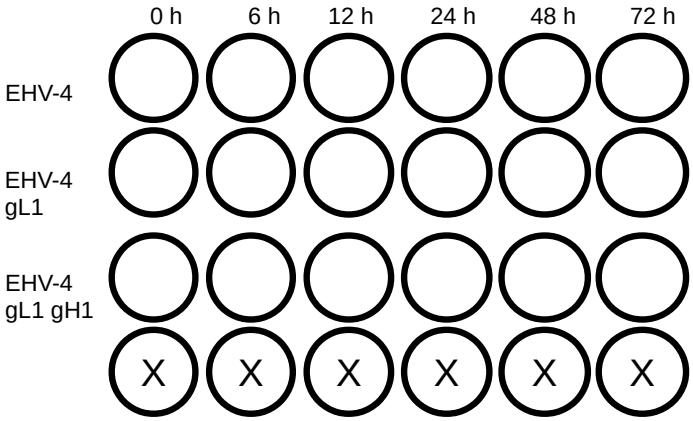


titrate all samples, not all dilutions from $10^{-1}$ to $10^{-7}$ are needed, example here:

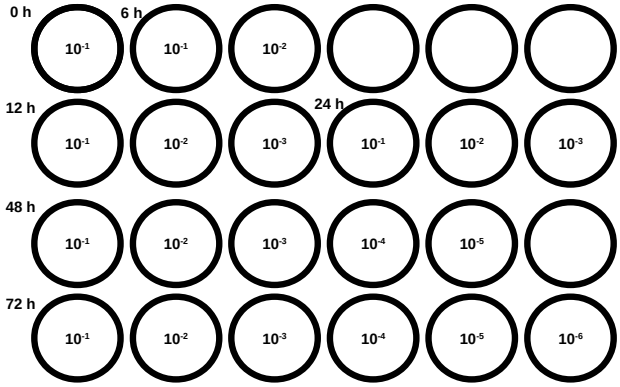


- statistical analysis can be done with one-way ANOVA and Bonferroni multiple comparison test

## Plaque size assay

- Infect cells in 6 well plate with all viruses that will be compared, measure at least 50 plaques each, you can use ImageJ for that or write a script in Python for automation

## A.2.8.

**IN GEL-VERDAU MIT TRYPSIN: (CHRIS WEISE/ STAND MÄRZ 2016)**

**Vorbereitung:**
- Gel dokumentieren und in Wasser lagern,
- Puffer 100mM $NH_4HCO_3$ neu aus 1 M Stammlösung ansetzen, pH-Wert prüfen (soll zwischen 7,9 und 8,5 liegen); daraus durch Verdünnung 1 ml 25mM $NH_4HCO_3$ herstellen und im Kühlschrank bei 4°C lagern

1.- Gel auf **saubere Unterfläche** legen und blau- oder silbergefärbte Banden oder Spots ausschneiden und in kleine Gelstücke von etwa 1x1 mm zerstückeln, **in einem kleinen Eppendorfgefäß (500 µl)** inkubieren in Acetonitril : 100 mM $NH_4HCO_3$ (1:1)
Volumen: 20µl für eine Minigel-Bande (bei fetten Banden evtl. größere Volumina verwenden)
Schütteln: 15 min. bei Raumtemperatur
– Kühlfalle der Trocknungsanlage (Speedvac) bereits einschalten

2.- Überstand abnehmen, ersetzen durch 100% Acetonitril
Volumen wie oben
stehenlassen, bis die Gelstücke milchig weiß sind,
wenn sie noch nicht weiß sind, Acetonitril wechseln und Schritt wiederholen
Dauer: ca. 5 min
(zwischenzeitlich DTT einwiegen 15,4mg/ml und Lösung ansetzen, siehe Schritt 4)

3.- Acetonitril entfernen und Gelstücke vakuum-trocknen (Speedvac)
Dauer: ca. 10 min
(Kühlfalle hinterher eingeschaltet lassen)

4.- REDUKTION:
(Disulfidbrücken werden geöffnet.)
inkubieren in 100 mM DTT in 100 mM $NH_4HCO_3$
Volumen wie oben – wichtig: Volumen an dieser Stelle genau dosieren und notieren
30 min. bei 56 °C
(zwischenzeitlich Iodacetamid einwiegen 10mg/ml und Lösung ansetzen, im Dunklen aufbewahren bis zur Benutzung, siehe Schritt 7)

5.- Proben kurz zentrifugieren, Überstand abnehmen (dabei das Volumen des Überstandes mit der Pipette genau bestimmen, damit man weiß, wieviel Flüssigkeit die Gelstückchen aufnehmen und nachher die Volumina der Trypsinlösung genau so dosieren kann, dass man ein Minimum an Überstand erhält.)

6.- Gelstücke mit 100% Acetonitril schrumpfen, bis sie milchigweiß sind
(Überschuss an Reduktionsmittel wird entfernt)
Volumen wie gehabt, ggf. wechseln
bei Raumtemperatur, ca. 5-10 min.

7.- CARBAMIDOMETHYLIERUNG
(Cysteine werden durch eine kovalente Reaktion so modifiziert, dass keine Rückbildung von Disulfid-Brücken mehr stattfinden kann. Für jeden Cystein-Rest kommt es dabei zu einer Massenzunahme von 57 Masseneinheiten.)
Überstand abnehmen, ersetzen durch 55 mM Iodacetamid in 100 mM $NH_4HCO_3$
Volumen wie gehabt
20 min bei Raumtemperatur im Dunklen (z.B. in einer Schublade) und ohne Schütteln

8.- Proben kurz zentrifugieren, Überstand abnehmen und verwerfen

9.- zum Spülen: 100 mM $NH_4HCO_3$,
Volumen wie oben
15 min bei Raumtemperatur

10.- Proben kurz zentrifugieren, Überstand abnehmen

11.- Gelstücke mit 100% Acetonitril schrumpfen, 5–10 min bei RT inkubieren, Überstand abnehmen
Vorgang wiederholen: noch einmal 100 % Acetonitril zugeben, 5 min bei RT inkubieren, Überstand abnehmen
(An dieser Stelle ist es wichtig, dass das Reagenz vollständig entfernt wird, da es bei der Spaltung später nicht mehr da sein darf, sonst werden auch nicht Cys-haltige Peptide modifiziert)

12.- Gelstücke vakuum-trocknen (Speedvac)
Dauer: ca. 10 min
währenddesssen schon mal ein Aliquot der Trypsin-Stammlösung (Trypsin sequencing grade, Sigma, 1mg/ml in 1mM HCl) auftauen und auf Eis lagern

13. - Aliquot der Trypsin-Stammlösung mit **25 mM $NH_4HCO_3$-Lösung** verdünnen (1:80, finale Trypsin-Konzentration in der Trypsinlösung: 12.5 ng/µl), vortexen, auf Eis stellen.
Trypsinlösung zu den Proben geben und die Proben sofort auf Eis stellen.
Volumen: Das oben bestimmte Volumen + ~ 5 µl, damit auch wirklich ein abnehmbarer Überstand entsteht (Rechnung meist: V=20µl – Überstand + 5µl)

Zunächst 30 Minuten auf Eis stehen lassen, dann bei $37^0$C über Nacht inkubieren.

(Falls erkennbar ein zu großer Überstand vorhanden ist, diesen Überstand von den Gelstücken abnehmen, ersetzen durch so viel 25 mM $NH_4HCO_3$, so daß die Gelstücke gerade eben bedeckt sind (kann 2-3 µl sein)

14.- Am nächsten morgen Eppis kurz zentrifugieren (Lösung kondensiert meist am Deckel ab.).
Bei RT mindestens 30 min. stehen lassen bzw schütteln.

15.- Eppis zentrifugieren und Verdauüberstand (S1) abnehmen; benötigt wird 1µl. (Falls kein abnehmbarer Überstand entstanden ist, das nötige Volumen Wasser zugeben und wiederum mindestens 30 min stehen lassen.)

Im Prinzip kann mit diesem Überstand S1 bereits ein MALDI-Massenfingerprint aufgenommen werden, durch den das Protein identifiziert wird. Allerdings ist die Qualität der Spektren wegen mangelhafter Kristallisation aufgrund des Salzgehaltes der Proben oft niedrig. Eine Verbesserung kann durch Ziptippen ($C_{18}$) oder durch Verdünnung der Proben, z.B 1:5 in Wasser oder in S2 (siehe unten), erreicht werden.

NB: Kann die Messung nicht sofort durchgeführt werden, können die Proben bei –20 °C eingefroren werden. Sie sind i.d.R. über Wochen bis Monate stabil.

**NACHEXTRAKTION**:
Im Gel verbliebene Peptide können weiter mit organischem Lösungsmittel und Säure eluiert werden (Schritte 16-17).

16.- Nach Abnehmen des 1.Überstandes 10µl 40% Acetonitril/0.1% Trifluoressigsäure (TFA) zusetzen und bei RT mehrere Stunden oder auch über Nacht/übers Wochenende schütteln.

17.- Überstand (S2) abnehmen und zur Messung einsetzen oder Probe bis zu einer späteren Messung bei –$20^0$C aufbewahren.

(Diese S2-Proben enthalten weniger Salz und kristallisieren daher besser; gegenüber dem ersten Überstand wird die Elution von großen und hydrophoben Peptiden aus dem Gel begünstigt; die Nachextrakte können ggf. aufkonzentriert werden. Bei ZipTip ist zu beachten, dass sie einen hohen Anteil organische Phase enthalten.)

S1 + S2 werden getrennt aufbewahrt.

PUFFER/REAGENZIEN:

| | |
|---|---|
| Puffer: | 100mM $NH_4HCO_3$ pH 7,9–8,5 |
| Verdaupuffer (Spaltung): | 25mM $NH_4HCO_3$ pH 7,9–8,5 |
| Reduktionslösung: | 100 mM DTT in 100 mM $NH_4HCO_3$ (=15,4mg/ml) |
| Carbamidomethylierung: | 55 mM Iodacetamid in 100 mM $NH_4HCO_3$ (=10mg/ml) |
| Trypsinlösung: | 12,5 µg/ml Trypsin* (bovin, Sequenzierungs-Reinheitsgrad) in 25 mM $NH_4HCO_3$ |

* Trypsin-Stammlösung (inaktiv) 1mg/ml in 1mM HCl; diese wird 1:80 mit Verdaupuffer verdünnt (z.B. 4µl ad 320µl) und zur Spaltung eingesetzt.

Alle Lösungen werden in $H_2O$ (HPLC- oder MQ-Reinheitsgrad) angesetzt.

Anm.: Der $NH_4HCO_3$-Puffer wird mitunter auch ABC-Puffer genannt (Ammoniumbicarbonat)

## Selbständigkeitserklärung

Hiermit erkläre ich, dass ich die vorliegende Arbeit selbstständig verfasst und keine anderen als die angegebenen Quellen und Hilfsmittel verwendet habe. Ich versichere, dass diese Arbeit in dieser oder anderer Form noch keiner Prüfungsbehörde vorgelegt wurde. Der Inhalt der Promotionsordung des Fachbereichs Biologie, Chemie, Pharmazie der Freien Universität Berlin vom 31. Mai 2018 ist mir bekannt.

Berlin,

Viviane Kremling